Biosynthesis of lignans in plant species of the section *Linum*: pinoresinol-lariciresinol reductase and justicidin B 7-hydroxylase

Inaugural-Dissertation

submitted to the Faculty of Mathematics and Natural Sciences

Heinrich-Heine University, Düsseldorf

in fulfillment of the requirement for doctoral degree

(Dr. rer. nat)

by

Shiva Hemmati

from Shiraz

Düsseldorf, 2007

From the Institut für Entwicklungs-und Molekularbiologie der Pflanzen,

Heinrich-Heine-Universität Düsseldorf,

Universitätsstr. 1, D-40225 Düsseldorf, Germany

Printed with the permission of the

Faculty of Mathematics and Natural Sciences,

Heinrich-Heine University, Düsseldorf

Referee: Prof. Dr. A. W. Alfermann

Coreferee1:   Prof. Dr. S. M. Li

Coreferee 2:   Prof. Dr. D. Ober

Date of oral examination: 19.11.2007

Table of contents

Abbreviations

A	Adenin
ATP	Adenosin triphosphate
Amp	Ampicillin
APS	Ammonium peroxidodisulfate
BLAST	Basic Local Alignment Tool
bp	Base pairs
BSA	Bovine serum albumin
C	Cytosine
CaMV	Cauliflower mosaic virus
cDNA	Complementary DNA
CLOT	Clotrimazole
CTAB	Hexadecyltrimethyl ammonium bromide
CYP	Cytochrome P450
Cyt *c*	Cytochrome *c*
dATP	Deoxyadenosine-5′-triphosphate
dCTP	Deoxycytidine-5′-triphosphate
DDC	Dehydrodiconiferyl alcohol
DIECA	Sodium diethyldithiocarbaminate-trihydrate
Diph	Diphyllin
DMSO	Dimethylsulfoxide
DNA	Deoxyribonucleic acid
dNTPs	Deoxynucleotide-5′-triphosphate
dsRNA	Double strand RNA
DTT	1,4-Dithiothreitol
DW	Dry weight
EB	Elution buffer
EDTA	Ethylenediamine tetraacetic acid
Fig	Figure
G	Guanine
gDNA	Genomic DNA
h	hour
His	Histidine
IFR	Isoflavone reductase
ihpRNA	Intron hairpin RNA
IPTG	Isopropyl-β-D-thiogalactopyranoside
Jus B	Justicidin B
JusB7H	Justicidin B 7-hydroxylase
kb	Kilobase
kDa	Kilodalton
Km	Michaelis-Menten constant
KPi	Kalium phosphate
Lari	Lariciresinol
L. perenne H	*Linum perenne* Himmelszelt
L. usitatissimum F	*Linum usitatissimum* Flanders
LB	Luria-Bertani

Matai	Matairesinol
min	Minute
mM	Milimolar
mRNA	Messenger RNA
MS	Mass spectrometry
NAA	Naphtyl acetic acid
NADH	Nicotinamide adenine dinucleotide
NADP+	Nicotinamide adenine dinucleotide phosphate (oxidized form)
NADPH	Nicotinamide adenine dinucleotide phosphate (reduced form)
NMR	Nuclear magnetic resonance
OD	Optical density
ORF	Open reading frame
p.A.	Pro analyse
PCBER	Phenylcoumaran benzylic ether reductases
Pino	Pinoresinol
PLR	Pinoresinol lariciresinol reductase
PMSF	Phenylmethansulfonyl fluride
PS	Pinoresinol synthase
Ri	Root inducing
RISC	RNA induced silencing complex
RNase	Ribonuclease
rpm	Round per minute
Rt	Retention time
s	seconds
SDG	Secoisolariciresinol diglucoside
SDS	Sodium dodecyl sulfate
SDS-PAGE	SDS-Polyacrylamide gel electrophoresis
Seco	Secoisolariciresinol
siRNA	Small interfering RNA
T	Thymine
Tab	Table
TAE	Tris-acetate-EDTA
T-DNA	Transfer DNA
TE buffer	Tris-EDTA
TEMED	N,N,N′,N′-tetramethyl ethylene diamine
Tris	Tris (hydroxymethyl) aminomethan
UTR	Untranslated region
v/v	Volume per volume
w/v	Weight per volume

1. Introduction

1.1. The genus *Linum* and its infrageneric taxa

The genus *Linum* is the type genus for the flax family, Linaceae (DC.) Dumort. The Linaceae family is geographically widespread with about 300 species worldwide (Diederichsen and Richards 2003). Several of the species are shrubs and occur in tropical areas, while perennial and annual species are found in temperate areas of the world. This family is positioned in the plant kingdom as follows: division: Spermatophyta; sub-Division: Angiospermae; class: Dicotyledoneae; sub-Class: Rosidae; order: Linales. Within the Linaceae family, *Linum*, is the largest genus and belongs to the tribe Linoideae. The infrageneric classification of the genus *Linum* with different morphological, cytological and biochemical characters is still controversial; it is usually divided into variable infrageneric groups, sometimes referred to as subgenera, sometimes as sections. However, none of the systems proposed can be regarded as satisfactory (Velasco and Goffman 2000). The wide range of diversity within the genus continues to challenge its systematic treatment. Ockendon and Walters (1968) have subdivided the genus *Linum* into 5 sections: *Linum*, *Linastrum*, *Syllinum*, *Dasylinum* and *Cathartolinum* in Flora Europaea. According to the recently established molecular phylogeny of the Linaceae (Kadereit and Repplinger, unpublished results, Fig.1.1) the genus *Linum* has two main clusters, one mainly consisting of the sections *Linopsis* and *Syllinum* and the other contains section *Linum*.

1.1.1. Section *Linum*

Alternate, glabrous leaves without basal glands; eglandular sepals; free, blue purple or pink petals; capitate, clavate or linear stigmas are the characteristics of plants in this section according to Flora Europaea (Ockendon and Walters 1968). They can be homo- or heterostylous; perennial, biennial or annual. 12 species of the section *Linum* have been reported from Europe. *L. narbonense*, *L. nervosum*, *L. aroanium*, *L. hologynum*, *L. virgultorum*, *L. decumbens*, *L. bienne*, *L. usitatissimum* and the *L. perenne* group. The *L. perenne* group contains 4 species as follows: *L. perenne*, *L. austriacum*, *L. punctatum* and *L. leonii*.
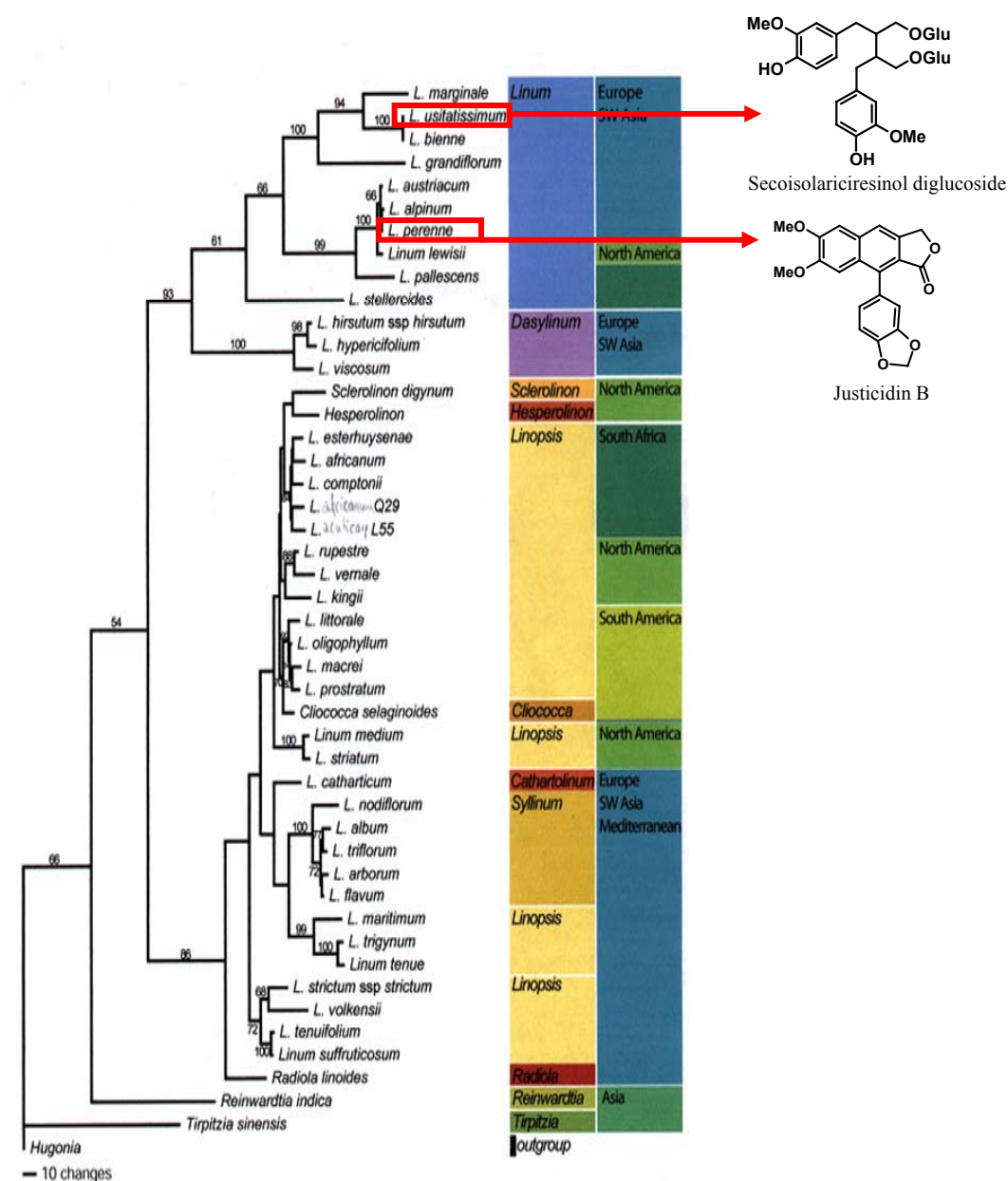
Fig. 1.1. Phylogenetic tree of the genus *Linum* based on ITS-analytics. Figure with permission of Prof. Dr. J. Kadereit & M. Repplinger, Institut für Spezielle Botanik, Universität Mainz; together with the type of lignans in *L. usitatissimum* and *L. perenne*.

1.1.1.1. *Linum usitatissimum* L.

L. usitatissimum does not occur as a wild plant. Its taxonomic characters are mentioned to be like its wild progenitor *L. bienne* Mill. (*L. angustifolium* Huds.), but *L. usitatissimum* L. is more robust and always annual. Stems are usually single, leaves are 1.5-3 mm wide, 3-veined,

with 6-9 mm sepals. Capsules are 6-9 mm. *L. usitatissimum* is an important summer crop for the production of oil and fiber. The translation of the Latin species epithet usitatissimum is "the most useful one", reflecting the several uses made of this plant.

1.1.1.2. *Linum perenne* **L**.

Stems are 10-60 cm, decumbent, ascending or erect. The middle cauline leaves are 1- to 3-veined. Inflorescence usually many-flowered. Inner sepals are acute or obtuse. Pedicels are erect. Capsules are 5-8 mm. Heterostylous. In Flora Europaea five subspecies are identified for *L. perenne* L. as follows: subsp. *perenne*, subsp. *anglicum*, subsp. *alpinum*, subsp. *montanum*, subsp. *extraaxillare*.

1.2. Primary and secondary metabolism

All organisms need to transfer and interconvert a vast number of organic compounds to enable them to live, grow, and reproduce. They need to provide themselves with energy in the form of ATP, and a supply of building blocks to construct their tissues. An integrated network of enzyme mediated and carefully regulated chemical reactions is used for this purpose, collectively referred to as intermediary metabolism, and the pathways involved are termed **metabolic pathways**. Despite the extremely varied characteristics of living organisms, the pathways for generally modifying and synthesizing carbohydrates, proteins, fats, and nucleic acids are found to be essentially the same in all organisms, apart from minor variations. These processes demonstrate the fundamental unity of all living matter, and are described as primary metabolism, with the compounds involved in the pathways being termed **primary metabolites**. There also exists an area of metabolism concerned with compounds which have a much more limited distribution in nature. Such compounds, called **secondary metabolites**, are only found in specific organisms, or groups of organisms, and are an expression of the individuality of species. Secondary metabolites are not necessarily produced under all conditions, and in the vast majority of cases the function of these compounds and their benefit to the organism is not yet known. But it is logical to assume that all do play some vital role for the well-being of the producer (Dewick 2002). Hartmann (1996) defined primary metabolism as universal, uniform, conservative, and indispensable, and secondary metabolism as singular

diverse, adaptive, dispensable for growth and development, but indispensable for survival. Many of the secondary metabolites have important ecological functions in plants: they protect plants against herbivores and microbial pathogens, they serve as attractants for pollinators and seed-dispersing animals, and they function as agents of plant-plant competition and plant-microbe symbioses (Taiz and Zeiger 2006). Undoubtly, the great utility of secondary metabolites as medicinal drugs, flavoring agents, dyes, polymers, fibers, glues, oils, waxes and perfumes have made them interesting for humankinds (Croteau et al. 2000). The above generalizations distinguishing primary and secondary metabolism leave a grey area at the boundary, so that some groups of natural products could be assigned to either division. Hartmann (1996) suggested using "primary" and "secondary" in the sense of function; e.g. Canavanine (**1**) as a nitrogen reservoir, is a primary metabolite, and as a toxic defense chemical, is a secondary metabolite. Secondary metabolites are low molecular weight compounds and their production is often low (less than 1% dry weight). More than 100,000 secondary metabolites have been described, with many more yet to be discovered; estimates of total number in plants alone exceed 500,000 (Oksman-Caldentey and Inzé 2004; Hadacek 2002).

1.2.1. The building blocks of secondary metabolites

The building blocks for secondary metabolites are derived from primary metabolism as indicated in Fig. 1.2. This scheme outlines how metabolites from fundamental processes of photosynthesis, glycolysis, and the Krebs cycle are tapped off from energy generating processes to provide biosynthetic intermediates. By far the most important building blocks employed in the biosynthesis of secondary metabolites are derived from the intermediates acetyl coenzyme A (acetyl-CoA), shikimic acid, mevalonic acid and 1-deoxyxylulose 5-phosphate.

1.3. The shikimate-chorismate pathway

The shikimate pathway is the major metabolic route leading to the formation of aromatic compounds especially L-phenylalanin, L-tyrosin and L-tryptophan in microorganisms and in plants.
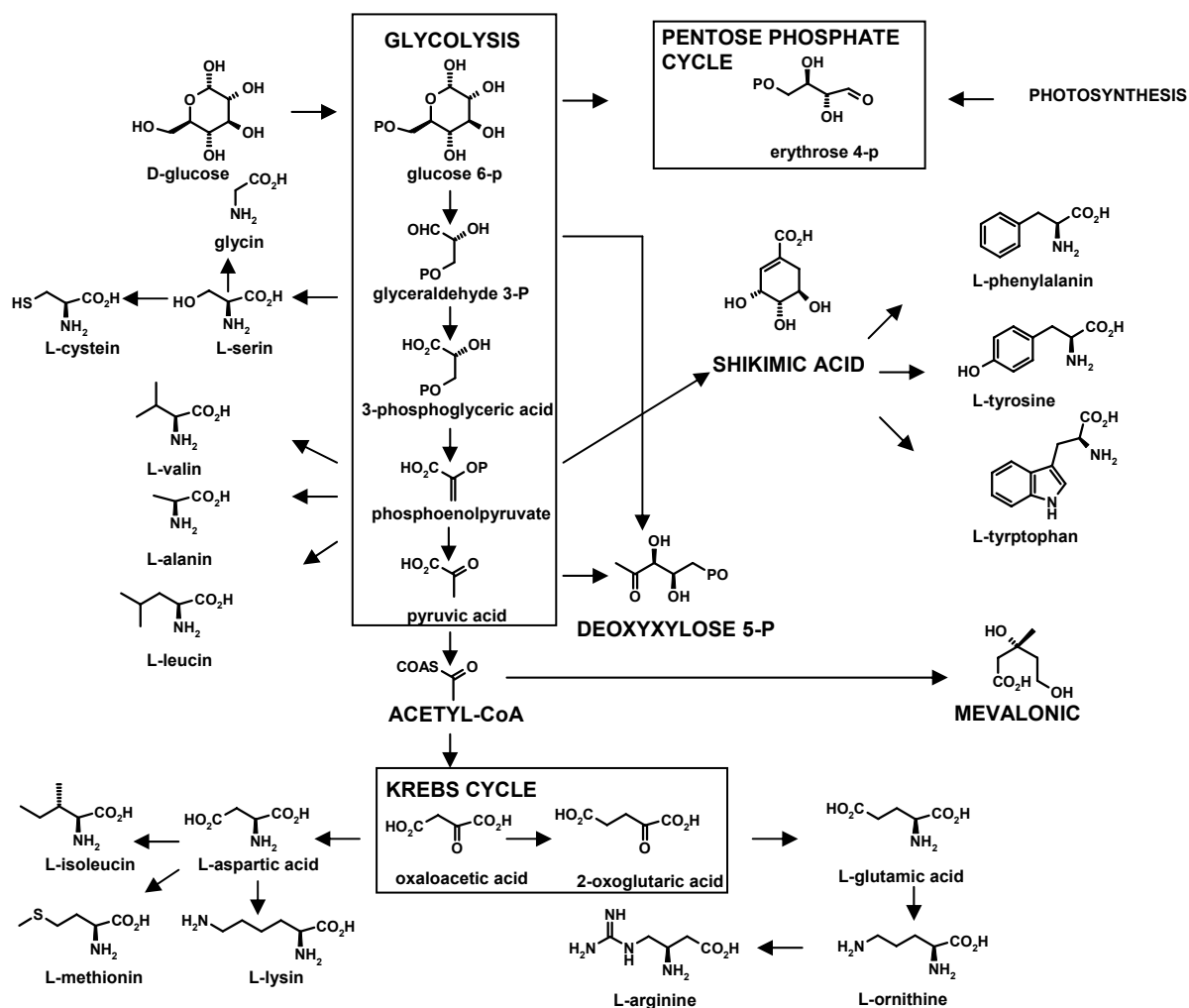
Fig. 1.2. The building blocks for secondary metabolites are derived from primary metabolism (adopted from Dewick 2002).

The shikimate pathway begins with the coupling of phosphoenolpyruvate (PEP) and D-erythrose 4-phosphate to give 3-deoxy-D-arabino-heptulosonic acid 7-phosphate (DAHP) (Fig. 1.3). Elimination of phosphoric acid from DAHP followed by an intramolecular aldol reaction generates the first carbocyclic intermediate 3-dehydroquinic acid. Reduction of 3-dehydroquinic acid leads to quinic acid. Shikimic acid itself is formed from 3-dehydroshikimic acid by dehydration and reduction steps. A very important branchpoint compound in the shikimate pathway is chorismic acid, which has incorporated a further molecule of PEP as an enol ether side chain. Shikimic acid 3-phosphate is produced in a simple ATP-dependent phosphorylation reaction. Shikimic acid 3-phosphate combines with PEP and produces 5-enolpyruvylshikimic acid 3-phosphate (EPSP) by EPSP synthase. The transformation of EPSP to chorismic acid involves a 1,4-elimination of phosphoric acid. By a

singular rearrangement, chorismic acid transforms into prephenic acid. Decarboxylative aromatization of prephenic acid yields phenylpyruvic acid. L-phenylalanin forms after transamination. In the presence of an NAD^+-dependent dehydrogenase, decarboxylative aromatization occurs with retention of the hydroxyl function for prephenic acid and results in the formation of 4-hydroxyphenylpyruvic acid which after transamination forms L-tyrosin. (Floss 1979; Strack 1997; Dewick 2002)
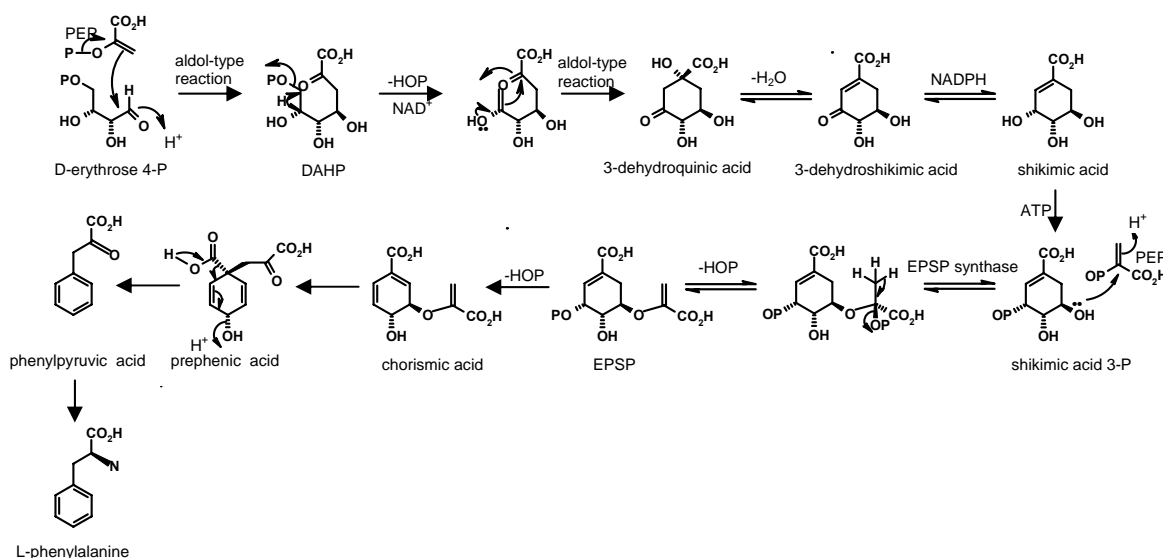
Fig. 1.3. The shikimate-chorismate biosynthetic pathway leads to the formation of L-phenylalanine (adapted from Dewick 2002).

1.4. The general phenylpropanoid pathway

C_6C_3 refers to a phenylpropyl unit and is obtained from the carbon skeleton of either L-phenylalanin or L-tyrosin, two of the shikimate-derived aromatic amino acids (Fig. 1.3). C_6C_3 building blocks are routinely employed into many biosynthetic pathways like the monolignol pathway. The biosynthesis of monolignols e.g. coniferyl alcohols (Fig. 1.4), is initiated with deamination of phenylalanine by phenylalanine ammonia lyase (PAL) to form cinnamic acid, which is hydroxylated by a P450 enzyme, cinnamate 4-hydroxylase (C4H), to form *p*-coumaric acid. 4-coumarate is then activated to the coenzyme A-thioester by 4-coumarate:CoA ligase (4CL). (Formation of the coenzyme A ester facilitates the NADPH reduction steps by introducing a better leaving group $CoAS^-$).

4-coumarate-CoA is the precursor for many phenylpropanoid compounds including flavonoids, stilbenes, coumarins and lignin. The latter is constituted mainly of subunits derived from coniferyl (G-lignin subunits) and sinapyl (S-lignin) alcohols.

Fig. 1.4. General phenylpropanoid and monolignol pathway (adapted from Humphreys and Chapple 2002).

To form these, and the corresponding aldehydes (coniferaldehyde and sinapaldehyde) and acids (ferulate and sinapate), the aromatic ring of 4-coumarate needs to be hydroxylated at the 3- and 5-positions respectively, followed by methoxylation of the hydroxy groups. It was long thought that these hydroxylations occur at the level of the free acids. But, in recent years it became clear that the predominant pathway proceeds via 3'-hydroxylation of coumaroyl-shikimate and coumaroyl-quinate derivatives and 5-hydroxylation of coniferaldehyde. *p*-coumarate 3-hydroxylase (C3H) converts the 5-*O*-shikimate and 5-*O*-D-quinate esters of *p*-coumaric acid into their corresponding caffeic acid conjugates. The operation of the "shikimate/quinate ester shunt" is catalyzed by hydroxycinnamoyl CoA:shikimate hydroxycinnamoyltransferase (CST) and hydroxycinnamoyl CoA:quinate

hydroxycinnamoyltransferase (CQT), respectively. CST and CQT are reversible and would have to function in both forward and reverse directions. Methylation of caffeoyl-CoA by caffeoyl-CoA *O*-methyltransferase leads to formation of feruloyl-CoA. Ferulate 5-hydroxylase (F5H) and caffeic acid/5-hydroxyferulic acid *O*-methyltransferase (COMT) act in the level of aldehyde and alcohol respectively and result in the formation of sinapyl alcohol. In any event, the feruloyl-CoA undergoes successive reduction reactions catalyzed by cinnamoyl CoA reductase (CCR) and cinnamyl alcohol dehydrogenase (CAD), respectively, to form coniferyl alcohol (Anterola et al. 2002; Humphreys and Chapple 2002; Dixon and Reddy 2003).

1.5. Lignans
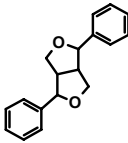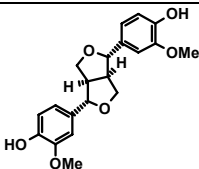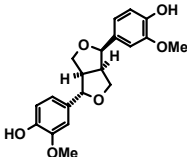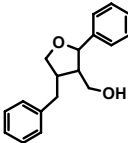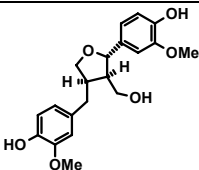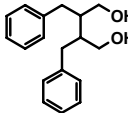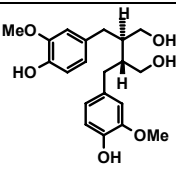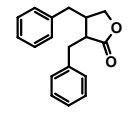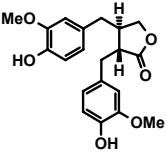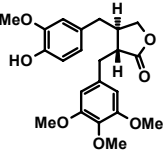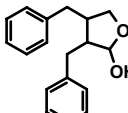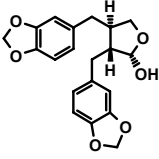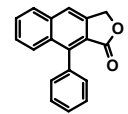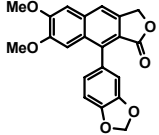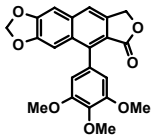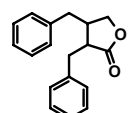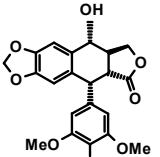
Lignans and neolignans are a large group of naturally occurring phenolic compounds characterized by the coupling of two C_6C_3 units. When the two C_6C_3 units are linked by a bond between positions 8 and 8' the compound is named lignan (Fig 1.5). If the two C_6C_3 units are linked by other carbon-carbon bonds it is referred to as neolignan. When the carbons are linked by an ether oxygen atom the compound is named oxyneolignan. Sesquineolignans and dineolignans have three and four C_6C_3 units respectively (Moss 2000).
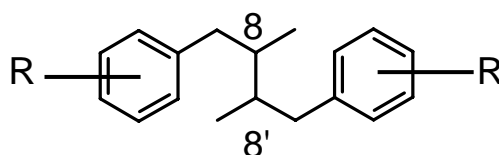
Fig. 1.5. General structure of lignans. Two C_6C_3 units are linked between 8 and 8' carbon atoms.

1.5.1. Distribution of lignans

In terms of evolutionary patterns, lignans are apparently absent in algae but are present in primitive early land plants, such as the liverworts (Cullmann et al. 1993). Lignans are also widely distributed in the Pteridophytes like ferns and Lycopsidae like *Selaginella* species (Lin et al. 1994). The gymnosperms were evolutionary accompanied by a massive increase in lignan structures.

Lignan subgroups	Examples
Furofuran type	(+)-pinoresinol (+)-epipinoresinol
Furan type	(+)-lariciresinol
Dibenzylbutan type	(-)-secoisolariciresinol
Dibenzylbutyrolacton type	(-)-matairesinol (-)-yatein
Dibenzylbutyrolactol type	(-)-cubebin
Arylnaphthalene type	justicidin B dehydrodeoxypodophyllotoxin
Aryltetralin type	(-)-podophyllotoxin

Fig. 1.6. Structural diversity of lignans. Baisic skeleton and examples of each group.

In a somewhat similar manner, the transition to angiosperms was also accompanied by an increase in lignan structural types/new skeletal forms. Lignan producing plants are distributed throughout the six subclasses of Magnoliopsida; in contrast Liliopsida plants are rather poor lignan sources. Umezawa (2003) have summerized the results on 108 families of lignan producing plants in the division of Magnoliophyta.

1.5.2. Structural diversity of lignans

Further derivatisation of the general structure of lignans leads to a broad variety of derivatives. Upon the way in which oxygen is incorporated into the skeleton and the cyclization pattern, lignans are classified into the following eight subgroups: furofuran, furan, dibenzylbutan, dibenzylbutyrolactone, aryltetralin, arylnaphthalene, dibenzocyclooctadiene and dibenzylbutyrolactol (Fig. 1.6). Lignans of each subgroup vary substantially in oxidation levels of both the aromatic rings and propyl side chains. Some lignans of furan, dibenzylbutane, and dibenzocyclooctadiene have no oxygen at C9 (C9'), while some lignans have extra hydroxyl groups at C7 (C7') or C8 (C8'). 3-methoxy-4-hydroxyphenyl (guaiacyl), 3,4-dimethoxyphenyl (veratryl), 3,4-methylenedioxyphenyl (piperonyl), 3,5-dimethoxy-4-hydroxyphenyl (syringyl) and 3,4,5-trimethoxyphenyl (Fig. 1.7) are the most occurring aromatic rings found in lignans (Umezawa 2003).
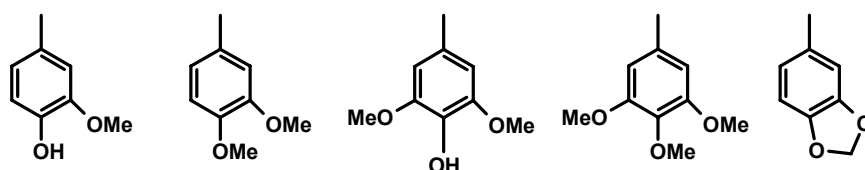
Fig. 1.7. Principle aromatic structures of lignans (adapted from Umezawa 2003).

1.5.3. Enantiomeric diversity of lignans

Most lignans contain chiral carbon atoms. They can be either optically active, racemic or optically inactive coupling products. As the result, in addition to the structural diversity, lignans vary substantially with respect to their enantiomeric composition. Most naturally occurring lignans have been found to exist exclusively as one enantiomer or as enantiomeric

mixtures with various enantiomeric compositions. Comparing the enantiomeric composition of lignans from various species in different plant families Umezawa (2003) has concluded the following statements: dibenzylbutyrolactone lignans are optically pure (>99% e.e.) while furofuran and furan lignans are mixture of both enantiomers and exhibit various enantiomeric compositions. For instance pinoresinol (Pino) which was isolated from cell suspension cultures of *L. album* and *L. usitatissimum* was the mixture of both enantiomers (von Heimendahl et al. 2005). Dibenzylbutyrolactone lignans are in most cases levorotatory except that the lignans from Thymelaeaceae plants and *Selaginella doederleinii* are dextrorotatory. Predominant enantiomers of furofuran, furan and dibenzylbutane lignans vary among plant species, and even within different organs in a single plant species. Petiols of *Arctium lappa* accumulate mainly (+)-secoisolariciresinol (Seco), but the seeds contain lignans with opposite stereochemistry like (-)-matairesinol (Matai) and (-)-arctigenin (Suzuki et al. 2002). Seeds of *L. usitatissimum* contain almost 99% (+)- and 1% (-)-SDG; whereas its aerial parts during flowering stage contain (-)-enantiomers of lignans (Schmidt et al. 2006). It should be mentioned that there are several conventions used for nominating chiral compounds. Based on the actual geometry of each enantiomer (+)-Pino, (+)-lariciresinol (Lari) and (-)-Seco all have R,R configuration at C-atoms 8,8′. (-)-Pino, (-)-Lari and (+)-Seco all have S,S configuration at C-atoms 8,8′.

1.5.4. Pharmacological effects of lignans

Lignans are of considerable pharmacological and clinical interest in the treatment of cancer and other diseases (Lee and Xiao 2003). The most important lignan for human health is probably the cytotoxic aryltetralin lignan podophyllotoxin because its semisynthetic derivatives like etoposide are used in cancer therapy (Imbert 1998). Justicidin B (Jus B), an arylnaphthalene lignan without any optically active center can attract interest, because of its fungicidal and antiprotozoal properties (Gertsch et al. 2003). It shows antiviral and anti-inflammatory activities as well as inhibition of platelet aggregation (Chen et al. 1996; MacRae et al. 1989; Rao et al. 2006). In addition, it is used as a lead compound for the design of antirheumatic drugs (Baba et al. 1996). Recently, its strong cytotoxicity on chronic myeloid and chronic lymphoid leukemia cell lines was shown (Vasilev et al. 2006). Diphyllin (Diph) derivatives are putative remedies for topical chronic inflammatory disorders such as

dermatitis and psoriasis while an acetylapioside derivative of Diph is a 5-lipoxygenase inhibitor (Prieto et al. 2002).

Besides various physiological roles in plants, lignans such as Seco and Matai, which are present in certain dietary components (e.g. flax (*L. usitatissimum*) seed), are thought to substantially reduce incidence rates of breast, prostate and other hormonally linked cancers, in humans on high fiber diets (Westcott and Muir, 2003). This so called chemoprotection occurs through their metabolism by the action of gastrointestinal flora such as *Clostridia* species into the mamelian lignans enterodiol and enterolactone, respectively (Axelson and Setchell, 1981; Setchell et al. 1981). It's now considered that dietary lignans impart these protective effects because of one or more of their antioxidant, weak estrogenic/antiestrogenic, anti-aromatase, antiangiogenic and anticarcinogenic/antitumor properties (Adlercreutz et al. 1993; Martin et al. 1978; Osawa et al. 1985).

1.6. Biosynthesis of lignans

In terms of biosynthesis the enzymatic steps leading to formation of C_6C_3 monomeric units have been described (chapter 1.4). The subsequent enzymatic transformations involved in monomeeric coupling and post-coupling modifications are now being delinated. The lignan biosynthesis starts with the coupling of two molecules of coniferyl alcohol and results in the formation of Pino (chapter 1.6.1). Pino is reduced via Lari to Seco by the bifunctional NADPH dependent enzyme pinoresinol-lariciresinol reductase (PLR) (chapter 1.6.2.1). Secoisolariciresinol dehydrogenase (SDH) oxidizes Seco to Matai. The biosynthetic pathway of aryltetralin type lignans in various plant species has been described previously (Federolf et al. 2007, von Heimendahl et al. 2005; Kranz and Petersen 2003; Molog et al. 2001; Sakakibara et al. 2003; Seidel et al. 2002).

The biosynthetic steps of other type of lignans like arylnaphthalene lignans were not investigated up to now. But it is anticipated that the steps from coniferyl alcohol to Matai are common in all pathways. Matai is believed to be a central intermediate leading to all diverse lignan structures. Later steps in the biosynthesis of arylnaphthalenes most probably starting from Matai are poorly understood. We have found that cell cultures of *L. perenne* Himmelszelt accumulate Jus B and glycoside derivatives of Diph (Hemmati et al. 2007). Schmidt and Vößing (2006) reported on the occurrence of 7(8)-dihydroisojusticidin B as
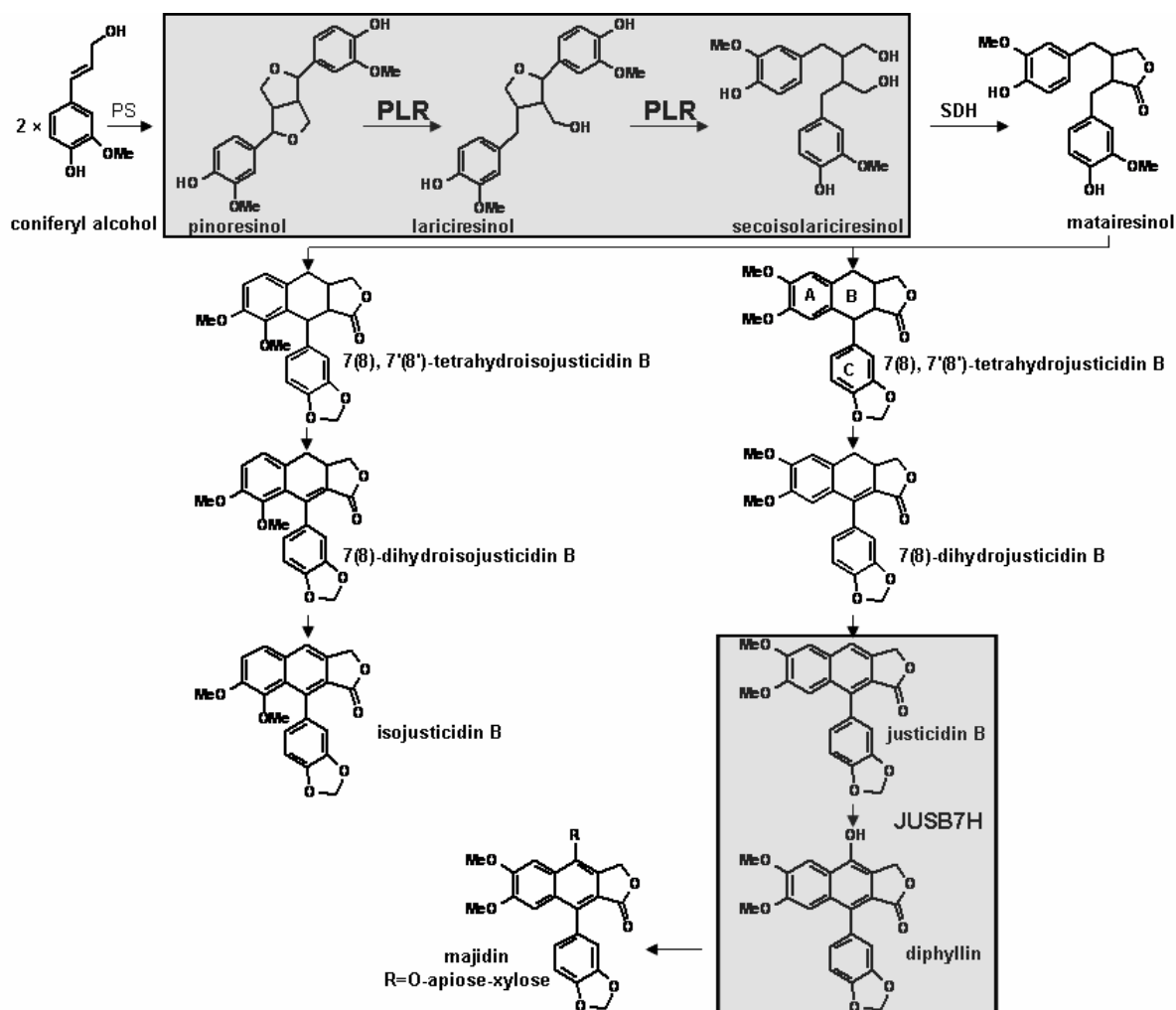
Fig. 1.8. Hypothetical biosynthetic pathway leading to diphyllin and isojusticidin B. PS: pinoresinol synthase, PLR: pinoresinol-lariciresinol reductase, SDH: secoisolariciresinol dehydrogenase, JusB7H: justicidin B 7-hydroxylase.

possible intermediate in the biosynthesis of isojusticidin B in the aerial part of *L. perenne*. Therefore, we have proposed a hypothetic biosynthetic pathway for arylnaphthalene lignans (Fig 1.8) suggesting that Matai is converted via cyclisation to form ring B and further derivatisation of ring C to 7(8),7'(8')-tetrahydroisojusticidin B and in parallel to 7(8),7'(8')-tetrahydrojusticidin B, which is converted by two dehydrogenation steps to 7(8)-dihydroisojusticidin B, respectively 7(8)-dihydrojusticidin B and then isojusticidin B and JusB. JusB can be further hydroxylated at position 7 to form Diph. As the cell cultures of *L. perenne* H accumulate not Diph but Diph diglycosides, glycosyltransferases are responsible

for the formation of majidin. Aspects of stereoselective coupling for the formation of Pino and the consequent reductive steps by PLR are described in the following chapters.

1.6.1. Dimerization of two coniferyl alcohols

Monolignol monomers, such as coniferyl alcohol are postulated to be dehydrogenated to phenoxy radicals; One-electron oxidation of a simple phenol allows delocalization of the unpaired electron, giving resonance forms. Radical pairing of resonance structures can then provide a range of dimeric systems containing reactive quinonemethides, which are susceptible to nucleophilic attack from hydroxyl groups in the same system, or by external water molecules. Thus, coniferyl alcohol monomers can couple, generating linkages as exemplified by guaiacylglycerol β-coniferyl ether (β arylether or 8-*O*-4' linkage), dehydrodiconiferyl alcohol (DDC) (phenylcoumaran or 8-5' linkage) and Pino (resinol or 8-8' linkage) Fig. 1.9.

1.6.1.1. Stereoselective coupling by dirigent proteins

As mentioned in chapter 1.5.3, plant lignans occur mainly as stereochemically pure (+)- or (-)- enantiomers. It has been concluded that dimerization of monolignols would occur either by a non-specific peroxidase followed by stereoselective biosynthetic steps or that the dimerization is already stereospecific. Following incubation of [8-^{14}C] coniferyl alcohol with *Forsythia suspensa* soluble cell-free enzyme preparations, the racemic Pino was formed only when H_2O_2 was supplied as cofactor, indicative of non specific peroxidase catalyzed coupling. The insoluble residue from *F. suspensa* (free of soluble and ionically bound enzymes) was able to catalyze the synthesis of Pino with enantiomeric excess for (+)-Pino. This fact provides the first evidence for a direct highly stereoselective coupling process. The so-called (+)-pinoresinol synthase (PS) was also detected in "crude cell wall preparations" of *F. intermedia*, where it catalyzed the stereoselective 8-8' dimerization of two molecules of *E*-coniferyl alcohol (Paré et al. 1994). (+)-PS has been purified and characterized, showing an enzyme system consisting of two proteins, an oxidase and a dirigent protein, the later without catalytic activity (Davin et al. 1997).
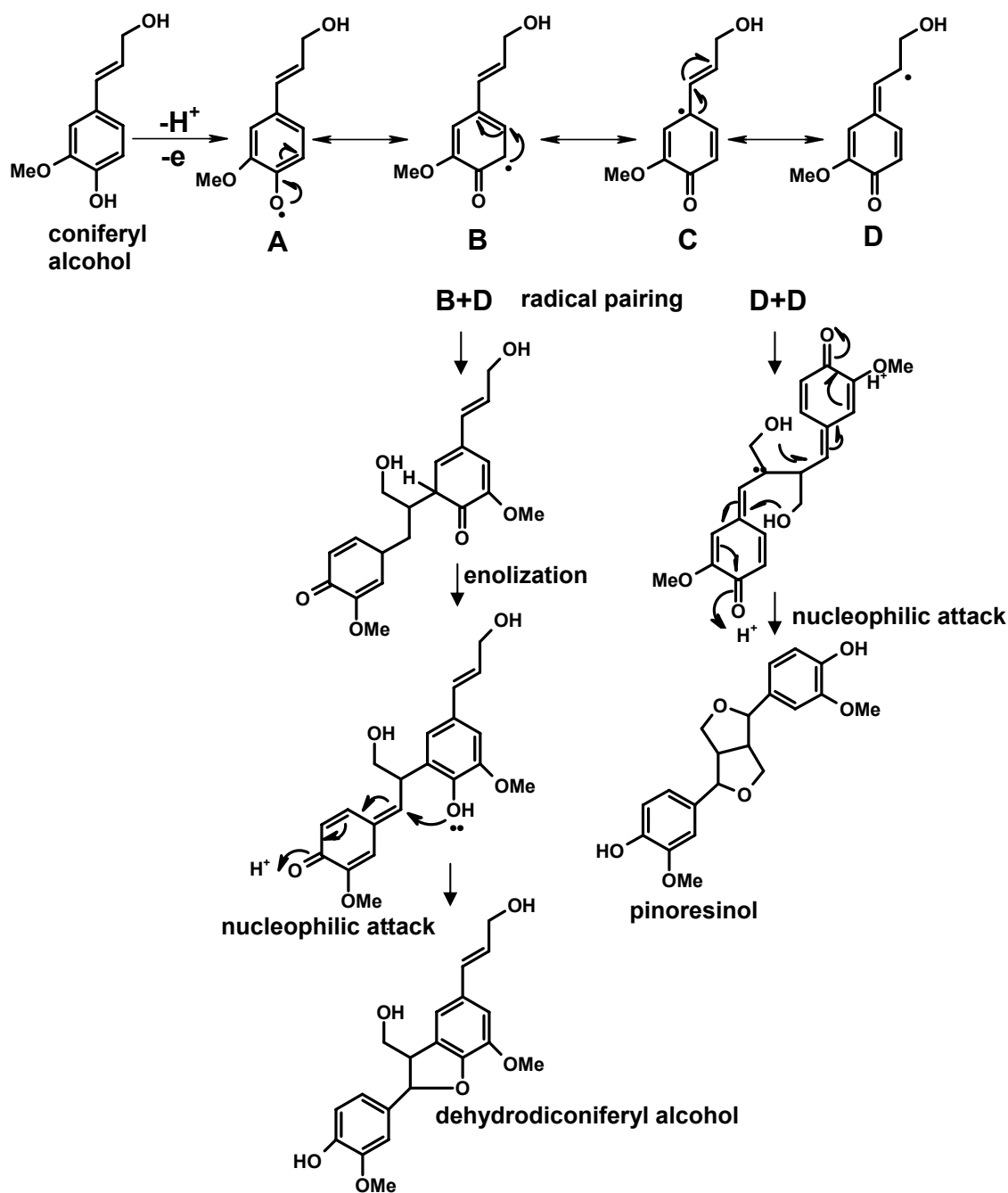
Fig. 1.9. Nonspecific (racemic) coupling products of coniferyl alcohol radicals, following one electron oxidation of coniferyl alcohol (modified according to Dewick 2002).

Both proteins have been solubilized from cell wall enriched homogenates and purified. The last purification step yielded four fractions: fraction I did not have significant dimerization activity, whereas fraction III catalyzed unspecific coupling of *E*-coniferyl alcohol to (±)-Pino and other dimers. Combination of the two fractions resulted in the original "(+)-PS" activity with full regio- and stereospecificity. An oxidase, most probably a plant laccase generating

free radicals of *E*-coniferyl alcohol, was found in fraction III. Fraction I contained a protein with an approximate MW of 78 kDa, possibly a trimer of 27 kDa subunits. The protein has no catalytically active center. Since this protein determines the region- and stereospecificity without having any catalytic properties, it was named "dirigent protein" from the latin *dirigere*: to guide or to align. It was shown that chemical formation of coniferyl alcohol radicals, with the help of flavin mononucleotide (FMN), flavin adenine dinucleotide (FAD) or ammonium peroxidisulfate, was sufficient to form (+)-Pino in presence, but not in the absence, of the "dirigent protein". Therefore, it was proposed that the phenoxy radicals formed by the oxidase (fraction III) are captured by the "dirigent protein", leading to a stereospecific and regiospecific coupling of the monomers. (+)-PS was strictly specific for coniferyl alcohol; 4-coumaroyl and sinapoyl alcohols were not accepted (which gave racemic products due to non-specific coupling). Formation of (+)-Pino in *Forsythia*, therefore, is made possible by concomitant of two proteins (Fig. 1.10). The corresponding gene encoding the dirigent protein was cloned and found to encode a protein of *circa* 18 kDa, which differed from the native *Forsythia* protein of ~26 kDa due to post-translational glycosylation of the native protein (Gang et al. 1999a).

1.6.2. Pinoresinol-lariciresinol reductase (PLR)

One of the first documented examples in the nature of benzylic ether reduction in plant systems and the specificity of the reductase step(s) in terms of enantiospecificity and diastereomic preferences was examined when the (+)- and (-)- enantiomers of Pino were individually incubated with the *Forsythia intermedia* cell-free extracts (Katayama et al. 1993). In the presence of NADPH, preferential conversion was observed into both (+)-Lari and (-)-Seco, respectively. Incubation with (±)-Lari also established that only the (+)-antipode was converted into (-)-Seco. This proves the existence of a bifunctional enantiospecific pinoresinol-lariciresinol reductase (PLR) in the soluble protein extract of *F. intermedia*. Isolation of a cDNA encoding a PLR from *F. intermedia* (*PLR-Fi1*) and its heterologous expression showed the same enantiospecificity as for the crude extracts. The polypeptide had a 312 amino acids and a calculated MW of 34.9 kDa. The presence of cDNAs corresponding to two stereochemically distinct classes of *PLRs* in a single plant species western red cedar (*Thuja plicata*), has been demonstrated by Fujita et al. (1999).
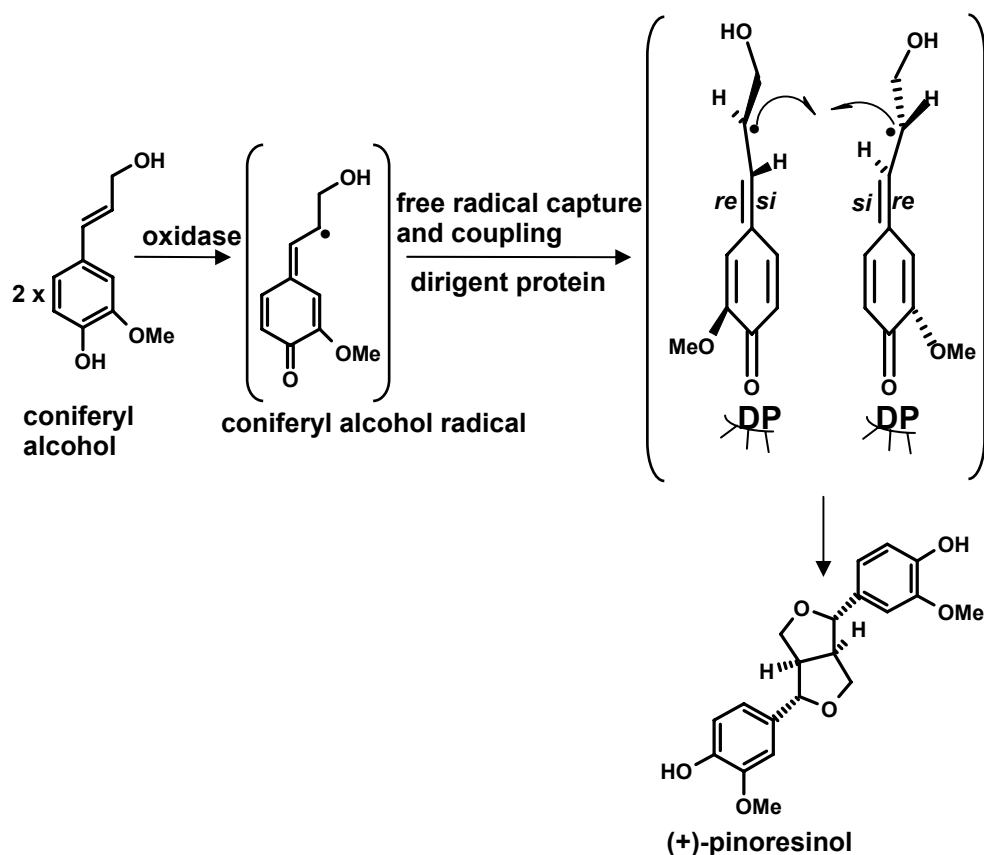
Fig. 1.10. The formatation of dirigent protein (DP) mediated (stereoselective) coupling products of coniferyl alcohol radicals, following one electron oxidation of coniferyl alcohol (adopted from Davin and Lewis 2005).

Four cDNAs were grouped two by two in two distinct classes of *PLRs*. In the first class *PLR-Tp1* had the highest similarities to *PLR-Tp3* and in the second class *PLR-Tp2* had the highest similarities to *PLR-Tp4*. Heterologously expressed PLR-Tp1 reduces (-)-Pino into (+)-Seco. On the other hand consumption of (±)-Pino with recombinant PLR-Tp2 resulted in the accumulation of both (+) and (-)-Lari, in which only the (+)-Lari was converted into (-)-Seco. However, the (-)-Lari was not further transformed into (+)-Seco. Thus *T. plicata* PLRs can reduce both (+)- and (-)- enantiomers of Pino, but they are highly enantiospecific toward Lari. As both classes of Tp-PLRs, were isolated from mRNA from stems of a single tree; it is therefore, probable that both reductase classes are involved in parallel lignan biosynthetic pathways in *T. plicata*. In *Arctium lappa*, enzyme preparations of petioles catalyze the formation of mainly the (+)-enantiomers of Pino, Lari and Seco. On the contrary extracts from seeds catalyze the formation of an enantiomeric excess of lignans with opposite optical

rotation. This observation can be accounted for by postulating that *A. lappa* has PLR isoforms with different enantioselectivity and expression. However no *PLR* cDNAs to prove this assumption were cloned (Suzuki et al. 2002).

L. usitatissimum seeds accumulate secoisolariciresinol diglucoside (SDG) to a very high percentage (2%-4% by dry weight). There are two distinct diastereomers of SDG present in flaxseed; the dominant form (~99%) is (+)-Seco. (Ford et al. 2001; Sicilia et al. 2003). Experiments with radiolabeled phenylalanine revealed that (-)-Pino is converted to (+)-Seco in flaxseed (Ford et al. 2001). The corresponding *PLR* cDNA (*PLR-Lu1*) encoding this conversion was isolated and expressed heterologously by von Heimendahl et al. (2005).

On the basis of the SDG diastereomer, there also appears to be another pathway to SDG, with the minor road being that to (-)-Seco. Recently, six lignans of the dibenzylbutyrolactone type were identified in the aerial parts of flowering *L. usitatissimum* plants (Schmidt et al. 2006); all were found to be laevorotatory and possess the absolute stereochemistry (8*R*, 8'*R*), corresponding to (-)-bursehernin, (-)-yatein, (-)-hinokinin, (-)-matairesinol dimethyl ether, (-)-thujaplicatin trimethyl ether and (-)-*E*-anhydropodorhizol. This finding gives further hints for the demand of a second PLR with opposite enantiospecificity to the *PLR-Lu1* In support of this contention we have proposed two parallel biosynthetic pathways for Seco biosynthesis in *L. usitatissimum* (Fig. 1.11).

Based on the high sequence similarity and reaction mechanism PLRs, phenylcoumaran benzylic ether reductases (PCBERs) and isoflavone reductases (IFRs) are the first three members of NADPH-dependent reductase enzymes forming the PIP reductase family (Fujita et al. 1999, Koeduka et al. 2006 PNAS) (Fig. 1.12). DDC and its 7'-8' (allylic bond)-reduced derivative dihydrodehydrodiconiferyl alcohol (DDDC), appear to be ubiquitous throughout the plant kingdom, being found in a wide array of plant families, such as the Asteraceae, Pinaceae and Urticaceae (Kraus and Spiteller 1997) suggesting the involvement of a universal defense system. The 8-5' linked lignans can also co-occur in many species with their phenylcoumaran benzylic ether reduced counterparts like isodihydrodehydrodiconiferyl alcohol (IDDDC) and tetrahydrodehydrodiconiferyl alcohol (TDDC). It can be considered that DDC and DDDC might undergo comparable reductive transformations, analogous to that catalyzed by PLRs. The cDNA encoding PCBER were cloned from the gymnosperm *Pinus taeda* and angiosperm *Populus trichocarpa*. The recombinant PCBER converted DDC and DDDC into the benzylic ether reduced lignans IDDDC and TDDC, respectively. Kinetic

studies have shown that the enzyme has higher affinity toward DDC rather than DDDC (Gang et al. 1999b), suggesting that the biosynthesis of TDDC may involve initial formation of the benzylic ether reduced intermediate prior to allylic bond reduction. PCBERs are regiospecific but not enantiospecific toward their substrates. IFRs catalyze the reduction of α-ß unsaturated ketones during isoflavonoid formation (Fig. 1.12).
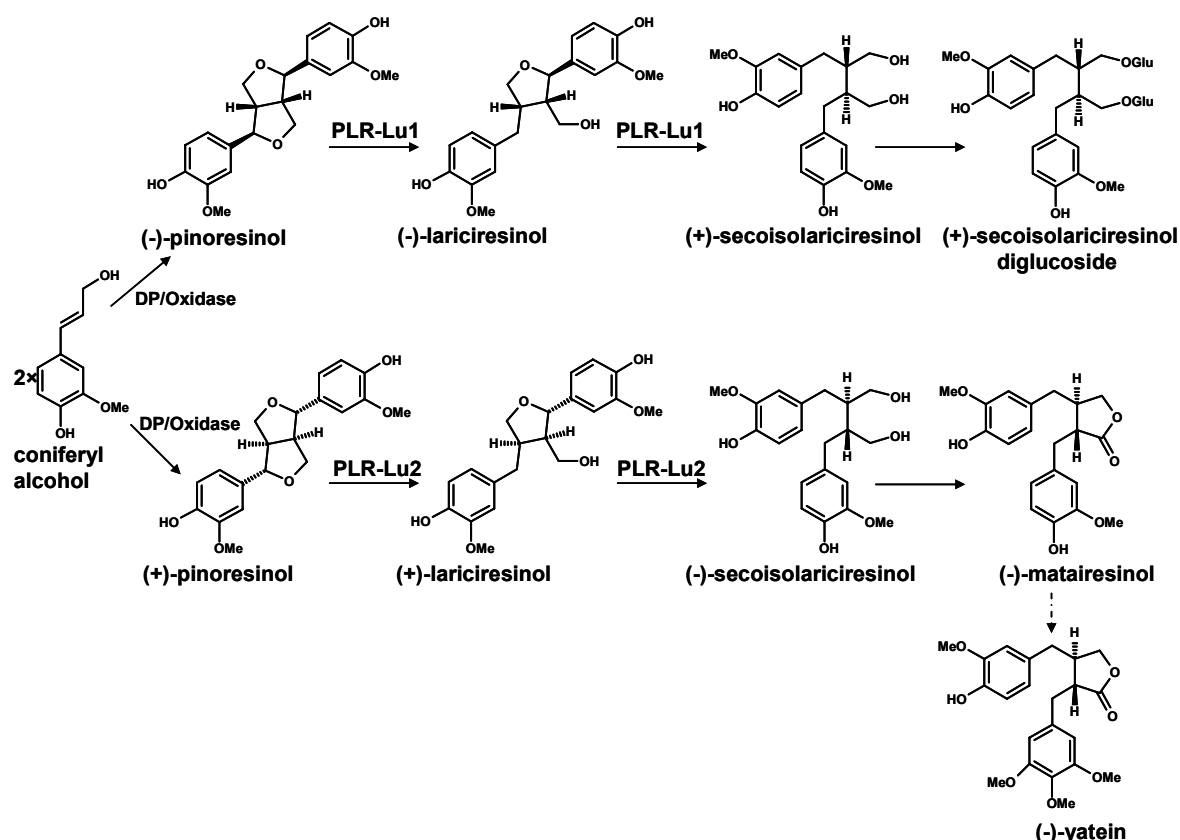
Fig. 1.11. Biosynthetic pathways of (+)- and (-)-secoisolariciresinol in *L. usitatissimum* respectively. DP/Oxidase: dirigent protein/oxidase complex; PLR: pinoresinol-lariciresinol reductase.

1.6.2.1. Mechanism of hydride transfer

The hydride transfer by PLR is highly stereospecific. By partially purified PLR from *F. intermedia* Chu et al. (1993) and Dinkova-Kostova et al. (1996) have shown that (+)-PLR abstract the *4pro-R* hydrogen of NADPH in such a manner that the incoming hydride took up the *pro-R* position at C-7' in Lari and at C-7/C-7' in Seco, respectively, the overall of each is
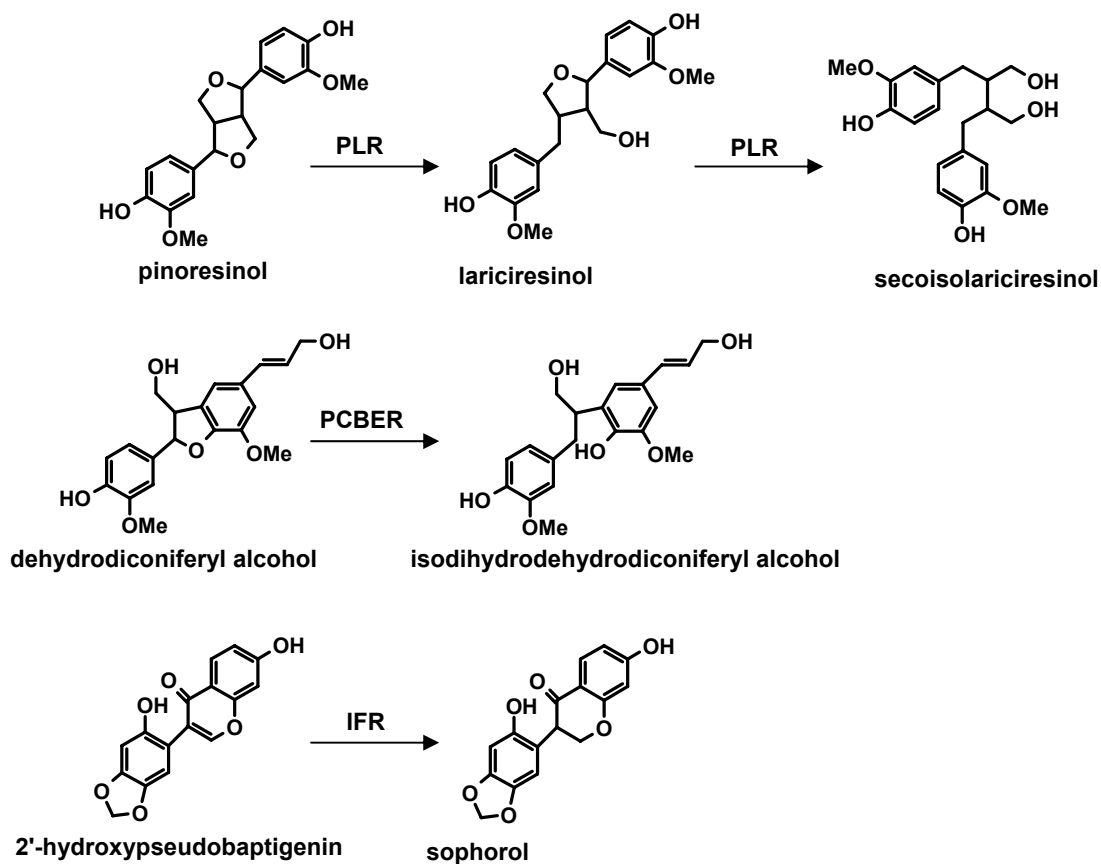
Fig. 1.12. Reactions catalyzed by PIP reductases. PLR: pinoresinol-lariciresinol reductase; PCBER: phenylcoumaran benzylic ether reductases; IFR: Isoflavone reductases.
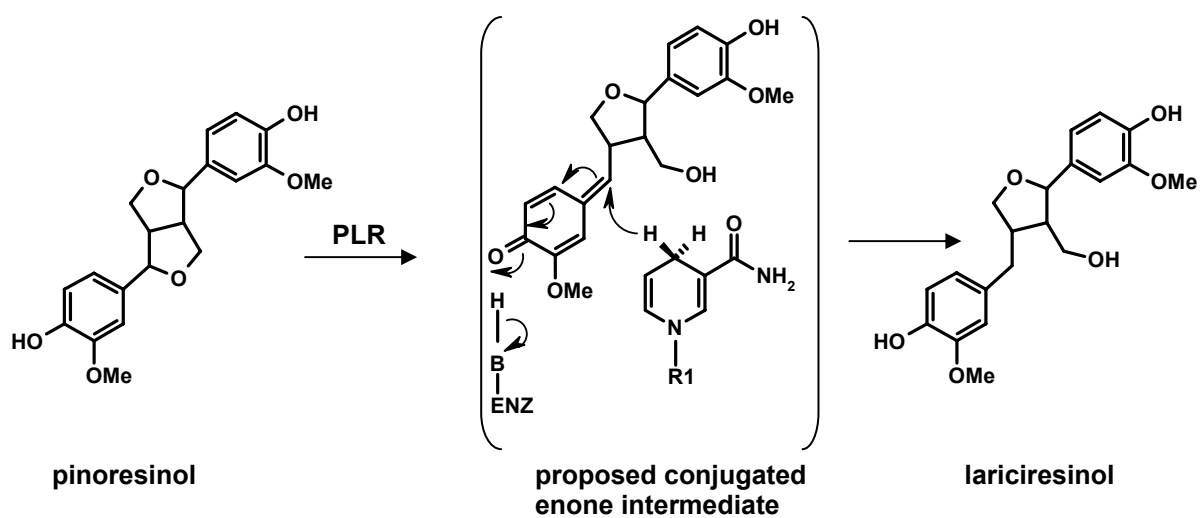
Fig. 1.13. Mechanism of hydride transfer by PLR. (Fujita et al. 1999).

an inversion of configuration at these positions. Therefore these findings, rule out the possibility of a S_{N1} mechanism involving a planar quinine methide transition state with random hydride delivery from either side of the molecule (Fig. 1.13).

1.7. Plant cell cultures

Plant in vitro cultivation has several advantages over collecting plants from wild or cultivating them on fields (Alfermann et al. 2003). Metabolites like lignans can be produced under controlled and reproducible conditions, independent of geographical and climate factors. Usually, it is not necessary to use herbicides or insecticides. Especially suspension cultures can show high growth rates combined with high accumulation of the desired metabolite in short time. There are a few examples where the in vitro cultivation of plants led to the commercialization of the process for the production of red pigment shikonin in cell cutures of *Lithospermum erythrorhizon* which was followed by the company Mitsui Petrochemical Inc. Ltd. The cytotoxic paclitaxel (Taxol®) which is used in anticancer therapy is produced by the Phyton Ges. für Biotechnik mbH in cell cultures of *Taxus* species. On the other hand, plant cell cultures are an ideal system to study various aspects of secondary product formation, including the molecular biology and enzymology of biosynthesis. They are a "pot of gold", as expressed by Zenk (1991). E.g. all enzymes for the production of rosmarinic acid were found in cell cultures of *Coleus blumei* (Petersen et al. 1995). In some cases the isolation of the enzymes has allowed the cloning of the corresponding cDNAs or genes (Kutchan et al. 1991 & 1995).

Cell cultures of *Linum* species are a good source of different types of lignans. Podophyllotoxin and 6-methoxypodophyllotoxin were reported in the cell cultures of *L. album* and *L. flavum*. The arylnaphthalene type of lignans (e.g Jus B) was reported in the cell cultures of *L. austriacum*. Fuss (2003) has reviewed the accumulation of different lignans in cell cultures of *Linum* species. Despite the plant material, cell cultures are in access during the whole year which makes them a valuable source for isolation of genes an characterization of enzymes.

1.8. Plant transformation by *Agrobacterium rhizogenes*

Various species of bacteria are capable of transferring genes to higher plant species (Chung et al. 2006). Among them, *Agrobacterium tumefaciens* is most widely studied. The soil bacteria *A. rhizogenes* infects the plant tissues and leads to the formation of adventitious roots called "hairy roots". Fast and hormone independent growth and high genetic stability make hairy root cultures superior in comparison to cell cultures. Hairy roots are known to produce the same or even higher amounts of the metabolites found in normal roots. Integration of new genes into hairy roots has opened another way for metabolic engineering (Guillon et al. 2006) which is based on the ability to transform plant cells with the root-inducing (Ri) plasmid of *A. rhizogenes*. Two important regions in the Ri plasmid are essential for transformation by transferred DNA (T-DNA). These are the T-DNA itself as a mobile element and the virulence region (*vir*) (Klee et al. 1987). The T-DNA is flanked by 25 bp directly repeated sequences. Any DNA between these sequences will be transferred to the plant cell. The Ri plasmids are grouped into two main classes according to the opines synthesized by hairy roots: agropine-type (e.g., A4, 15834, LBA9402, 1855) and mannopine type (e.g., 8196, TR7, TR101) strains (Sevón and Oksman-Caldentey 2002). The T-DNA of the agropine-type Ri-plasmid consists of two separate T-DNA regions the TL-DNA and TR-DNA. The genes encoding auxin (*tms1* and *tms2*) have been localized on the TR-DNA of the agropin type Ri plasmid. The mannopine type Ri-plasmids contain only one T-DNA that shares considerable DNA sequence homology with the TL-DNA of the agropine-type plasmids. The TL-DNA contains four genetic loci, *rol*A, *rol*B, *rol*C and *rol*D, the first three of which mainly contribute to the root initiation and maintenance. A plant cell becomes susceptible to *Agrobacterium* when it is wounded. The wounded cells release phenolic compounds such as acetosyringone, that activate the *vir* region of the bacterial plasmid and results in the formation of a T-strand as a single strand copy of T-DNA. Control of *vir* gene expression is mediated by Vir A and Vir G proteins. Vir A detects the released phenolic compounds, resulting in autophosphorylation, finally activate *vir* gene transcription. Two other proteins (Vir D1 and Vir D2) recognize the 25 bp border sequence and produce single strand endonucleolytic cleavage in the bottom strand of each border. After nicking the Vir D2 remains tightly associated with the 5' end of the T-strand. The Vir E2 protein completely coates the T-strand, to prevent T-strand nucleolytic degradation before integration.

The T-strand with Vir D2 and Vir E2 makes a T complex by passing through the bactereial and plant membranes and finally will integrate into the plant chromosome (Zupan and Zambryski 1995).

Binary vectors contain origins of replication from a broad host-range plasmid. Using the binary vector strategy a plasmid containing the left and right borders of T-DNA -but not the virulence region- is modified in vitro to carry the gene to be transferred together with a selectable marker. The modified plasmid DNA is transferred into *E. coli* and afterwards to an *Agrobacterium* strain containing a helper plasmid that provides the *vir* functions. During infection of plants the activated *vir* functions recognizes the left border sequence of the modified plasmid and transfers all DNA between left and right borders to change a plant chromosome (Hellens et al. 2000).

1.9. RNA interference (RNAi)

RNAi would be a useful approach to demonstrate if our cloned gene is involved in the biosynthetic pathway of the corresponding metabolite. Most of the biosynthetic pathways for secondary plant metabolites are still partially hypothetical. Reduction of the levels of a special mRNA decreases the accumulation of the corresponding compound or group of compounds which helps on the elucidation of the biosynthetic pathways. Alteration of the expression level of our cloned gene can clarify its influence on the biosynthesis of arylnaphthalene lignans. RNA silencing might have arisen as an ancient RNA surveillance system that is conserved among eukaryotes, and that acts as a natural defense mechanism against invasive nucleic acids, including viruses, transposons and perhaps other highly repetitive genomic sequences. RNA silencing also plays a pivotal role in plant and animal development by providing an elegant system of gene control that can occur through RNA degradation, translational inhibition or chromatin modification (Wang and Metzlaff 2005).

The first report on a RNA interference (RNAi) type of phenomenon was reported in 1990 (Napoli et al. 1990; van der Krol et al. 1990; Smith et al; 1990). It was described that the introduction of transcribed sense transgenes could down regulate the expression of homologous endogenous genes, named co-suppression. Since in this type of silencing the transcription is still active and the system is targeted after transcription level, the phenomenon renamed to post transcriptional gene silencing (PTGS) (Fagard and Vaucheret 2000).
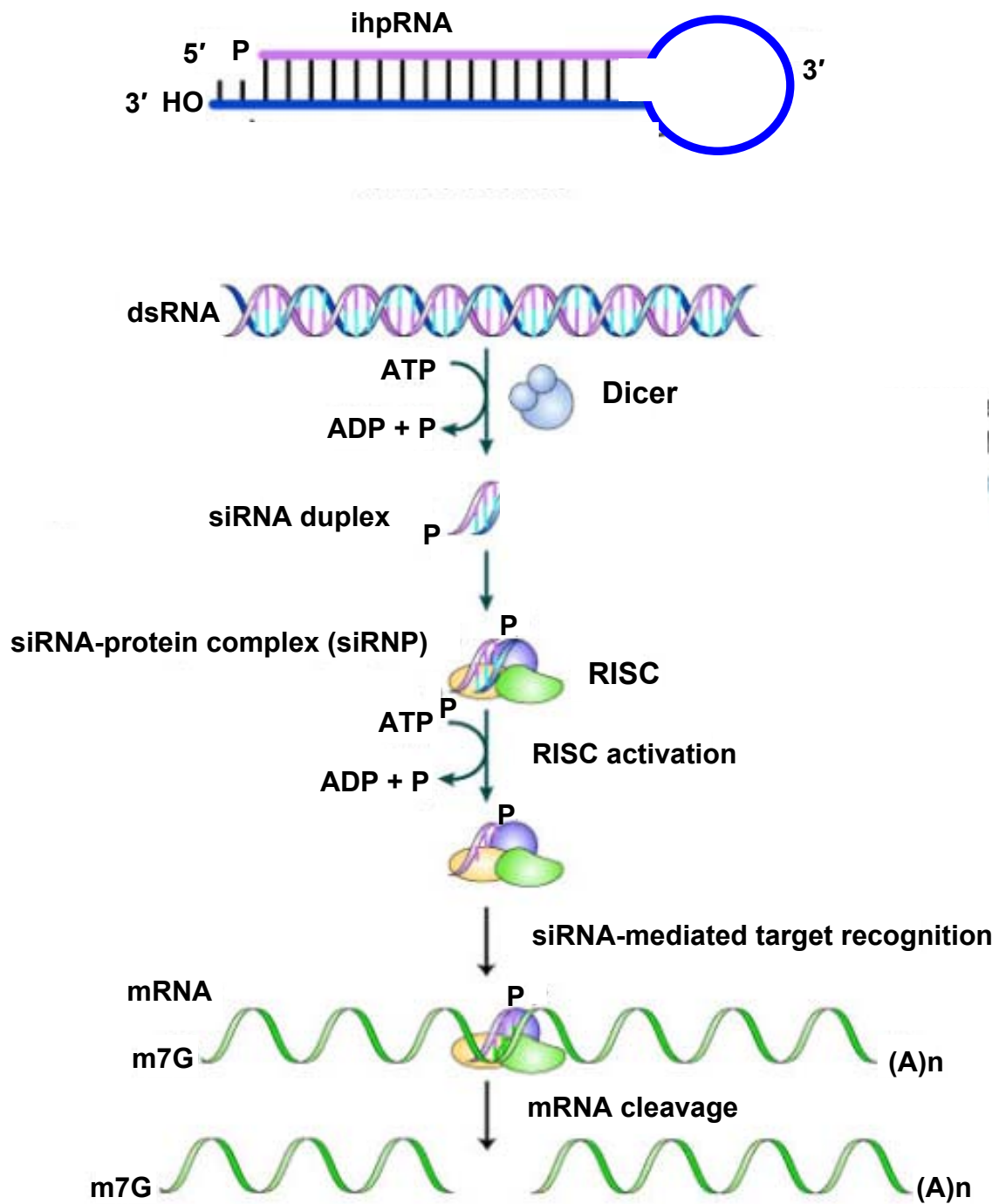
Fig. 1.14. RNAi induced with ihpRNA.

(modified according to: http://www.ocf.berkeley.edu/~edy/genomics/functional.html)

The term RNAi was first coined when it was observed that both sense and antisense RNA were able to silence gene expression in the nematode *Caenorhabditis elegans* (Fire et al. 1998). It was explained that the strongest trigger for gene silencing was the double stranded RNA (dsRNA). DsRNA triggers the specific degradation of homolgous RNAs only within the region of identity with the dsRNA (Elbashir et al. 2001).

1.9.1. Mechanism of RNAi

The RNAi pathway is initiated by recognition of dsRNA by a processing enzyme "Dicer" in the cytoplasm (Fig. 1.14). Dicer is a ribonuclease in the RNase III family that cleaves dsRNA into short double-stranded RNA fragments called small interfering RNA (siRNA) which are about 20-25 nucleotids long, usually with a two base overhang on the 3' end (Hamilton and Baulcombe 1999; Zamore et al. 2000). One of the two strands of each fragment, known as the guide strand, is then incorporated into a complex named as the RNA-induced silencing complex (RISC). The catalytically active components of the RISC complex are endonucleases called argonate proteins, which cleave the target mRNA strand complementary to the bound siRNA (Bernstein et al. 2001). The other anti-guide strand or passenger strand is degraded during RISC activation. Degrading the mRNA results in substantially decreased levels of protein translation and effective turning off the gene.

RNAi can be induced in plants by expressing artificial microRNAs (amiRNA), long hairpin RNAs, modified viral RNAs or by directly inducing synthetic small interfering RNAs (siRNAs) (Small 2007). An amenable approach of silencing has been to clone both sense and antisense sequences, which are separated by an intron, under the same promoter. Upon transcription, these sequences form a hairpin RNA (hpRNA) molecule that triggers gene silencing (Smith et al. 2000). The silencing efficiency of hpRNA and antisense RNA has been compared in a range of plant species: the hp strategy generally increases gene silencing by 90-100% (Wesley et al. 2001) and is now the most widely used system for silencing genes in plants (Mansoor et al. 2006). Hairpin RNAs are predominantly processed by the enzyme Dicer-like 4 (DCL4). The produced siRNAs are loaded into the RNAi silencing complex of which AGO1 is a major component. Gene discovery and metabolic engineering of plants are two important usages of RNAi in plants. On the basis of the plant genomes sequenced so far there is no true experimental evidence of function for the majority of sequenced genes.

RNAi offers an easy, cost effective approach to generate "phenocopies" of genetic mutants (Small 2007). Mansoor et al. (2006) have reviewed the engineering of novel traits in plants through RNAi.

1.10. Cytochrome P450 monooxygenases

Based on our suggested biosynthetic pathway leading to the arylnaphthalene lignans Diph and its glycosides (Fig. 1.8) the detection of the enzyme justicidin B 7-hydroxylase (JusB7H) which catalyzes the reaction from JusB to Diph in *L. perenne* H suspension cultures confirms one of the last steps of our hypothetical biosynthetic pathway leading to Diph glycosides. We describe the properties of the JusB7H as a cytochrome P450-dependent monooxygenase.

Cytochrome P450s are a diverse superfamily of heme-thiolate proteins, named for the absorption band at 450 nm of their carbon monoxide bound form and P for pigment (Omura and Sato 1964). Usually they are a part of multicomponent electron chains in enzymatic reactions like hydroxylations, methylen dioxybridge and ring closure reactions, epoxidations, N-,S- and O-dealkylation reactions, N-oxidations, sulfoxidations, dehydrogenations and deamination catalysis. Canonical P450s use electrons from NAD(P)H to catalyze the activation of molecular oxygen, leading to attack of a plethora of substances. Depending on how electrons from NAD(P)H are delivered to the catalytic site of P450s, they can be divided into four classes (Werck-Reichhart and Feyereisen 2000). Class I are the proteins that the electrons of NAD(P)H are transferred through an FAD-containing reductase and an iron sulfur redoxin (most bacterial P450s and P450s found in mitochondria of eukaryotes). Class II proteins are microsomal and require NADPH:cytochrome P450 reductase (FAD/FMN containing P450 reductase) as the only electron transfer partner (found in the endoplasmic reticulum of eukaryotes). Class III enzymes are self-sufficient and require no electron donor, while class IV receive electrons directly from NAD(P)H. Fig. 1.15 shows a class II CYP450 in an animal system where different CYP450s are serviced by the same cytochrome reductases. Sequence identity of P450 proteins is often extremely low and may be less than 20%. Highest structural conservation is found in the core of the protein around the heme and reflects a common mechanism of electron and proton transfer and oxygen activation. The heme binding loop containing the most characteristic P450 consensus sequence (Phe-X-X-Gly-X-Arg-X-Cys-X-Gly), located on the proximal face of the heme.
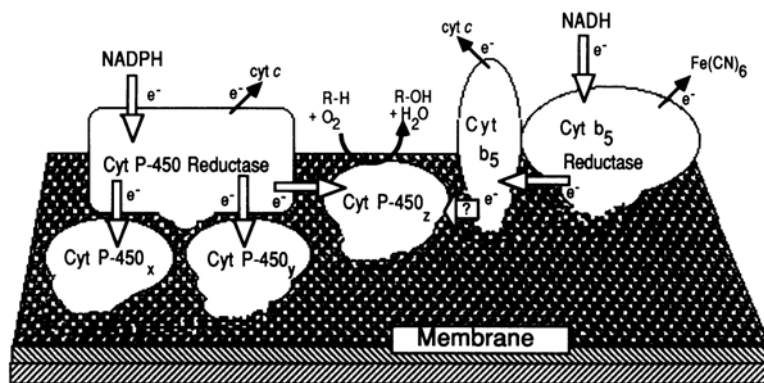
Fig. 1.15. Protein components of the CYP450 enzyme system in the cytosolic face of the endoplasmic reticulum. Electrons flow from cytosolic NADPH through NADPH: CYP450 reductase. In some cases Cyt *b5*, which receives electrons from NADH:Cyt *b5* reductase, may donate electrons to a CYP450. There are many different CYP450s indicated as x, y and z. Some CYP450s are specific hydroxylases as shown (R-H $\longrightarrow$ ROH). In vitro Cyt *c* or ferricyanide ($Fe(CN)_6$) can accept electrons as indicated (from Donaldson and Luster 1991).

The cysteine is conserved and serves as fifth ligand to the heme iron. The Glu-X-X-Arg motife, also on the proximal side of the heme which probably need to stabilize the core structure is absolutely conserved. Finally, the sequence considered as P450 signature (Ala/Gly-Gly-X-Asp/Glu-Thr-Thr/Ser), which corresponds to the proton transfer groove on the distal side of the heme (Graham and Peterson 1999; Werck-Reichhart and Feyereisen 2000). Most eukaryotic P450s are associated with microsomal membranes, and very frequently have a cluster of prolins ([Pro]-Pro-Gly-Pro-X-[Gly/Pro]-X-Pro) that form a hinge and is required for optimal rotation of the enzyme with regard to the membrane. On the basis of overall identity and sequence conservation in these domains, phylogenetic analysis of plant P450s has led to the identification of "group A" and "non-group A" proteins. The non-group A P450s are a disparate set of families that cluster closer to animal and fungal enzymes. Group A which mostly involved in the biosynthesis of natural products appear to have evolved since the divergence of plants from the common ancestor they share with animal and fungi (Chapple 1998).

1.10.1. The reaction mechanism of cytochrome P450s

In the most common CYP450 oxygenase rections two electrons from CYP450 are donated to O_2, then one oxygen atom combines (hydroxylates) with the substrate and the second oxygen atom is used to form a molecule of water:

$$NADPH + H + O_2 + R\text{-}H \longrightarrow NADP + H_2O + ROH$$
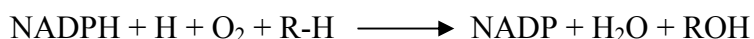
The active center for catalysis is the iron-protoporphyrin IX (heme) with the thiolate of the conserved cysteine residue as fifth ligand. Resting P450 is in the ferric form and partially six-coordinated with a molecule of solvent.

The well characterized portion of the catalytic sequence involves four steps, which are indicated in Fig. 1.16. The first step is substrate binding, with displacement of the sixth ligand solvent inducing a shift in the maximum of absorbance, spin state and redox potential of the heme protein system; the second is one-electron reduction of the complex to a ferrous state, driven by the increase in the redox potential which results from the previous step; the third is binding of molecular oxygen to give a superoxide complex; and the fourth is a second reduction step leading to an "activated oxygen species". The exact nature of the very short-lived activated oxygen species that carries on substrate attack long remained uncertain, but the most recent data, from crystallography and mechanistic probes (Schlichting et al. 2000) strongly suggest that it is actually a mixture of two electrophilic oxidants ([B]⁻ and [C] in Fig. 1.16.). Both iron-peroxo [B]⁻ and iron-oxo [C] complexes are formed by protonation of the two-electrons-reduced dioxygen, a process that is allowed when a water channel forms in the groove of the I-helix upon binding of O_2. The oxo (oxyferryl) species, resulting from the cleavage of the O-O bond - one atom of oxygen leaves with the two electrons and two protons as water - is apparently the most abundant. The iron-hydroperoxo species inserts the elements of OH^+, producing protonated alcohols that can give cationic rearrangement products. The iron-oxo species inserts an oxygen atom.

Carbon monoxide can bind ferrous P450 instead of dioxygen, inducing a shift of the maximum of absorbance of the heme (called the Soret peak) to 450 nm (Omura and Sato 1964). CO is bound with high affinity and prevents binding and activation of O_2. The result is an inhibition of P450 activity. CO binding and inhibition can be reversed by light, with maximal efficiency at 450 nm. Other ligands, substrates and inhibitors, induce absorbance shifts of the Soret in P450 enzymes.

Differential spectrophotometry is thus widely used to monitor binding of such ligands (Jefcoate 1978). Substrates that displace the six-coordinated solvent in the resting P450 usually induce a shift to the blue (420 to 390 nm) which reflects a low- to high-spin transition of the iron. Inhibitors with an sp_2 hybridized nitrogen (nitrogens in heterocycles such as azoles, pyridines, or pyrimidines) replace the sixth ligand for coordination with iron and induce a shift to the red (400 to 430 nm).
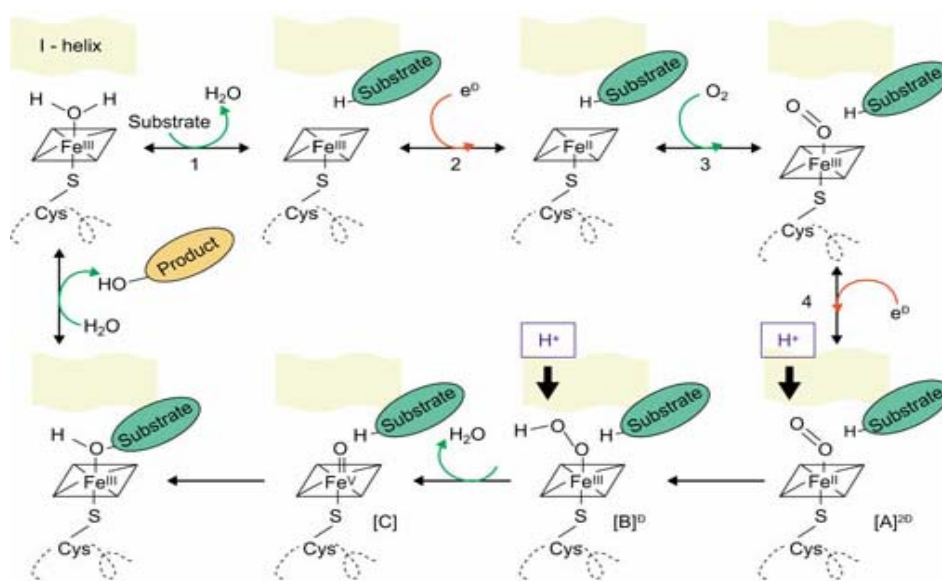
Fig. 1.16. Catalytic mechanism of P450 enzymes (adopted from Werck-Reichhart and Feyereisen 2000).

1.11. Scope of the work

Seeds of *L. usitatissimum* as a plant species of the section *Linum* (Linaceae) contain almost 99% (+)- and 1% (-)-Seco. The *PLR* cDNA which was responsible for the formation of (+)-Seco was cloned previously. In the aerial parts of *L.usitatissimum* lignans of the dibenzylbutyrolactone type were identified (Schmidt et al. 2006); all were found to be (-) isoforms. The question is that whether consequent reductive transformations to (+)- and (-)-Seco are performed by a nonspecific PLR enzyme or via at least two PLR isoforms with different enantiospecificity.

We have found that *L. perenne* H, as a typic example of the section *Linum*, accumulate arylnaphthalene lignan types like Jus B and Diph without any chiral center. The question was if the biosynthetic pathway of arylnaphthalene lignans starts with PLR. Cloning and aspects of the enantiospecificity of the corresponding PLR is described in this work. This suggests but does not prove that the PLR is involved in Jus B biosynthesis. Therefore, we intended to down regulate the corresponding cloned gene by RNAi to see the influence on Jus B biosynthesis.

Regarding the lignans which were found in *L. perenne* we have proposed a biosynthetic pathway for arylnaphthalene lignan biosynthesis. Herein we describe the detection of the enzyme justicidin B 7-hydroxylase (JusB7H) which catalyzes the reaction from JusB to Diph in *L. perenne* H suspension cultures confirming the late steps of our hypothetical biosynthetic pathway leading to Diph. We describe the properties of the JusB7H, a cytochrome P450-dependent monooxygenase.

2. Materials and Methods

2.1. Materials

2.1.1. Oligonucleotides

Primers were synthesized by MWG-Biotech (Martinsried) or Operon Biotechnologies GmBH (Köln) companies*.

PLRdegF1: 5′-GGNACIGGITWYATNGGIAARMG-3′

LPLR4F: 5′-CCITCIGARTTYGGIATGGAYCC-3′

LPLR6R: 5′-GTRTAYTTIACYTCIGGGTA-3′

LuPLR-GSP1-5′: 5′-GCAATTGGCGGAAATG-3′

LuPLR-GSP2-5′: 5′-GCTCTAGAGGATCCATCTTGTCGTCGAACGTCACTC-3′

LuPLR-GSP3-5′: 5′-GCTCTAGAGGATCCCGGCTTCTTTGATGGCATCAAC-3′

LuPLR-GSP1-3′: 5′-GCTCTAGAGGATCCCAATTGCTTCGCCGGTTACTTC-3′

LuPLR-GSP2-3′: 5′-GCTCTAGAGGATCCAGGACGATATTGCGCGATACAC-3′

LUBPLRORF-F: 5′-CCTATTCCATATGGGATCCCTCCCGGCCATC-3′

LUBPLRORF-R: 5′-CCGCTCGAGTTAAACATATCGTTTCATATACTC-3′

SemiLu1-F: 5'-AAGAAACAGGGCGCCCAC-3'

SemiLu1-R: 5'-GTCTTGTGAAGAAAGCTCAG-3'

SemiLu2-F: 5'-CGTTTAAAAAGGCCGGTGCAAG-3'

SemiLu2-R: 5'-CTCTTCCACGGACAGGGTTG-3'

LpPLR-GSP1-5′: 5′-CTCCATAGATGATGACC-3′

LpPLR-GSP2-5′: 5′-GCTCTAGAGGATCCAGCTGCGAAAGATTGCCGACGAAG-3′

LpPLR-AAP: 5′-GGAATTCGAGCTCGGTACCACGGGIIGGGIIGGGIIG-3′

LpPLR-GSP3-5′: 5′-GCTCTAGAGGATCCTGAACCTCTTAACATTCCCCGCCTCC-3′

LpPLR-AUAP: 5′-CCGGAATTCGAGCTCGGTACCAC-3′

LpPLR-AAP-3′: 5′-GGAATTCGAGCTCGGTACCACTTTTTTTTTTTTTTTTT-3′

LpPLR-GSP1-3′: 5′-GCTCTAGAGGATCCACTTCG TCGGCAATCTTTCGCAGCTC-3′

LpPLR-GSP2-3′: 5′-GCTCTAGAGGATCC TAACCCCGCCTTCCGATAAGGTCATC-3′

LpPLRORF-F: 5′-GGAATTCCATATGAAGCCGTGTAGTGTGCTCG-3′

LpPLRORF-R: 5′-GGGGATCCTCAAAGGTAGATCTTCAAGTAATCATGG-3′

LPPLRhanF: 5′-CCTCTAGACTCGAGACATCGAGAAGCTCCAGCTCTTGC-3′

LPPLRhanR: 5′-CCATCGATGGTACCCAAACGGCCACCAACTCTCTTTGAC-3′

35 S: 5′-GTAAGGGATGACGCACAATCC-3′

PKFactin5′: 5′-ATGGARAARATNTGGCATC-3′

PKFactin3′: 5′-ACATCTGMTGGAANGTGC-3′

ROLCFOR: 5'-ATGGCTGAAGACGACCTGTGTT-3'

ROLCREV: 5'-TTAGCCGATTGCAAACTTGCAC-3'

VIRCFOR: 5'-ATCATTTGTAGCGACT-3'

VIRCREV: 5'-AGCTCAAACCTGCTTC-3'

* I = inosine, M = A+C, N = A+C+T+G, R = A+G, Y = C+T, W = A+T

2.1.2. Enzymes for molecular biology

Enzyme	Company
Apa I (10 U/µl)	MBI Fermentas, St. Leon-Roth
BamH I (10 U/µl)	MBI Fermentas, St. Leon-Roth
Bgl II (10 U/µl)	MBI Fermentas, St. Leon-Roth
Cla I (10 U/µl)	MBI Fermentas, St. Leon-Roth
EcoR I (10 U/µl)	MBI Fermentas, St. Leon-Roth
EcoR V (10 U/µl)	Roche, Mannheim
HiFi Taq-Polymerase	Roche, Mannheim
Hind III (10 U/µl)	MBI Fermentas, St. Leon-Roth
Kpn I (10 U/µl)	MBI Fermentas, St. Leon-Roth
Lysozyme (from chicken egg)	Fluka Chemie GmbH, Buchs, Swizerland

Enzyme	Company
Nde I (10 U/µl)	MBI Fermentas, St. Leon-Roth
Not I (10 U/µl)	MBI Fermentas, St. Leon-Roth
RNase A	MBI Fermentas, St. Leon-Roth
RNasin (RNAse inhibitor)	MBI Fermentas, St. Leon-Roth
T4 DNA ligase (1 U/µl)	Invitrogen, LIFE TECHNOLOGIES
Xba I (10 U/µl)	MBI Fermentas, St. Leon-Roth
Xho I (10 U/µl)	MBI Fermentas, St. Leon-Roth

2.1.3. Vectors

pGEM®-T	Promega, Madison, WI, USA
pET-15b	Novagen, Darmstadt,
pHANNIBAL	Wesley et al. 2001
pART27	Gleave, 1992

2.1.4. Bacterial strains

E. coli (DH5α):   F⁻, *gyr*A96, (Nal^r), *rec*A1, *rel*A1, *end*A1, *thi*-1, *hsd*R17, (rk-mk$^+$), *gln*V44 *deo*R, Δ(*lac*ZYA-*arg*F)U169 [Φ80dΔ(*lac*Z)M15]   Invitrogen GmbH, Karlsruhe

E. coli BL21
(DE3)-RIL: F⁻ *omp*T *hsd*S$_B$ (r⁻$_B$m⁻$_B$) *dcm*$^+$ Tet^r *gal*λ (DE3) *end*A Hte [*arg*U*ile*Y*leu*WCam^r) Stratagene, La Jolla, USA

A. rhizogenes: wild type (TR-105; Hector E. Flores; Louisiana State University; USA)

2.1.5. General chemicals

The compounds used were of p.A. grade quality unless otherwise mentioned.

Material	Company
1 kb Plus DNA Ladder	Invitrogen GmbH, Karlsruhe
1st Strand cDNA Synthesis Kit for RT-PCR	Roche Diagnostics GmbH, Mannheim
Acetic acid	Merck KgaA, Darmstadt
Aceton	Sigma-Aldrich Laborchemikalien GmbH, Seelze
Acetonitrile	VWR International GmbH, Wien, Austria
Acetosyringone	Carl Roth GmbH & Co. Kg, Karlsruhe
Acrylamid/bisacrylamid	Carl Roth GmbH & Co. Kg, Karlsruhe
Agar-Agar	Duchefa, Haarlem, The Netherlands
Agarose	Invitrogen Life Technologies, Paisley, Scotland
Albumin, bovine (BSA) 96-99% Fraction V	Sigma Chemical Co, St. Louis, USA
Ammonium nitrate	Merck KgaA, Darmstadt
Ammonium sulfate	Carl Roth GmbH & Co. Kg, Karlsruhe
Ampicillin (sodium salt)	Grünenthal GmbH, Aachen
APS (ammonium peroxodisulfate)	Sigma Aldrich Chemie GmbH, Steinheim
Bacto®-Peptone	Carl Roth GmbH & Co. Kg, Karlsruhe
Bacto®-Trypton	DIFCO laboratories, Detroit, USA
Boric acid	Carl Roth GmbH & Co. Kg, Karlsruhe
Brom phenol blue	Serva GmbH & Co, Heidelberg
Calcium chloride dihydrate	Merck KgaA, Darmstadt
Cellulose acetate filter, 0.2 μm	Sartorius AG, Göttingen
Chloroform	Merck KgaA, Darmstadt
Chemiluminescent detection film	Roche Diagnostics GmbH, Mannheim

Clotrimazole (solvent MeOH)	Sigma Aldrich Chemie GmbH, Steinheim
Coniferyl alcohol	Fluka Chemie GmbH, Buchs, Switzerland
Coomasie-Brilliant blue G-250	Merck KgaA, Darmstadt
CTAB (cetyltrimethyl ammonium bromide)	Serva GmbH & Co, Heidelberg
Cupper (II)-sulfate pentahydrate	Fluka Chemie GmbH, Buchs, Switzerland
Cytochrome c (solvent H_2O)	Fluka Chemie GmbH, Buchs, Switzerland
Denhardt´s solution (100×)	Eppendorf, Netheler
Developer: Kodak X-Ray developer LX24	Kodak, Darmstadt
Dichloromethane	Sigma-Aldrich Laborchemikalien GmbH, Seelze
DIECA	Merck KgaA, Darmstadt
(sodium diethyldithiocarbaminate trihydrate)	
Dipotassium hydrogen phosphate trihydrate	Merck KgaA, Darmstadt
DNA-Agar	Marine Bioproducts Inc., Delta, Canada
DNeasy Plant Mini Kit	Qiagen GmbH, Hilden
dNTPs	Carl Roth GmbH & Co. Kg, Karlsruhe
DTT (1,4 dithiothreitol)	Applichem GmbH, Darmstadt
Ethidiumbromide	Fluka Chemie GmbH, Buchs, Switzerland
EDTA	Merck KgaA, Darmstadt
Ethyl acetate	Fisher Scientific UK, Loughborough, UK
Expand High Fidelity PCR System	Roche Diagnostics GmbH, Mannheim
Ficoll 400	Serva GmbH & Co, Heidelberg
Fish sperm DNA	Roche Diagnostics GmbH, Mannheim
Fixer G334 Rapid Fixer	Agfa, Mortsel, Belgium

Glucose 6-phosphate	Sigma Aldrich Chemie GmbH, Steinheim
Glucose 6-phosphate dehydrogenase	Sigma Aldrich Chemie GmbH, Steinheim
Glycin	Carl Roth GmbH & Co. Kg, Karlsruhe
n-Hexan	Merck KgaA, Darmstadt
n-Hexan, HPLC grade	VWR Prolabo, France
Imidazol, 99%	Acros Organics, New Jersey, USA
Iron sulfate heptahydrat	Merck KgaA, Darmstadt
Isoamylalcohol	Mallinckrodt Baker B.V., Deventer, The Natherlands
Isopropanol	Merck KgaA, Darmstadt
IPTG	Carl Roth GmbH & Co. Kg, Karlsruhe
(isopropyl-β-D-thiogalactopyranoside) Leupeptin	USB, Cleveland, USA
Low DNA Mass^{TM} Ladder	Invitrogen GmbH, Karlsruhe
Low Melting Point Agarose	AppliChem GmbH, Darmstadt
Magnesium chloride hexahydrate	Merck KgaA, Darmstadt
McCown woody Plant Medium	Duchefa Biochemie B.V., Haarlem, The Netherlands
Methanol	Merck KgaA, Darmstadt
Miracloth	Calbiochem-Novabiochem Corp., USA
myo-Inositol	Merck KgaA, Darmstadt
NADH	Biomol Feinchemikalien, Hamburg
NADP$^+$ (disodium salt)	Biomol Feinchemikalien, Hamburg
NADPH (tetrasodium salt)	AppliChem, Darmstadt
Nescofilm$^®$	Azwell Inc., Osaka, Japan
Nick Translation System	Invitrogen GmbH, Karlsruhe

Ni-NTA Agarose	Qiagen GmbH, Hilden
NAA (naphthyl acetic acid)	Merck KgaA, Darmstadt
Nylon membrane (Hybond^{TM}-N$^+$)	Boehringer, Ingelheim
Paromomycin	Duchefa Biochem Haarlem, The Netherlands
PD10 columns	Amersham Biosciences, Freiburg
PMSF (Phenyl methane sulfonyl fluoride)	Carl Roth GmbH & Co. Kg, Karlsruhe
o-Phosphoric acid (85%)	Janssen Chimica, Beerse, Belgium
Polyclar 10	ISP Technologies INC., Wayne, New Jersey
PVP (Polyvinyl pyrrolidon)	Sigma Aldrich Laborchemikalien GmbH, Seelze
Potassium dihydrogen phosphate	Merck KgaA, Darmstadt
Potassium hydroxide	Merck KgaA, Darmstadt
Potassium nitrate	Riedel-de Haën, Seelze
Protein Molecular Marker	Fermentas GmbH, St. Leon-Roth
QIAprep® Spin Miniprep Kit	Qiagen GmbH, Hilden
QIAquick® Gel Extraction Kit	Qiagen GmbH, Hilden
QIAquick® PCR Purification Kit	Qiagen GmbH, Hilden
Revert Aid M-MuL V reverse transcriptase	MBI Fermentas, St. Leon-Roth
RNeasy® Plant Mini Kit	Qiagen GmbH, Hilden
Rubidium chloride	Merck KgaA, Darmstadt
Saccharose	Pfeifer&Langen, Köln
Silica gel 60 (0.040-0.063 mm)	Merck KgaA, Darmstadt
Sodium chloride	Mallinckrodt Baker B.V., Deventer, The Netherlands
SDS (sodium dodecyl sulfate)	Serva GmbH & Co, Heidelberg

Sodium hydroxide	Merck KgaA, Darmstadt
Sodium molybdate dihydrate	Merck KgaA, Darmstadt
Sodium pyrosulfate	Merck KgaA, Darmstadt
Sodium sulfate	Grüssing GmbH, Filsum
Sorbitol	Carl Roth GmbH & Co. Kg, Karlsruhe
Spectrophotometer (Uvikon 930)	Kontron Instrument, Tegimenta, Swizerland
Spectinomycin	Duchefa Biochemie B.V., Haarlem, TheNetherlands
TEMED	Serva GmbH & Co, Heidelberg
Tetcyclasis (NDA)	Dr. W. Rademacher, BASF AG, Ludwigshafen
Timentin	Duchefa Biochemie B.V., Haarlem, TheNetherlands
Titriplex III (Na_2-EDTA)	Merck KgaA, Darmstadt
Tris (Trizma base)	Sigma Aldrich Chemie GmbH, Steinheim
Tryptone	Difco, Sparks, USA
Water, E-PURE, ultra pure water system	Wilhelm Werner GmbH, Leverkusen,
X-GAL	Bts, St. Leon-Roth
Yeast extract	Invitrogen Life Technologies, Paisley, Scotland
α-^{32}P-dATP (3000 Ci/mmol)	Amersham Buchler, Braunschweig
β-Glucosidase (7.1 U/mg)	Carl Roth GmbH & Co. Kg, Karlsruhe
β-Mercaptoethanol	Carl Roth GmbH & Co. Kg, Karlsruhe

2.1.6. Instruments

Agarose gel electrophoresis	Buffer reservoir and gel combs, University of Düsseldorf
	Power supply: 2303 Multidrive 1 Power Supply, Pharmacia
Analytical balance	MC 210 S (Sartorius AG, Göttingen)
Autoclave	Webeco Type No. 5, Lüdenscheid
Ball mill	Retsch, Haan
Centrifuges	Biofuge A, Heraeus Christ, Osterode
	Eppendorf 5415 C, Hamburg
	Eppendorf 5804 R, Hamburg
	Sorvall Superspeed RC-5B, Rotor SS34 + HB-4, Kendro Laborating Products GmbH, Langenselbold
Conductometer	Battery conductometer LF 91 with standard measure cell KLE 1/T, WTW Weilheim
Evaporator Centrifuge	Univapo 150 H + Unijet II Waterjet Aspirator with cooling pump, Uniequip, Martinsried, Germany
Freeze dryer	Alpha 1-4, Christ, Osterode Vacuum pump: Pfeiffer, Balzers Gruppe, Vaduz
Hybridization oven	Appligene mini hybridization oven, Heidelberg
HPLC	Thermoquest, Thermo Separation® Products, Egelsbach, with:
	Degaser
	Autosampler: Spectra System AS1000
	Detector: Spectra System KO, UV 6000 LP
	Pump: Spectra System P2000
	LDC/Milton Roy, Riviera Beach, USA with:
	Controler: LDC Analytical MP3000E
	Pump: Milton Roy constaMetric® I & II
	Detector: LDC Analytical spectroMonitor®3200

HPLC columns	GROM-SIL 120 ODS-5 ST GROM, Herrenberg-Kayh
	Hypersil HypurityTM Elite C18, Thermoquest, Kleinostheim
	Chiracel OD-H, Daicel GmbH, Eschborn
Ice machine	Ziegra UBE 125-100, Isernhagen
Magnetic Stirrer	Ikamag Ret-G (IKA-Labortechnik, Janke and Kunkel GmbH & Co. KG, Staufen
pH-electrode	Mettler Toledo, Udorf, Swiss
pH-meter	WTW pH 523, Knick, Weilheim
Photometer	GeneQUANT II, Pharmacia, Uppsala, Switzerland
	Uvikon 930, Kontron Instruments, Tegimenta, Swiss
Refractometer	Hand refractometer, Krüss, Hamburg
Rotation evaporator	Rotavapor RE 111, Water bath 461, Büchi, Switzerland
SDS gel chamber	SE250/SE260 Mighty Small II (Hoefer, Inc., San Francisco, USA)
Shaker	G53, New Brunswick Scientific Co., New Jersy, USA
Shaking water bath	Julabo SW 20, Seelbach
Sterile bench	ASW-UP 1320 T, Bleymehl, Inden-Pier
Thermocycler	T-personal Combi, T-Gradient, Biometra GmbH, Göttingen
Ultrasonic bath	SONOREX SUPER RK 103 H, Bandelin electronics, Berlin
Ultrasonic rod	Sonifier B12, Branson Sonic, USA
Ultra TURRAX	Janke and Kunkel, Staufen im Breisgau
UV-table	N90, MW 302 nm, Konrad Blenda, Wiesloch
UV-table camera	Cosmicar/Pentax, Englewood, USA
UV-table monitor	Hitachi Ltd., Tokyo, Japan
UV-table thermo printer	Video Copy Processor, Mitsubishi, Tokyo, Japan
UV-table tripod	Dunco Sdn Bhd, Kota Kinabalu, Malaysia
Vacuum pump	Vacuubrand CVC 2, vacuubrand GmbH-co, Wertheim
Vortex	Vortex Genie 2^{TM}, Bender & Habein, Zürich, Swizerland
Water bath	Thermomix, B. Braun, Melsungen
Water system (ultra pure)	E-PURE, Wilhelm Werner GmbH, Leverkusen

2.1.7. Media

For buffers and other solutions ultra pure water was used. All mediums were autoclaved for 20 min, 118 °C and 1.7 bar, after adjustment of pH.

Tab. 2.1. Components of **MS medium** for *L. perenne* cell suspension cultures.

	Components	**Concentration (mg/l)**
Macro elements	KNO_3	1900
	NH_4NO_3	1650
	$CaCl_2. 2H_2O$	440
	$MgSO_4. 7H_2O$	370
	KH_2PO_4	170
Micro elements	Na_2-EDTA	37.3
	$FeSO_4. 7H_2O$	27.8
	$MnSO_4.H_2O$	16.9
	$ZnSO_4. 7H_2O$	10.6
	H_3BO_3	6.2
	KI	0.83
	$Na_2MoO_4. 5H_2O$	0.25
	$CuSO_4. 5H_2O$	0.025
	$CoCl_2. 6H_2O$	0.025
Vitamins	Nicotinic acid	0.5
	Pyridoxol hydrochloride	0.5
	Thiaminchloride- hydrochloride	0.1
Hormone	NAA	0.4
Others	myo-Inositol	100
	Saccharose	30 g/l
	Glycin	2
pH value	Adjusted to 5.6 with KOH	

Tab. 2.2. B103 medium for seed germination.

Components	Concentration
Coconut milk	1 ml/l
Agar-Agar	1% w/v
pH value	Adjusted to 5.8 with 0.5 N HCl or KOH

Tab. 2.3. LB medium for *E. coli* cultures. *1.5% w/v Agar-Agar was added to prepare LB solid medium.

Component	Concentration (g/l)
Bacto®-trypton	10
Yeast extract	5
NaCl	10
PH value	Adjusted to 7.0 by NaOH

Tab. 2.4. YEB medium for *A. rhizogenes*. *1.5% w/v Agar-Agar was added to prepare YEB solid medium.

Components	Concentration (g/l)
Bacto®-trypton	5
Yeast extract	1
Bacto®-peptone	5
Saccharose	5
$MgSO_4 . 7H_2O$	0.5
pH value	7.4

2.1.8. Buffers and solutions

* Add just before use. ** Should not be autoclaved; stirring for a long time is necessary to bring everything in solution. *** For TFB1, $CaCl_2$, Glycerin and potassium acetate were added and pH was adjusted, $RbCl_2$ and $MnCl_2$ was added afterwards. The medium was sterilized by passing through a 0.22 µl filter.

100 × Denhardt's solution	BSA	2% (w/v)
	Ficoll 400	2% (w/v)
	PVP	2% (w/v)
2.5 × Separating gel buffer for SDS-PAGE	Tris-HCl (pH 8.9)	1.875 M
	SDS	0.25% (w/v)
2 × SDS-PAGE sample buffer	Tris-HCl pH 7.5	124 mM
	Glycerin	20% (v/v)
	β-Mercaptoethanol	10% (v/v)
	SDS	4% (w/v)
	Bromphenol blue	0.2% (w/v)
20 × SSPE	NaCl	3 M
	NaH2PO4	200 mM
	EDTA	20 mM
	pH 7.4 (with NaOH)	
5 × Electrophoresis buffer	Tris	0.5 M
	Glycine	1.92 M
	SDS	0.5%
5 × Stacking gel buffer for SDS-PAGE	Tris-HCl (pH 6.7)	0.3 M
	SDS	0.5% (w/v)
50 × TAE	Tris	2 M
	EDTA	0.25 M
	Acetic acid	1 M
Bradford reagent	Coomassie G-250	100 mg/l
	Ethanol (96%)	50 ml/l
	Phosphoric acid (85%)	100 ml/l
	H_2O	to 1 l
Coomasie-Brilliant-Blue Solution for staining the SDS-PAGE	Coomassie R-250	3.6 g/l
	Acetic acid	12% (v/v)
	Ethanol	30% (v/v)
DNA loading buffer	Saccharose	50% (w/v)
	Bromphenol blue	0.25% (v/v)
	in 1× TAE	

Extraction buffer for gDNA isolation	Sorbitol	350 mM
	Tris	100 mM
	EDTA	5 mM
	pH 7.5 (autoclave)	
	Sodium pyrosulfate*	20 mM (0.114 g/30 ml)
KPi buffer	KH_2PO_4	0.1 M
	K_2HPO_4	0.1 M
	pH 7.1	
Lysis buffer for gDNA isolation**	Tris (pH 7.5)	200 mM
	EDTA (pH 8.0)	50 mM
	NaCl	2 M
	CTAB	2%
TE-RNase	Tris	10 mM
	EDTA	1 mM
	pH 8.0	
	RNase*	20 µg/ml
Transformation buffer TFB1	KAc	30 mM
	$MnCl_2$	50 mM
	$RbCl_2$	100 mM
	$CaCl_2$	10 mM
	Glycerin	15% (v/v)
	pH 5.8 (acetic acid)***	
Transformation buffer TFB2	NaMops	10 mM
	$CaCl_2$	75 mM
	$RbCl_2$	10 mM
	Glycerin	15% (v/v)
	pH 7.0 (NaOH)	

2.2. Methods

2.2.1. Plant materials

Flax (*L. usitatissimum* L.) plants (var. Flanders) were harvested 9 weeks after sowing the seeds (at the early capsule stage), from the botanical garden, University of Duesseldorf, Germany, in summer 2006 and 2007. Roots, stems, leaves and young immature seeds were separated for the RNA isolation. The plant material was immediately frozen in liquid nitrogen after harvesting and stored at -80 °C prior to analysis.

L. perenne Himmelszelt seeds were purchased (Jelitto, Schwarmstedt, Germany) and germinated under sterile conditions on B103 medium at 25 °C in the dark. Shoot cultures were established from seedlings on MS-medium (Murashige and Skoog 1962) without hormone and incubated under permanent light. Single seedlings were used to initiate calli and, subsequently, suspension cultures in MS-medium. Cells (5 g fresh weight) were transferred every 7 days into 50 ml of fresh medium in 300 ml Erlenmeyer flasks and incubated on a gyratory shaker at 120 rpm in the dark at 25 °C.

2.2.2. Isolation of RNA

RNA was extracted from the *L. usitatissimum* plant or a four day old suspension culture of *L. perenne* by using the RNeasy® Plant Mini Kit.

2.2.3. First strand cDNA synthesis

cDNA of *L. perenne* was synthesized with the AMV cDNA synthesis kit. 2 µg RNA in the final volume of 7 µl (H_2O) was heated at 65 °C for 15 min and cooled on ice-water. 2 µl of 10 × reaction buffer, 4 µl $MgCl_2$ (25 mM), 2 µl dNTP (10 mM), 2 µl Oligo p(dT)$_{15}$ primer (from AMV 1st strand cDNA synthesis kit), 1 µl RNase inhibitor, 0.8 µl AMV reverse transcriptase and 0.8 µl gelatin in a final volume of 13 µl with H_2O were mixed. The master mix was added to the prepared RNA and incubated in a PCR cycler at 25 °C for 10 min, 42 °C for 60 min, 99 °C for 5 min, eventually cooled upto 20 °C.

cDNA from *L. usitatissimum* was synthesized with M-Mul V reverse transcriptase as follows: 2 µg RNA were mixed with 1 µl LppLR-AAP-3′ (10 pmol/µl) and H_2O until 12.5 µl. The mixture was cooled on ice-water after 5 min incubation at 70 °C (for 3′- and 5′-RACE experiment incubation at 70 °C was extended until 10 min). 4 µl of 5 × reaction buffer (from Revert Aid M-Mul V RT, Fermentas), 2 µl dNTP (10 mM) and 0.5 µl RNase inhibitor was added to the RNA mixture. After 5 min preincubation of the mixture at 37 °C, 1 µl M-Mul V RT (200 U) was added. The mixture was incubated at 42 °C and 70 °C for 60 and 10 min. For 3′-RACE the synthesized cDNA was mixed with 1 µl of RNase H. After 20 min incubation at 37 °C, the cDNA was purified with the PCR Purification Kit (QIAgen).

For 5′-RACE, 2 µg RNA of *L. usitatissimum* or *L. perenne* was mixed with 1 µl of LuPLRGSP1-5′ (2.5 pmol/µl) or LpPLRGSP1-5′ (2.5 pmol/µl). H_2O was added to a final volume of 15.5 µl. This was added to the Master mix with M-Mul V RT containing 5 µl of 5 × reaction buffer to give a final volume of 24 µl. The synthesized cDNA was briefly centrifuged and after 2 min preincubation at 37 °C 1 µl RNase H + 1 µl RNase T1 was added. 10 µl of the purified cDNA was used for tailing in combination with 5 µl of 5 × tailing buffer and 2.5 µl dCTP (2.5 mM) in a final volume of 24 µl. After 3 min incubation at 94 °C, cooling on ice and brief centrifugation, 1 µl TdT enzyme was added. The mixture was incubated at 37 °C and 65 °C each for 10 min.

2.2.4. PCR components and programs

Polymerase chain reaction (PCR) was used to amplify the synthesized cDNA. All PCR sets were performed according to Tab. 2.5. and Tab. 2.6. unless otherwise mentioned. As negative control 2 µl sterile water was used instead of DNA.

Tab. 2.5. Composition of a PCR standard mixture. **A):** Recombinant Taq polymerase* was from Arne Schwelm. **B):** PCR components with Expand High Fiedelity Kit containing a polymerase with proof reading activity. ** 3 µl of cDNA and 5 µl of dc-tailed cDNA were used for 3′-and 5′-RACE experiment respectively. 3′- & 5′-RACE nested PCR was performed with 10 µl of the first PCR product.

A)

Component	Amount
10 × PCR buffer	5 µl
MgCl$_2$ (50 mM)	1.5 µl
dNTPs (each 5 mM)	2 µl
Primer F (10 pmol/µl)	3 µl
Primer R (10 pmol/µl)	3 µl
cDNA	2 µl
Taq polymerase*	1 µl
H$_2$O	31.5 µl
total volume	**50 µl**

B)

Component	Amount
10 × PCR buffer + MgCl$_2$ (15 mM)	5 µl
dNTPs (each 10 mM)	1 µl
primer F (10 pmol/µl)	1.5 µl
primer R (10 pmol/µl)	1.5 µl
cDNA**	2 µl
HiFi-Taq polymerase	1 µl
H$_2$O	38µl
total volume	**50 µl**

Tab. 2.6. PCR program to amplify DNA. *Tm: melting temperature. **Elongation was performed for 1 min if the product was expected at ~ 1 kb, for shorter or longer products the time was adjusted.

1) predenaturation	94 °C	3 min	
2) denaturation	94 °C	30 s	
3) annealing	Tm*-4 °C	30 s	
4) Elongation**	72 °C	1 min	×35
5) final elongation	72 °C	3 min	
6) storage	20 °C	∞	

2.2.5. Cloning of a partial cDNA sequence of *L. usitatissimum* and *L. perenne*

Degenerated primers used to clone a first fragment of a *PLR* cDNA from *L. usitatssimum* and *L. perenne* were designed based on a multiple sequence alignment (ClustalW, version 1.82) of the following amino acid sequences: PLR-Fi1 (GenBank accession number U81158), PLR-Tp1 (GenBank accession number AF242503), PLR-Tp2 (GenBank accession number AF242504), PLR-Tp3 (GenBank accession number AF242505), PLR-Tp4 (GenBank accession number AF242506), PLR-Th1 (GenBank accession number AF242501), PLR-Th2 (GenBank accession number AF242502), PCBER-Fi-2 (GenBank accession number AF242492), PCBER-Pt1 (GenBank accession number AF242490), IFR-Mt1 (GenBank accession number AF277052), IFR-Ms1 (GenBank accession number U17436) and IFR-Ps1 (GenBank accession number S72472). The resulting primers were LPLRdegF1 and LPLR6R (Chapter 2.1.1). They were used to amplify a first PLR fragment by using a touch down PCR with annealing temperatures ranging from 46-56 °C. LPLR4F and LPLR6R primer pairs were used for a nested PCR.

2.2.6. Generation of full-length cDNAs

RACE experiments were used for rapid amplification of the 5′- and 3′- end of the obtained cDNA fragment. cDNA was synthesized and purified using the 5′-RACE system version 2.0 (Invitrogene) (Chapter 2.2.5). Five microliters of the dC-tailed cDNA was next used as the template in a 50 µl PCR reaction by using HiFi-Taq polymerase according to the manufacturer with the gene specific primer LpPLR-GSP2-5′ and the adaptor primer: LpPLR-AAP for *L. perenne* and LuPLR-GSP2-5′ and the adaptor primer: LpPLR-AAP for *L. usitatissimum*. PCR amplification was carried out as described in Tab. 2.6 except for an annealing temperature at 60 °C. A nested PCR was performed with LpPLR-GSP3-5′ and LpPLR-AUAP for *L perenne* and LuPLR-GSP3-5′ and LpPLR-AUAP as gene specific primers for *L. usitatissimum*. The reverse transcription for the 3′- end of the cDNA was the same as 5′-RACE with the poly(dT) primer LpPLR-AAP-3′. The cDNA was amplified with the LpPLR-GSP1-3′ primer and LpPLRAUAP for *L. perenne* and LuPLR-GSP1-3′ primer and LpPLRAUAP for *L. usitatissimum* as mentioned above. The nested PCR was performed with the gene specific primers LpPLR-GSP2-3′ and LpPLRAUAP for *L. perenne* and LuPLR-

GSP2-3′ and LpPLRAUAP for *L. usitatissimum*. The full length open reading frame of the cDNA of *L. perenne* was amplified by RT-PCR with the primers LpPLRORF-F and LpPLRORF-R, introducing an *Nde*I restriction site at the start codon and a *Bam*HI site behind the stop codon. The full length open reading frame of the cDNA of *L. usitatissimum* was amplified with the primers LUBPLRORF-F and LUBPLRORF-R introducing an *Nde*I restriction site at the start codon and a *Xho*I site behind the stop codon.

2.2.7. Cloning of the DNA fragment in cloning and expression vectors

pGEM®-T a circular double stranded vector which allows blue/ white screening, (chapter 5.3.) was used for ligation of the DNA fragments. Components were mixed (Tab. 2.7.) and stored at 4 °C overnight. The amount of DNA-insert was calculated by the vector ratio calculation:

$$\text{Amount of insert} = \frac{\text{amount of vector (ng)} \times \text{size of insert (kb)}}{\text{Size of vector (kb)}} \times 3$$

Tab. 2.7. Ligation mixture.

DNA-insert	calculated
pGEM®-T vector (Promega)	1 µl
T4-DNA ligase	1 µl
2 × ligation buffer (with ATP) (Promega)	10 µl
H₂O	up to 20 µl

To ligate the DNA insert into the expression vector pET15b (chapter 5.3.), 3-5 µg of the plasmid DNA of insert and vector (pET15b) were separately digested with *Nde* I and *Xho* I (each 3 µl) for pSHLUB6k6 and *Nde* I and *BamH* I for pSHORFk16 in a final volume of 100 µl. After purification with the PCR purification Kit and estimation of the amount by LM DNA Ladder; 80 ng of the insert was ligated in 100 ng of the expression vector (pSHETk11 & pSHLUB7k7).

2.2.8. Preparation of competent bacteria

E. coli DH5α bacteria were transformed to LB-Agar medium and incubated overnight at 37 °C. 5 ml LB medium was inoculated with a single colony and incubated overnight at 37 °C. The bacteria were transferred to 100 ml LB medium at 37 °C and grown until an $OD_{600} = 0.6$ was reached. After 15 min incubation on ice, the cells were transferred to a prechilled 50 ml centrifuge tube and centrifuged for 10 min at 4 °C, 3000 rpm. The pellet was dried by removing the supernatant and resuspended in 30 ml TFBI buffer (1/3 of the original volume). After 10 min incubation on ice the suspension was centrifuged 10 min at 4 °C, 3000 rpm. The supernatant was removed and the dried pellet was resuspended in 4 ml TFBII buffer (1/3 of the original volume). 200 µl of bacterial aliquets were dispensed in precooled eppendorf, frozen in liquid nitrogen and stored at -80 °C (modified according to Hanahan 1983).
.

2.2.9. Transformation of *E. coli*

The ligation mixture was added to 200 µl competent cell (DH5α or BL21) which was thawed on ice. The mixture was incubated on ice for 30 min (mixed each 10 min in between). Cells were incubated at 42 °C in a water bath for 90 s and immediately cooled on ice. 800 µl LB was added and the cells were incubated at 37 °C for 45 min (mixed in between). 100 µl of the bacteria was plated to an LB indicator agar for a blue/white selection (100 µg/ml ampicillin, 125 µg/ml X-Gal and 0.5 µM IPTG). The remaining transformation mixture was sedimented at 7000 rpm for 1 min, resuspended in 100 µl supernatant and plated on a separate LB indicator agar plate. The agar plates were incubated at 37 °C for 12-14 h.

2.2.10. Preparation of Plasmid DNA

20 white colonies grown on LB indicator agar were transferred to 3 ml LB (100 µg/ml ampicillin) and incubated at 37 °C overnight. 500 µl of the bacterial suspension was mixed with 500 µl of 60% glycerin in LB for long term storage at -80 °C. The remaining suspension was used for plasmid DNA preparation.

2.2.10.1. Mini plasmid preparation with the TENS reagents

For identification of positive clones, plasmid DNAs were isolated by an alkaline lysis method according to Zhou et al. (1990). 1.5-2 ml *E. coli* overnight cultures were centrifuged at 13000 rpm for 2 min. The supernatant was decanted (50-100 µl was remained). The bacteria were resuspended in the remaining media. 300 µl TENS solution (62.5 µl 1 M Tris pH 8.0, 12.5 µl 0.5 M EDTA pH 8.0, 4.456 ml H_2O, 1.563 ml 0.4 N NaOH and 156.3 µl 20% SDS for 20 preparations) was added. The mixture was vigorously mixed for 2-3 s and incubated for 10-30 min on ice. After addition of 150 µl 3 M potassium acetate solution (pH 5.2 by acetic acid), the reaction mixture was vortexed for 2-3 s and incubated for 10 min on ice. After centrifugation at 13000 rpm for 5 min, the supernatant was transferred to a new tube and mixed with 900 µl absolute ethanol. The mixture was centrifuged (13000 rpm 3-4 min) to sediment the plasmid DNA and the supernatant was removed. The pellet was washed with 300-500 µl 70% ethanol and centrifuged at 13000 rpm for 3-4 min. The pellet was dried for a few min and resolved in 70 µl TE-RNase buffer (chapter 2.1.8).

2.2.10.2. Plasmid preparation by using QIAgen Miniprep kit

Plasmid DNAs which were used for transformation, cloning and sequencing were prepared by using the QIAprep® Spin Miniprep Kit according to the manufacturer. The kit is based on a spin column technology. The DNA adsorbs to the silica membrane in the presence of "high salt" conditions while concomitants pass through the column. Impurities are efficiently washed away and the pure DNA is eluted with Tris buffer.

2.2.11. Restriction hydrolysis of plasmid DNA

5 µl plasmid DNA were mixed with 1 µl restriction enzyme (*Apa* I, *Pst* I when pGEM®-T vector was used), 2 µl 10 × reaction buffer until the final volume of 20 µl with H_2O. The mixture was incubated at 37 °C for 2 h. The hydrolysis result was analyzed by agarose gel electrophoresis.

2.2.12. Agarose gel electrophoresis

For DNA fragments > 1 kb and ≤ 1 kb, 0.8% and 1.5% (w/v) agarose in 1 × TAE buffer was prepared, respectively. DNA loading buffer (1/10 of the DNA sample) was added to the DNA and loaded on the gel. 1 kb Plus DNA Ladder was used to compare the size of the DNA. The gels were run at 80-90 V in 1 × TAE until the blue marker was migrated 2/3 of the gel. The gels were stained in ethidium bromide solution (5.2 μM ethidium bromide in 1 × TAE) for 20-30 min and photographed under UV light.

2.2.13. Determination of the purity and concentration of DNA and RNA

Low DNA Mass^{TM} Ladder and 1% Low Melting Agarose were used to estimate DNA amounts for ligation. DNA and RNA concentration and purity was also determined photometrically at 260 and 280 nm by GeneQuant II.

2.2.14. Sequence analysis

1-2 μg of the plasmid DNA was dried and sent for sequencing to MWG-BIOTECH AG in Martinsried or 100 ng/μl (20 μl) DNA plasmid was sent to Macrogen (Gasan-dong, Geumcheon-gu, Seoul, Korea). The sequence information was verified using Blast x at http://www.ncbi.nlm.nih.gov/blast/.

2. 2.15. Southern blotting

2.2.15.1. Isolation of genomic DNA

Genomic DNA was isolated with the DNeasy® Plant Mini Kit according to the manufacturer. For the genomic southern, gDNA was isolated by the CTAB method as follows: 3-7 g young tissue (for suspension culture day 3) was frozen in liquid nitrogen after harvesting. The material was ground to a fine powder with a precooled mortar and pistil. The powder was filled in a 50 ml centrifuge tube and 25 ml ice-cold extraction buffer (chapter 2.1.8) was added. The material was broken up on ice with an Ultraturrax (19000 rpm, thin pin) for 60 s.

The supernatant was separated and the pellet was resuspended in 2.25 ml extraction buffer and 3.15 ml lysis buffer by using a rod of glass (chapter 2.1.8) consequently. After addition of 1.05 ml 0.5% sarcosyl and vortexing for 10 s, the mixture was incubated at 65 °C for 90 min. 7.5 ml chloroform/isoamyl (24:1) alcohol was added and mixed. The hydrous supernatant (about 6 ml) was transferred to a 12 ml centrifuge tube after 15 min centrifugation at 5000 rpm. 6 ml isopropanol was added and the tube was inverted with caution until the DNA was observed as a bundle. The mixture was centrifuged two times at 5000 rpm for 3 min and the supernatant was pipetted off. The DNA pellet was dried for 5-10 min and resolved in 300-600 µl TE-RNAse at 65 °C for about 20 min.

2.2.15.2. Restriction hydrolysis of gDNA and electrophoresis

15 µl gDNA was mixed with 4 µl of the following restriction enzymes: *EcoR* I, *EcoR* V, *Hind* III, *Xba* I and *Bgl* II separately and 15 µl of the corresponding buffers in a final volume of 150 µl with H_2O. The mixtures were incubated at 37 °C for 4-6 h. 15 µl potassium phosphate solution (3 M, pH 5.2) and 150 µl isopropanol were added to the 150 µl reaction mixture and mixed by flicking. After centrifugation (13000 rpm, 2 min) the pellets were dried for 10 min and resolved in 30 µl Tris buffer (10 mM, pH 8.0) and incubated at 65 °C for 30 min. After gel electrophoresis the gel was photographed in the presence of a fluorescent ruler and the 1 kb Plus Ladder was cut from the gel.

2.2.15.3. Blotting

To denature the DNA, the gel was shaken in 1% HCl solution for 10-15 min (the marker changed from blue to a dark green color). After rinsing with millipore water, the gel was soaked and was shaken in NaOH solution (0.4 N) for 20 min. A plastic box was filled with NaOH (0.4 M), and a glass plate was laid upon the box. Two 3 mm Whatman papers were cut in pieces being longer than the glass plate, soaked in NaOH and laid upon the plate of glass with its ends in the NaOH. The air bubbles in between the papers and plate were removed. The gel was turned upside down and laid upon the paper. After rinsing few drops of NaOH on the gel, the nylon membrane which was cut in the same size as the gel, was laid upon the gel. Parafilm was used to form a barrier around the membrane, that the only route the moisture

could take was through the gel and the membrane. One wet and two dried whatman paper (cut in the size of gel), a pile of paper hand towels together with a mass of 1 kg were laid upon the gel. The blotting took place for 4 h or overnight. To stop the blotting the paper towels were removed, the sandwich assemble was rotated and the pockets on the gel were marked on the nylon membrane. The membrane was handled with forceps, washed with 2×SSPE + 0.1% SDS two times, dried and stored at 4 °C for hybridization.

2.2.15.4. Probe labelling and hybridization

The radioactive labelling of the DNA probe was performed by nick translation (Tab. 2.8). The mixture was incubated at 15 °C for 1 h. Unicorporated nucleotides were removed by using the QIAquick® PCR Purification Kit.

Tab. 2.8. Composition of the Nick Translation approach.

dNTP mix (without dATP)	2.5 µl
Sample of the DNA	100-500 ng
PolI/DNase I mix	2.5 µl
Millipore water	up to 22 µl
α-^{32}P dATP	3 µl

The DNA was eluted with 100 µl EB. 200 µl TE buffer was added. The DNA sample was denatured at 95-100 °C for 10 min and immediately cooled on ice.

To lower the background the membranes were first prehybridized. Fish sperm DNA was used to block unspecific nucleic acid binding sites of the membrane. The membrane was transferred to a roller bottle, 25 ml of the prehybridization solution (Tab. 2.9) was added and incubated in a 56 °C oven for 1 h.

Tab. 2.9. Prehybridization solution.

5 × SSPE	6.25 ml 20 × SSPE
5 × Denhardt's solution	1.25 ml 100 × Denhardt's solution
0.5% SDS	625 µl 20% SDS
Millipore H$_2$O	16.9 ml
Fish sperm DNA	250 µl

For the hybridization process, 15 ml of prehybridized solution was rinsed and the labeled DNA sample was added to the roller bottle. Hybridization was performed overnight at 56 °C.

2.2.15.5. Stringency washes and detection

To get rid of excess unbound and unspecific bound labeled probes, the membrane was washed with washing solutions with different ionic strength. The hybridization solution was poured off in a 50 ml tube and the membrane was washed in the roller bottles consequently with 50 ml 2 × SSPE + 0.1% SDS and 50 ml 1 × SSPE + 0.1% SDS each for 15-20 min. The membrane was transferred to a plastic box with a forceps and washed with prewarmed 100 ml 0.2 × SSPE + 0.1% SDS for 15-30 min. The radioactivity of the membrane was monitored in each step during the washing. If the radiation was low, washing was terminated earlier or prolonged in case of very strong signals. The membrane was shortly dried with paper and wrapped in a plastic foodwrap. Chemiluminescent detection films were exposed to the membranes in a development case in the dark room. Signals were detected by developing the autoradiograph films after storage at -80 °C for a week. The film was laid in the detection (developing) solution until the signals appeared and washed with water. After at least 4 min soaking in the fixating solution and washing with water, the film was dried at 37 °C for 30 min.

2.2.16. Heterologous expression of PLR in *E. coli*

Purified plasmid DNA from pSHLUB7k7 (*PLR-Lu2*) or pSHETk11 (*PLR-Lp1*) was transformed into *E. coli* BL2-Codonplus® (DE3)-RIL cells. Transformed cells were grown at 37 °C with shaking (200 rpm) until the A_{600} reached to 0.8-1.0 in LB medium supplemented with 100 μg/ml ampicillin. After growth of the cells at 28 °C for 30 min, IPTG (isopropyl β-D-thioglycopyranoside) was added to a final concentration of 1 mM. The cells were grown for 5 h at 28 °C. They were harvested by centrifugation and frozen at -20 °C. After thawing at room temperature the cells were resuspended in [5 ml/200 ml culture] extraction buffer (20 mM Tris/HCl pH 7.2, 2 mM EDTA, 5 mM DTT, 1 mM PMSF, 5 μg leupeptin and 100 μg lysozyme) and lysed by sonication (6 × 30 s) (Sonifier B12, Branson Sonic, USA). The supernatant of a centrifugation (13000 rpm, 30 min) was desalted by using a PD10 column

(Amersham, Freiburg, Germany), and the following buffer: 5 mM imidazol, 20 mM Tris pH 8.5, 5 mM mercaptoethanol, 100 mM NaCl. 6 ml of the eluted protein were mixed with 2.5 ml Ni-NTA solution (Qiagen, Hilden, Germany) and shaked at 4 °C with 200 rpm for 1 h. The suspension was filled into an empty PD10 column and washed with 8 ml wash buffer (50 mM NaH_2PO_4, 300 mM NaCl, 20 mM imidazol, pH 8.0 [NaOH]). The His-tagged PLR protein was eluted in 7 steps with 0.8 ml elution buffer each (50 mM NaH_2PO_4, 300 mM NaCl, 250 mM imidazol, pH 8.0 [NaOH]). Fractions containing the His-tagged PLR-Lu2 were pooled, desalted by using a PD10 column with extraction buffer and used for PLR activity assays. All protein concentrations were determined according to chapter 2.2.18.

2.2.17. Extraction of soluble proteins from plant cells (PLR)

The suspension cells of *L. perenne* were separated under vacuum. 0.2 g polyclar 10 and 1 ml extraction buffer were added to the cells [20 mM M Tris-HCl; 2 mM EDTA; (pH 7.1), 5 mM dithiothreitol] per gram fresh weight. The cells were homogenized with an Ultraturrax for 30 s with 30 s break on ice until no large aggregates were observable. After 20 min centrifugation (19000 rpm at 4 °C), an ice cold saturated ammonium sulfate solution (pH 7.1) was added to the supernatant dropwise while stirring on ice. Proteins were precipitated at different concentrations (0-20%, 20-40%, 40-60% and 60-80%). The mixture was stirred for an additional 30 min and centrifuged for 20 min (19000 rpm, 4 °C). The pellet was resolved in 2.5 ml extraction buffer as above, loaded on a PD10 column and eluted with 3 ml extraction buffer.

2.2.18. Determination of protein concentrations according to Bradford

The Bradford test involves the binding of the Coomasie-Brilliant blue (CBB) dye to the protein (Bradford 1976). The free dye in solution is the cationic form, which has an absorption maximum at 470 nm (red). The binding of the dye to protein causes a shift in the absorption maximum to 595 nm (blue). The protein concentration of the sample was determined by comparison to BSA (1 mg/ml) as standard. 5 µl protein sample was mixed with 1 ml of the Bradford dye. The measurement was performed in triplicate samples after 15 min. The linear range for the absorption was between 0.2-0.8. The samples with higher absorptions were diluted.

2.2.19. SDS polyacrylamide gel electrophoresis (SDS-PAGE)

The proteins were separated by SDS-PAGE according to Laemmli (1970). The separating and stacking gels were prepared for a 8.3 cm × 5.0 cm × 0.75 mm thick minigel (Tab. 2.10).

Tab. 2.10. SDS-PAGE gel components.

Components	Separating gel	Stacking gel
30% Acrylamide/0.8% bis-acrylamide	2.2 ml	0.28 ml
2.5 × Separating buffer or	2.2 ml	-
2.5 × Stacking buffer	-	0.33 ml
H_2O	1.1 ml	1 ml
TEMED	5 µl	2 µl
10% APS	50 µl	15 µl

The separating gel was poured upto 2/3, in between glass and aluminum plate and covered with H_2O. After at least 20 min that the polymerization was complete the H_2O was poured off and the gel surface was dried. The stacking gel was added and polymerized. The position of wells was marked before removing the comb. 10 µl protein solution (25 µg) was mixed with 1 µl of 2 × SDS sample buffer. The protein samples and the Protein Molecular Weight Marker were heated at 95 °C for 10 min. The samples were briefly centrifuged and vortexed. The plate containing the gel was laid in the electrophoresis chamber and filled with 1 × electrophoresis buffer (chapter 2.1.8). The samples were loaded and the gel started to run with 10 mA and 23 mA through stacking and separating gel, respectively. Finally the separating gel was stained with Coomasie-Brilliant blue solution for 45 min, briefly washed with H_2O, and shaked in 10% acetic acid overnight.

2.2.20. Chemical synthesis of pinoresinol and dehydrodiconiferyl alcohol

A solution of coniferyl alcohol (1 mmol, ~ 180 mg) in acetone (7 ml) was added to an aqueous solution of iron (III) chloride hexahydrate (2.6 mmol ~702 mg $FeCl_3$ was dissolved in 24 ml H_2O) and stirred at room temperature for 10 min. The mixture was extracted three

times with 30 ml diethyl ether in a separating funnel. The total 90 ml ethereal solution was washed with 20 ml millipore water to remove iron choloride and dried over sodium sulfate for approximately 1 h. By filtrating the sodium sulfate was taken away and the filtrate was evaporated to dryness using a rotavapor. The residue was resolved in 5 ml methylene chloride. To verify whether Pino was synthesized, an aliquote diluted in methanol (1:10) was analyzed by reverse phase HPLC. Column chromatography with silica gel was used (230-400 mesh) for purification. A column (19 cm × 2.5 cm) was packed with a slurry of silica gel (30 g) dissolved in the eluting solvent methylene chloride/diethyl ether (4:1) and washed with one liter of the same eluent. After addition of the sample to the column, at least 16 fractions (50 ml) were collected and evaporated to dryness. Residues were resolved in methanol (3 × 500 µl). Aliquots of fraction 4-13 were diluted with methanol (1:10) and other fractions without dilution were injected to the HPLC. Fractions which yielded Pino above 94% purity at 230 nm were unified and taken for PLR enzyme assays. After elution of Pino the Dichloromethane/aceton solvent system was used for elution of DDC from the same column (Tab. 2.11).

Tab. 2.11. solvent system for DDC elution.

Dichloromethane/aceton	No. and volume of fractions	Dilution for HPLC analysis
1 / 0	2 × 100 ml	1 : 5
1 / 0.15	1 × 100 ml	-
1 / 0.2	1 × 100 ml	-
1 / 0.25	7 × 50 ml	1 : 10
1 / 0.3	2 × 50 ml and 1 × 100 ml	1 : 5
1 / 0.4	1 × 100 ml	1 : 5

Fractions which yielded amounts of DDC above 90% purity at 230 nm were unified and taken for PCBER enzyme assays.

2.2.21. Enzyme assays for PLR

2.2.21.1. Enzyme assays for PLR extracted from cell suspension of *L. perenne*

Assays were performed in the presence of 400 µg enzyme extract, 10 µl Pino (10 mM) and 50 µl NADPH (25 mM) in 0.1 M Kpi buffer (pH 7.1) until the final volume of 500 µl. (NADPH was added after 15 min incubation of the reaction mixture at 30 °C). After overnight incubation the reaction was stopped and extracted with (3 × 500 µl in total) ethyl acetate.

2.2.21.2. Enzyme assays with recombinant purified PLRs

PLR eluted from PD10 column was used for the determination of enzyme activities. For PLR-Lp1, the assay mixtures (250 µl) consisted of KPi buffer (0.1 M, pH 7.1), 0.0925 mM racemic Pino, 2.5 mM NADPH and purified His tagged PLR-Lp1 in different concentrations (0.001, 0.005, 0.01, 0.05, 0.1, 0.5, 1, 3, 5, 7, 10, 15, 20 µg/assay). For PLR-Lu1 and PLR-Lu2 the mixture were the same as mentioned for PLR-Lp1 except for 0.12 mM racemic Pino, 2.5 µg purified His tagged PLR-Lu1 or 0.5 µg PLR-Lu2. Protein, buffer and Pino were preincubated for 15 min at 30 °C. The enzyme reaction was initiated by addition of NADPH and terminated by addition of 300 µl ethyl acetate after 3 h for PLR-Lp1. Assays for PLR-Lu1 was perfomed in a time scale of 2, 5, 10, 15 and 20 min and for PLR-Lu2 the assays were incubated for 2, 5, 10, 15, 20, 25, 30 and 40 min, respectively. The assays were extracted with ethyl acetate (3 × 300 µl in total). The combined ethyl acetate phases were dried under vaccum. The residue was dissolved in 100 µl methanol and subjected to HPLC analysis.

2.2.22. RNAi constructs and transformations

2.2.22.1 Construction of hpRNAi vectors

After cloning the first piece of *PLR* of *L. perenne*, a 652-bp fragment of the coding region of *PLR-Lp1* (pSH1) was selected and amplified by PCR using the primers LPPLRhanF and LPPLRhanR containing 2 sets of restriction sites at the 5' end. The forward primer contained *Xba*I and *Xho*I and the reversed primer contained *Cla*I and *Kpn*I restriction sites, respectively. The PCR product was first cloned into pGEM®-T vector and sequenced (pSH2). To clone the pSH2 in the sense orientation of a pHANNIBAL vector a restriction hydrolysis with three enzymes (*Xho*I, *Kpn*I and *Apa*I) were performed until a final volume of 100 µl. The mixture was incubated at 37 °C for 4 h and purified with QIAquick® PCR Purification Kit. 2 µg of the

pHANNIBAL vector was digested with *Kpn*I for 4 h and purified. After estimation of the amount of digested pSH2 and pHANNIBAL, 80 ng of insert was ligated to 100 ng of vector with the T$_4$-DNA ligase (It should be mentioned that vector and H$_2$O were heated at 45 °C for 5 min, cooled on ice and other components were added for ligation). The ligated DNA was cloned in DH5α (selection was on the LB media containing ampicillin) and sequenced (pSH3). pSH2 which was digested with *Xba*I, *Cla*I and *Sca*I was cloned in pSH3 (hydrolyzed with *Xba*I and *Cla*I) in the antisense direction with the same procedure as above (pSH4). pSH4 was digested with *Not* I at 37 °C for 4 h and purified to ligate into pART27 binary vector. 3 μg of the vector was also digested with *Not* I. After 20 min heating at 65 °C, the pART27 was treated with alkaline phosphatase (1 μl) in the presence of corresponding buffer, incubated at 37 °C for 70 min and purified. pSH4 was ligated into pART27 cloned in DH5α and sequenced (pSH5). Its notable that, selection of clones which were contained pART27 was a blue/white selection on a LB media containing spectinomycin. To prepare the control constructs without sense and antisense *PLR*s, the expression cassette of the *Not* I hydrolyzed pHANNIBAL was cloned into pART27 (pDI25).

2.2.22.2. Preparation of *A. rhizogenes* competent cells

The Agrobacteria (TR105) were streaked on an YEB agar plate from a glycerol stock and were grown at 28 °C for app. 3 days until single colonies were appeared. 4 ml YEB broth medium was inoculated with a single colony and incubated at 28 °C for 2 days. 100 ml YEB medium was inoculated with the above 4 ml culture and was grown 28 °C for an additional 3-4 h. The cultures were centrifuged at 5000 rpm in 50 ml tubes for 15 min. The pellet was resuspended in 2 ml medium and stored in 200 μl aliquots at -80 °C.

2.2.22.3. Transformation of the competent *Agrobacteria* with hpRNAi constructs

100 ng-1 μg plasmid DNA was mixed with the thawed *Agrobacteria* and incubated on ice for 5 min. After 5 min incubation in liquid nitrogen, the mixture was incubated at 37 °C for 5 min. 800 μl YEB was added on ice to the mixture and incubated at 28 °C for 3-4 h (inverted meanwhile). The spreaded bacteria on YEB agar plates containing spectinomycin, were incubated at 28 °C for 3 days.

2.2.22.4. Plasmid preparation from *Agrobacteria*

Agrobacteria colonies were inoculated to 15 ml YEB media with spectinomycin (in 100 ml erlenmeyer flasks) and grown for 1-2 days at 28 °C, 200 rpm. After centrifugation in a 15 ml tube at 5000 rpm for 15 min, plasmid DNA was isolated with the QIAprep® Spin Miniprep Kit by using double volumes of the buffers P1-P3. The DNA was eluted with 50 µl elution buffer. 15 µl DNA was used for restriction digest with *Not* I.

2.2.22.5. Transformation of *L. perenne* shoot cultures

Transformed agrobacteria were grown on YEB medium in a 200 ml flask with 100 µg/ml spectinomycin and 20 µM acetosyringone at 28 °C for 2 days until the OD_{600} was between 0.8-1.2. Medium was centrifuged in 5000 rpm for 15 min and the pellet was transformed with a sterile scalpel to the young shoots. Shoots from in vitro cultures were wounded and infected with the agrobacteria. After 2 days of cocultivation the explants were washed in 50 ml water contained timentin® and incubated on hormone free McCown agar medium with 2% sugar and 200 µg/ml timentin® in the dark. The hairy roots appeared 2 weeks after the infection. The root segments were cut and transferred onto new medium when they were at least 25 mm in length. Paromomycin (200 µg/ml) was used for selection of hairy roots carrying the ihpRNAi construct with and without the *PLR-Lp1* partial sequence. Hairy root clones were kept in the dark at 25 °C and routinely subcultured every 25 days. After several subcultivation cycles, hairy roots were transferred to liquid McCown medium. Subcultivation was performed every 2 weeks by transferring 2 g fresh weight in liquid McCown medium (50 ml per 450 ml jar) with 2% sugar on a rotary shaker (80 rpm).

2.2.23. Analysis of transgenic lines

2.2.23.1. Molecular analysis of transgenic lines

The DNeasy Plant Mini Kit was used to isolate total genomic DNA from 20 mg freeze dried material from 7 day old hairy roots. The transformed status of hairy roots was verified by PCR for the genes *rol*C and *vir*C according to (Yang and Choi 2000). The PCR mixture and

program was as mentioned in Tab. 2.5 and Tab. 2.6. The annealing temperature for *rol*C amplification with ROLCFOR and ROLCREV primer pairs and VIRCFOR and VIRCREV primer pairs for *vir*C amplification was 63 °C and 48 °C, respectively.

2.2.23.2. Detection of *35S-PLR* in transgenic hairy roots

The oligonucleotide primers used for amplification of the *PLR* gene were 35 S and LPPLRhanR. PCR amplification for the inserted *plr* gene was the same as mentioned in Tab. 2.6 with an annealing temperature at 59 °C.

2.2.23.3. Semiquantitative RT-PCR

First strand cDNA was reverse transcribed from 1 μg total RNA using Revert Aid M-MuL V reverse transcriptase. PKFactin5′ and PKFactin3′ were used to amplify a 850 bp *actin* cDNA fragment with an annealing temperature at 46 °C. Primer pairs and the PCR programme for amplification of *PLR-Lp1* cDNA from hairy roots of *L. perenne* were PLRORFF and PLRORFR as mentioned in Tab. 2.5 and Tab. 2.6. DNA fragments were compared after 29 cycles of amplication. PCR products were analysed on a 0.8% agarose gel stained with ethidium bromide.

The level of *PLR-Lu1* and *PLR-Lu2* in normal *L.usitatissimum* plant was also estimated by semiquantitative RT-PCR. Gene specific primer pairs SemiLu1-F and SemiLu1-R were used to amplify a *PLR-Lu1* fragment and SemiLu2-F and SemiLu2-R for *PLR-Lu2*. DNA fragments were compared after 26 cycles of amplication.

2.2.23.4. Preparation of protein extracts from hairy roots

Seven day old hairy roots of *L. perenne* H were separated from the medium. Protein was extracted as described in chapter 2.2.17. The protein was precipitated between 0% and 60% ammonium sulfate. Protein concentrations were determined as mentioned in chapter 2.2.18.

2.2.23.5 Enzyme assays for hairy roots

In order to determine the range of linearity of product formation PLR assays were either conducted with 40 μg protein for different time intervals in the range from 30 to 180 min or with different protein concentrations in the range from 0 to 100 μg protein/assay for 90 min. Finally, specific enzyme activities of different ihpRNAi and control lines were compared with assays containing 40 μg protein incubated for 90 min at 30 °C. PLR activity was calculated as follows:

$$\text{Absolute enzyme activity [nkat]} = \frac{\text{Aprobe} \times \text{Cst} \times \text{Vtest}}{\text{Ast} \times \text{t}}$$

$$\text{Specific enzyme activity [mkat/kg]} = \frac{\text{Absolute enzyme activity [nkat]}}{C_{protein} \times V_{protein}}$$

A_{probe}: Integration level of sample peaks

C_{st}: Concentration of standard [mM]

V_{test}: Volume of assay mixture [μl]

A_{st}: Integration level of standard peak

t: Incubation time [s]

$C_{protein}$: Protein concentration [mg/ml]

$V_{protein}$: volume of protein solution/assay [μl]

2.2.24. Biochemical characterization of JusB7H

2.2.24.1. Preparation of microsomes

Five-day-old suspension cells of *L. perenne* H were harvested by vacuum filtration. All further steps were carried out at 0-4 °C. Cells were homogenized by using a prechilled mortar and pestele together with 0.2 g Polyclar 10, 0.17 g sea sand and 1 ml buffer [0.1 M Tris-HCl (pH 7.5), 1 mM dithiothreitol, 1 mM diethyldithiocarbaminate] per gram fresh weight. The homogenate was centrifuged at 8000 g for 20 min. The supernatant was adjusted to 50 mM $MgCl_2$ and stirred on ice for 30 min. The sediment containing aggregated membranes was resuspended in buffer (as above) by a Potter and Elvehjem glass homogeniser after-centrifugation at 48000 g for 25 min. Crude cell-free extracts for enzyme assays were obtained by passing the resuspended pellet through a preequilibrated PD10 column using the same buffer. Protein concentrations were determined according to chapter 2.2.18.

2.2.24.2. Determination of general parameters

pH, temperature, time and protein dependency of the JusB7H were characterized. 0.1 M Tris-HCl buffer with the following pH values 6.0, 6.5, 7.0, 7.2, 7.5, 7.8, 8.0, 8.5 and 9.0 were prepared to determine pH dependency. The assay condition was as mentioned in Tab. 2.12. To determine the protein dependency, 0, 300, 500, 600, 700, 800 and 1000 μg microsome preparations were added to the assay mixture. Enzyme assays which were stopped after 0, 15, 30, 45, 60, 75, 90, 105 and 120 min, used to determine time dependency of JusB7H. To determine the optimum temperature for JusB7H, reactions were incubated at 0, 4.0, 20, 26, 28, 30, 32, 34, 37, 40, 50, 60 and 100 °C.

2.2.24.3. Standard enzyme assay for JusB7H

Standard assays contained 50 μM Jus B, 1 mM NADPH and 0.7 mg protein in a total volume of 500 μl Tris-HCl (pH 7.5) with 1 mM dithiothreitol and 1 mM diethyldithiocarbaminate. After vigorous mixing assays were routinely incubated for 75 min at 26 °C, stopped by addition of 50 μl 6 M HCl and cooled on ice. An NADPH regenerating system consisting of

10 mM glucose-6-phosphate, 0.07 unit glucose-6-phosphate dehydrogenase and 4 mM DTT were added to the assay, which was incubated for 5 h for the identification of the reaction product Diph by HPLC-SPE-NMR. Stopped assays were extracted with ethyl acetate (3×500 μl). The combined ethyl acetate phases were dried under vaccum. The residues were redissolved in 80μl methanol and subjected to HPLC analysis.

2.2.24.4. Determination of kinetic constants for JusB7H and NADPH

To determine the substrate (JusB) and cosubstrate (NADPH) dependency for JusB7H, their concentrations for each enzyme assay were varied as Tab. 2.13. The determination of Km values was the mean of at least three independent assays, each in duplicate. Km values were calculated according to Lineweaver-Burk, Hanes-Woolf and Eadie-Scatchard equations.

Tab. 2.12. JusB7H standard assay. * To determine the optimum pH, values were in between 6-9. ** To determine protein dependency, values were in between 0-1000 μg protein.

Substance (solution)	Volume
0.1 M Tris-HCl pH 7.5* (with 1 mM DTT, 1mM DIECA)	x μl
Microsome**	y μl
100 mM NADPH (in H_2O)	5 μl
2.5 mM JusB (in DMSO)	10 μl
Volume of the assay	500 μl

Tab. 2.13. Jus B and NADPH concentrations for JusB7H assays to determine kinetic constants. Jus B stock solution was dissolved in DMSO.

Jus B stock solution	Jus B end concentration	NADPH stock solution	NADPH end concentration
0 mM	0 µM	0 mM	0 µM
0.05 mM	1 µM	2.5 mM	25 µM
0.1 mM	2 µM	5 mM	50 µM
0.5 mM	10 µM	10 mM	100 µM
1 mM	20 µM	25 mM	250 µM
1.5 mM	30 µM	50 mM	500 µM
2 mM	40 µM	75 mM	750 µM
2.5 mM	50 µM	100 mM	1000 µM
5 mM	100 µM		
7.5 mM	150 µM		
10 mM	200 µM		

2.2.24.5. Preparation of JusB7H inhibitors

Cytochrome P450 enzyme activity can be inhibited by specific inhibitors. Effects of different inhibitors on JusB7H were tested in vitro. Cytochrome *c* (Cyt *c*), tetcyclacis (NDA), clotrimazole (CLOT), ancymidol and aminobenzotriazol (ABT dissolved, in MeOH) solutions were tested. As the first three inhibitors have shown inhibition effects, different concentrations (Tab. 2.14) were used in the assay to find the 50% inhibition concentration.

Tab 2.14. Concentrations of inhibitors used for JusB7H assay. Cyt *c* was dissolved in 0.1 M Tris-HCl. NDA and CLOT were resolved in DMSO and MeOH respectively.

Inhibitor stock solution (Cyt c)	Inhibitor end concentration (Cyt c)	Inhibitor stock solution (CLOT or NDA)	Inhibitor end concentration (CLOT or NDA)
0 µM	0 µM	0 mM	0 mM
12.5 µM	0.25 µM	0.2 mM	0.001 mM
25 µM	0.5 µM	0.4 mM	0.002 mM
37.5 µM	0.75 µM	1 mM	0.005 mM
50 µM	1 µM	2 mM	0.01 mM
62.5 µM	1.25 µM	10 mM	0.05 mM
75 µM	1.5 µM	20 mM	0.1 mM
87.5 µM	1.75 µM	40 mM	0.2 mM
100 µM	2 µM	100 mM	0.5 mM
112.5 µM	2.25 µM		
125 µM	2.5 µM		

2.2.25. HPLC analysis

Analysis of lignans and collection of the enzyme assay products were performed by reverse phase HPLC analysis. Enantiomeric compositions were determined by normal phase HPLC (Tab. 2.15).

Tab. 2.15. HPLC columns, solvent systems and gradient programs.

Analysis	Column	Solvent A	Solvent B	Time [min]	Flow [ml/Min]	A [%]	B [%]
PLR and PCBER enzyme assay	GROM-Sil 120 ODS-5 ST (250 × 4 mm, 5 μm) Precolumn: (20 × 4 mm, 5 μm)	H_2O + 0.01% H_3PO_4 (85%)	Acetonitrile	0 22 29 32 33 36 40	1 1 1 1 1 1 1	75 75 57 25 25 75 75	25 25 43 75 75 25 25
Isolation of Pino, Lari and Seco	GROM-Sil 120 ODS-5 ST (250 × 8 mm, 5 μm) Precolumn: (20 × 4 mm, 5 μm)	H_2O	Acetonitrile	0 16 26 28 29 32 40	2 2 2 2 2 2 2	71 69 54 25 25 71 71	29 31 46 75 75 29 29
Seperation of all lignans, and JUSB7H enzyme assays	GROM-Sil 120 ODS-5 ST (250 × 4 mm, 5 μm) Precolumn: (20 × 4 mm, 5 μm)	H_2O + 0.01% H_3PO_4 (85%)	Acetonitrile	0 25 43 46 54 56 60	0.8 0.8 1 1 1 1 0.8	75 62 57 45 30 85 85	25 38 43 55 70 25 25
Chiral analysis for Pino	CHIRACEL OD-H (250 × 4 mm, 5 μm) Precolumn: (0.4 cm Ø × 1 cm) Chiracel	Ethanol	n-Hexan	0 45	0.5 0.5	50 60	50 40
Chiral analysis for Seco	CHIRACEL OD-H (250 × 4 mm, 5 μm) Precolumn: (0.4 cm Ø × 1 cm) Chiracel	Ethanol	n-Hexan	0 35	0.5 0.5	25 25	75 75
Chiral analysis for Lari	CHIRACEL OC (250 × 4.6 mm, 5 μm) Precolumn: (0.4 cm Ø × 1 cm) Chiracel	Ethanol	n-Hexan	0 30	0.5 0.5	80 80	20 20

2.2.25.1. LC-ESI/MS analysis

HPLC-ESI/MS analysis was performed in the laboratory of Prof. Dr. Schmidt with a Finnigan LCQ Deca XP mass spectrometer (Thermo Finnigan, Dreieich, Germany) coupled to an Agilent (Agilent, Waldbronn, Germany) 1100 series HPLC system. Separations were achieved with a Knauer (Berlin, Germany) Eurosphere RP C_{18} column (250 × 2 mm i.d., 5 μm) using acetonitrile:water (containing 0.1% formic acid) for elution in a gradient from 3:7 to 7:3 in 30 min, followed by isocratic elution with 7:3 between 30 and 40 min, a further increase from 7:3 to100:0 between 40 and 55 min, and finally isocratic elution with acetonitrile from 55 to 65 min. The flow rate was 0.4 mL/min throughout.

2.2.25.2. LC-SPE-^{1}H NMR analysis

LC-NMR analysis for identification of Diph was performed in the laboratory of Dr. B. Schneider with the following conditions: HPLC on a LiChrospher 100 RP-18 column (250 × 4 mm, particle size 5 μm) using acetonitrile : water (0.1% trifluoroacetic acid) as a mobile phase (flow rate 1.0 ml min^{-1}). The following gradient was applied: 0 min 25% MeCN, 25 min 38%, 43 min 43%, 46 min 55%, 54 min 70%. HPLC was performed on an Agilent 1100 chromatography system (quaternary pump G1311A; autosampler G1313A; J&M photodiode array detector, monitoring wavelength 230 nm and 254 nm). The HPLC system was connected to a Prospekt 2 SPE unit (Spark Holland), which was used for trapping. The post-column eluent flow was diluted with H_2O by a makeup pump before trapping the peak eluting at R_t 28.5 min on a poly(divinylbenzene) SPE cartridge (HySphere resin GP, Spark Holland). The SPE device was connected by a capillary to a Bruker Avance 500 MHz spectrometer equipped with a Cryofit^{TM} flow insert (30 μl active volume). The cartridge containing the trapped peak was dried with a stream of nitrogen gas for 30 min. Then the compound was eluted with MeCN-d_3 and directly transferred to the NMR spectrometer for data acquisition at 300 K. A ^{1}H NMR spectrum was measured in MeCN-d_3. Jus B was also trapped from the LC-SPE-NMR of the assay mixture (R_t 37.3 min) and the ^{1}H NMR was measured. In order to compare the ^{1}H NMR spectra of the product directly with that of the authentic standard, a sample of Diph was run under identical LC-SPE-NMR conditions.

3. Results

3.1. Analysis of lignans in *Linum usitatissimum* and *Linum perenne* H

3.1.1. Fragmentation pattern of lignans by LC-MS analysis

Electrospray ionization (ESI) is currently one of the most used ionization methods because it allows analysis of non-volatile compounds, and produces multiply charged ions from high molecular weight compounds. Furthermore, as an atmospheric pressure source, it is easy to couple directly to liquid chromatography. Understanding the fragmentation mechanism of compounds, helps in identifying pure substances or those separated by LC-MS from crude extracts (Stévigny et al. 2004).

The lignans occuring in the Linaceae family have a common basic skeleton (Fig. 1.6) and may show, under appropriate mass spectrometric conditions, fragmentation pathways amenable to straightforward structural interpretation. It is also worth exploring the possibility of identifying these ingredients using their mass spectrometric data, with the aim of predicting the structure of new compounds and also registering a diagnostic profile for each plant in the absence of reference standards (Wong et al. 2000). The LC-MS method was used for achieving this objective for lignans in *L. usitatissimum* L. (Schmidt et al. 2006) and *L. perenne* H (Hemmati et al. 2007). The fragmentation pattern of different groups of lignan standards were determined. It should be mentioned that the fragmentation observed in the negative ion mode was much less informative than in case of the positive ion spectra.

Pinoresinol: UVmax (nm): 232, 280; Mw: 358; **MS**: 359 (25%) $[M+H]^+$, 341 (100%) $[M+H-H_2O]^+$; **MS/MS**: 323 (100%) $[341-H_2O]^+$, 311 (15%) $[341-CH_2O]^+$, 291 (95%), 271 (70%).

Lariciresinol: UVmax (nm): 230, 280; Mw: 360; **MS**: 219 (100%) $[M+H-H_2O-124$ (=guaiacol)$]^+$; **MS/MS**: 189 (100%) $[219-OCH_2]^+$, 159 (15%) $[189-OCH_2]^+$

Secoisolariciresinol: UVmax (nm): 228, 282; Mw: 362; **MS**: 363 (30%) $[M+H]^+$, 345 (80%) $[M+H-H_2O]^+$, 327 (100%) $[M+H-2H_2O]^+$; **MS/MS**: 295 (100%), 203 (5%) $[M+H-2H_2O-124$ (=guaiacol)$]^+$, 163 (55%), 137 (17%)

Matairesinol: UVmax (nm): 230, 282; Mw: 358; **MS**: 359 (100%) $[M+H]^+$, 341 (30%) $[M+H-H_2O]^+$; **MS/MS**: 323 (100%), %) $[M+H-2H_2O]^+$, 163 (17%), 137 (42%)

Hydroxymatairesinol: UVmax (nm): 230, 280; Mw: 374; **MS**: 357 (50%) $[M+H-H_2O]^+$, 233 (100%) $[M+H-H_2O-124 (=guaiacol)]^+$

Yatein: UVmax (nm): 230, 286; Mw: 400; **MS**: 401 (100%) $[M+H]^+$, 383 $[M+H-H_2O]^+$; **MS/MS**: 365 (50%) $[M+H-2H_2O]^+$, 161 (10%), 181 (30%)

Deoxypodophyllotoxin: : UVmax (nm): 238, 292; Mw: 398; **MS**: 399 (100%) $[M+H]^+$, 231 (70%) $[M+H-trimethoxyphenyl]^+$, 187 (15%) $[231-CO_2]$

Podophyllotoxin: UVmax (nm): 238, 292; Mw: 414; **MS**: 415 (45%) $[M+H]^+$, 397 (100%) $[M+H-H_2O]^+$, 247 (17%) $[M+H-trimethoxyphenyl]^+$; **MS/MS**: 313 (100%) $[M+H-H_2O-lacton]^+$, 229 (4%) $[247-H_2O]^+$

6-Methoxypodophyllotoxin: UVmax (nm): 216, 280; Mw: 444; **MS**: 445 (10%) $[M+H]^+$, 427 (100%) $[M+H-H_2O]^+$; **MS/MS**: 343 (100%) $[M+H-H_2O-lacton]^+$

α-peltatin: UVmax (nm): 274; Mw: 400; **MS**: 401 (70%) $[M+H]^+$, 247 (100%) $[M+H-syringyl]^+$, 203 (10%) $[247-CO_2]$

β-peltatin: UVmax (nm): 276; Mw: 414; **MS**: 415 (100%) $[M+H]^+$, 247 (85%) $[M+H-trimethoxyphenyl]^+$, 203 (20%) $[247-CO_2]$

β-peltatin-A-methylether: UVmax (nm): 280; Mw: 428; **MS**: 429 (100%) $[M+H]^+$, 261 (80%) $[M+H-trimethoxyphenyl]^+$, 217 (14%) $[261-CO_2]$

Justicidin B: UVmax (nm): 260, 312; Mw: 364; **MS**: 365 (100%) $[M+H]^+$; **MS/MS**: 335 (5%) $[M+H -OCH_2]^+$, 321 (16%) $[M+H -CO_2]^+$

5′-demethyl justicidin B: UVmax (nm): 260, 320; Mw: 350; **MS**: 351 (100%) $[M+H]^+$; **MS/MS**: 321 (20%) $[M+H -OCH_2]^+$, 307 (15%) $[M+H -CO_2]^+$

3.1.2. Analysis of lignans in cell suspension culture of *L. perenne* Himmelszelt

We have isolated from a cell suspension culture of *L. perenne* H Jus B as the main lignan beside two further arylnaphthalene lignans not detected in *Linum* species before (Fig. 1.8). The two latter compounds were found by HPLC/ESI-MS to be glycosides of 7-hydroxyjusticidin B (diphyllin) (Schmidt et al. 2006). The ESI-MS spectrum of the first substance displayed a quasimolecular ion $[M + H]^+$ at *m/z* 645, followed by fragments at *m/z* 513 and 381, corresponding to loss of one, and two, pentose moieties, respectively. The second compound, occurring only in minor amounts, differed from the first by showing an $[M + H]^+$ at *m/z* 675 and fragments due to successive loss of a pentose (*m/z* 543) and a hexose (*m/z* 381) moiety. Both compounds were also present in a cell culture of *L. perenne* H, from which they were isolated by column chromatography and analysed by NMR spectroscopy. Thus, the first compound was unambiguously identified by its ^{1}H, ^{13}C as well as a series of 2D NMR measurements (COSY, HMQC, HMBC) as diphyllin-7-(2-β-xylopyranosido)-β-apiofuranoside, whose data were found identical (Al-Abed et al. 1990). This diphylline glycoside (Fig. 1.8) is known under the generic name majidine as a constituent of *Haplophyllum* species (Rutaceae). In case of the second compound, unambiguous identification as a further diphyllin glycoside followed from its ^{1}H NMR data which were very similar to those of majidine with respect to the aglycone part. The small sample amount precluded measurement of ^{13}C NMR spectra and massive signal overlap in the ^{1}H NMR spectrum precluded unambiguous assignment of the pentosido-hexoside disaccharide moiety, so that the full structural assignment must remain open at present. This is the first report on the occurrence of 7-oxygenated arylnaphthalenes and their glycosides within a *Linum* species.

3.1.3. Biosynthesis of lignans in *L. usitatissimum*

Two distinct diastereomers of SDG present in flaxseed the dominant form (~99%) is (+)-Seco and ~1% is (-)-Seco. The aerial parts of flowering *L. usitatissimum* plants accumulate (-)-bursehernin, (-)-yatein, (-)-hinokinin, (-)-matairesinol dimethyl ether, (-)-thujaplicatin-

trimethyl ether and (-)-*E*-anhydropodorhizol, which should be derivatives of (-)-Seco (Schmidt et al. 2006). Based on the enantiomeric composition of lignans in *L. usitatissimum*, we have proposed two parallel biosynthetic pathways for the biosynthesis of (+)- and (-)-Seco, respectively (Fig. 1.11).

3.2. PLRs from *L. usitatissimum*

3.2.1 Cloning of a sequence encoding a *PLR* (*PLR-Lu2*) from leaves of *L. usitatissimum*

A full length cDNA with 1203 bp encoding a putative PLR (*PLR-Lu2*, GenBank accession number EU029951) was cloned by an RT-PCR with degenerated primers followed by 5'- and 3'-RACE experiments. The translational start of the ORF is at nucleotide 58, the TAA stop at nucleotide 1048 encoding a polypeptide of 330 amino acids (Fig. 3.1).

A blast search with the translated amino acid sequence of (+)-pinoresinol/(+)-lariciresinol reductase [(+)-PLR] against the nonredundant peptide data base at the National Center for Biotechnology (NCBI) was conducted. Significant similarities were noted for PLR-Lu2 to the PLR of *L. album* (83% identity and 92% similarity) and the PLR of *F. intermedia* (76% identity and 88% similarity) on the amino acid level. PLRs, isoflavone reductases (IFRs) and phenylcoumaran benzylic ether reductases (PCBERs) are the first three members of NADPH-depenent reductase enzymes forming the PIP family showing high sequence similarities and also comparable reaction mechanisms (chapter 1.6.2). PLR-Lu2 shows lower similarities to these members of the PIP family. 47% identity and 66% similarity to a PCBER of *Pinus taeda* and 49% identity and 64% similarity to a PCBER of *Populus trichocarpa* was observed for PLR-Lu2. PLR-Lu2 shows 41% identity and 60% similarity to an IFR of *Medicago truncatula* and 40% identity and 60% similarity to an IFR of *Glycine max*. PLR-Lu2 also had sequence similarities to the new members of PIP family like eugenol synthases (EGSs), isoeugenol synthases (IGSs), (Koeduka et al. 2006) leucoanthocyanidin reductases (LARs) (Peiffer et al. 2006) and pterocarpan reductases (PTRs) (Akashi et al. 2006). 40% identity and 60% similarity to the EGS of *Ocimum basilicum*, 41% identity and 60% similarity to the IGS of *Petunia × hybrida*, 39% identity and 58% similarity to the LAR of *Pinus taeda* and 41% identity and 60% similarity to the PTR1 of *Lotus japonicus* was identified for PLR-Lu2.

```
                                                                    M
  2   ATATCAAATCCCCTTAACCTTCACAGTATCAAATCCATCTCCGACGAATCCGACAAAATG

      A   A   G   F   L   F   H   M   G   S   L   P   A   I   A   T   V   G   H   K
 62   GCCGCGGGATTCCTATTCCATATGGGATCCCTCCCGGCCATCGCCACCGTCGGCCACAAG

      S   K   V   L   V   I   G   G   T   G   Y   L   G   K   R   L   V   T   A   S
122   AGCAAGGTCCTGGTGATCGGAGGCACAGGTTACTTAGGCAAGAGGCTAGTGACGGCCAGC

      L   A   A   G   H   E   T   Y   V   L   Q   R   P   E   I   G   V   D   I   E
182   TTAGCCGCCGGTCACGAAACCTACGTCCTCCAACGTCCGGAGATCGGCGTCGACATCGAG

      K   I   Q   L   L   L   S   F   K   K   A   G   A   S   L   V   S   G   S   F
242   AAGATCCAGCTCCTGCTTTCGTTTAAAAAGGCCGGTGCAAGCCTCGTCAGCGGCTCGTTC

      N   D   Y   R   S   L   V   D   A   V   K   L   V   D   V   V   I   C   A   V
302   AACGACTACCGCAGCCTCGTCGATGCCGTCAAGCTCGTCGACGTCGTGATCTGCGCCGTC

      S   G   V   H   I   R   S   H   Q   I   L   L   Q   L   K   L   V   D   A   I
362   TCCGGCGTCCACATCCGTAGCCACCAGATCTTGCTCCAGCTCAAGCTCGTTGATGCCATC

      K   E   A   G   N   V   K   R   F   L   P   S   E   F   G   T   D   P   A   T
422   AAAGAAGCCGGTAACGTTAAGAGGTTCTTGCCTTCGGAGTTTGGAACGGATCCGGCAACG

      M   E   N   A   M   E   P   G   R   V   T   F   D   D   K   M   V   V   R   K
482   ATGGAGAACGCGATGGAACCGGGGAGAGTGACGTTCGACGACAAGATGGTGGTGAGGAAG

      A   I   E   E   A   G   I   P   F   T   Y   I   S   A   N   C   F   A   G   Y
542   GCGATAGAGGAAGCTGGGATTCCGTTCACATACATTTCCGCCAATTGCTTCGCCGGTTAC

      F   L   G   G   L   C   Q   P   G   F   I   L   P   S   R   E   Q   V   T   L
602   TTCCTCGGCGGCCTTTGCCAGCCTGGCTTTATTCTTCCTTCACGTGAACAAGTGACTTTG

      L   G   D   G   N   Q   K   A   V   Y   V   D   E   D   D   I   A   R   Y   T
662   CTCGGAGACGGTAACCAGAAAGCTGTTTATGTTGACGAGGACGATATTGCGCGATACACG

      I   K   M   I   D   D   P   R   T   L   N   K   T   V   Y   I   K   P   P   K
722   ATCAAAATGATAGACGATCCTCGTACTCTGAACAAGACGGTCTACATCAAGCCGCCGAAA

      N   V   L   S   Q   R   E   V   V   G   I   W   E   K   Y   I   G   K   E   L
782   AATGTATTGTCCCAACGGGAAGTCGTCGGAATTTGGGAGAAATACATCGGTAAAGAGCTA

      K   K   T   T   L   S   V   E   E   F   L   A   M   M   K   E   Q   D   Y   A
842   AAAAAGACAACCCTGTCCGTGGAAGAGTTCCTCGCGATGATGAAAGAACAAGATTATGCA

      E   Q   V   G   L   T   H   Y   Y   H   V   C   Y   E   G   C   L   T   N   F
902   GAGCAAGTCGGATTGACGCACTACTACCATGTGTGCTACGAAGGGTGCCTTACGAACTTC

      E   I   G   D   E   A   G   E   A   T   K   L   Y   P   E   V   G   Y   T   T
962   GAGATCGGAGATGAAGCCGGTGAGGCTACTAAGCTGTACCCGGAAGTTGGGTACACGACT

      V   V   E   Y   M   K   R   Y   V   -
1022  GTTGTAGAGTATATGAAACGATATGTTTAATATTTTTACAGTATATTATGTGGTACTGTA

1082  ACGTGACTAAAAAAAAGTTCATTATTATAACTTGGTGTTATTGTACCCAAGAAAGAGTGAT

1142  GTCATGATATATATATAATATTTCGTGACAAATTTGGGCTTCAAATTAAAAAAAAAAAAAA

1202  AAA
```

Fig. 3.1. Full length cDNA sequence (untranslated regions and open reading frame) of *PLR-Lu2* and the corresponding amino acids (Accession number EU029951). The start and stop codons are shown in red.

3.2.2. Heterologous expression of PLR-Lu2 in *E. coli*

With the *PLR-Lu2* cDNA putatively encoding a (+)-PLR, our next objective was to prove the functionality of the enzyme by heterologous expression of PLR-Lu2 in active form. The ORF of *PLR-Lu2* was cloned in an expression vector as N-terminal 6-His fusion protein (Fig. 3.2.) in *E. coli*. The protein was purified with Ni-NTA agarose column.

T7-Prom.	Lac operator	rbs	6-His-tag	thrombin	MCS	T7 term.

PLR-ORF

*Nde*I   *Bam*HI
                         or *Xho*I

Fig. 3.2. Schematic structure of the expression region of the pET15b vector with the cloned *PLR*-ORFs.

Catalytic activity was established by the formation of Lari and Seco consequently via incubating purified recombinant PLR-Lu2 with (±)-Pino in the presence of NADPH. No activity was detected either in the absence of substrate and cofactor or when the protein was denatured by boiling. Extracts from cells containing the expression vector lacking an insert did not show any catalytic activity. A time course experiment was performed with 0.5 µg PLR-Lu2 fusion protein. The product formation and substrate utilization was monitored after 0, 2, 5, 10, 15, 20, 25, 30 and 40 min of incubation at 30 °C and a pH of 7.1. Half of the substrate (Pino) was converted to Lari within 10 min; Lari was then completely depleted with concomitant formation of Seco (Fig. 3.3A). Attention was next directed towards the enantiospecificity of PLR-Lu2. The remaining substrate and the formed products corresponding to Pino, Lari and Seco from the above assays were collected by reverse phase HPLC and subjected to chiral column HPLC analysis (Fig. 3.3B).

The remaining Pino and the formed Seco in the assays with PLR-Lu2 fusion protein consist of the pure (-)-enantiomer. There is a rapid depletion of (+)-Pino in the assay mixture, whereas the content of the (-)-antipode remains essentially unchanged. (+)-Lari then builds up and levels off consequently while the (-)-Seco content increases.

A)
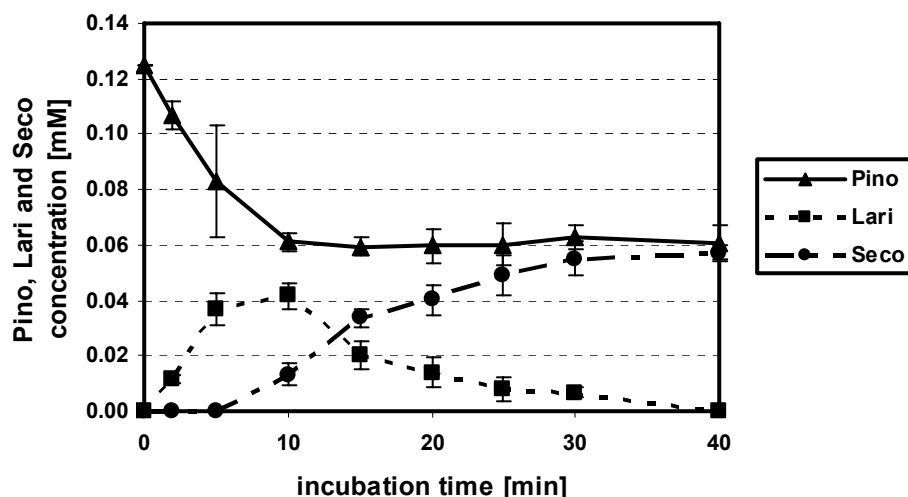
B)
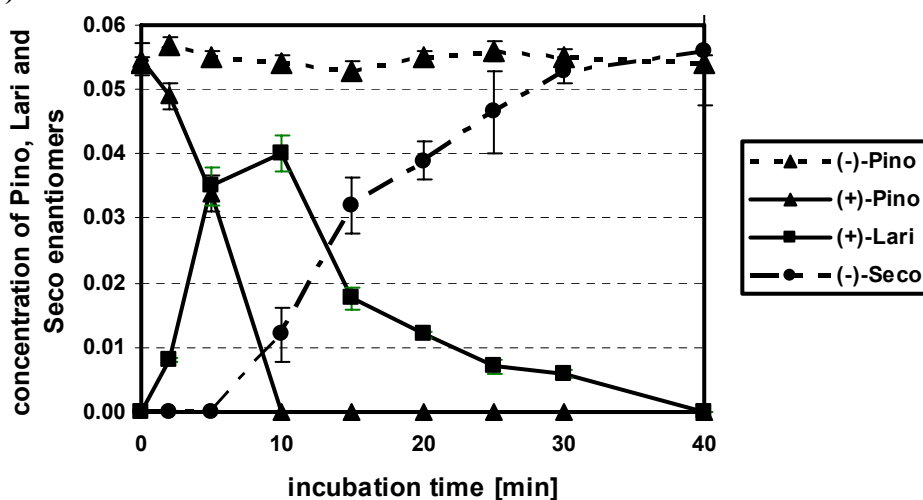
Fig. 3.3. A) Turnover of pinoresinol (Pino) and formation of lariciresinol (Lari) and secoisolariciresinol (Seco) following incubation of racemic Pino with 0.5 μg of recombinant purified PLR-Lu2 with different time intervals. Experiments were carried out three times each in duplicate. **B)** Enantiomeric composition of Pino, Lari and Seco antipodes.

PLR-Lu1 which was cloned by von Heimendahl et al. (2005) and is assumed to be responsible for the formation of (+)-Seco, was characterized for time intervals up to 20 min (Fig. 3.4A).

Seco was formed while the amount of Pino decreased until half of the Pino was used. Lari was not observed as an intermediate. Therefore, we assume that it is immediately reduced to Seco. The chiral analysis of the educts and products shows that from the racemic mixture of Pino, only (-)-Pino was used to form only (+)-Seco. (Fig. 3.4B).

A)

B)
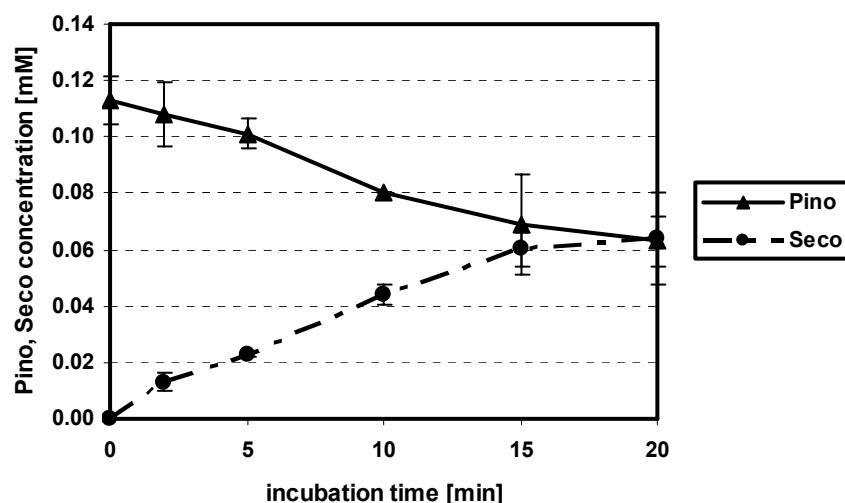

Fig. 3.4. A) Turnover of pinoresinol (Pino) and formation of secoisolariciresinol (Seco) following incubation of racemic Pino with 2.5 µg of recombinant purified PLR-Lu1 with different time intervals. Experiments were carried out three times each in duplicate. **B)** Enantiomeric composition of Pino and Seco antipodes.
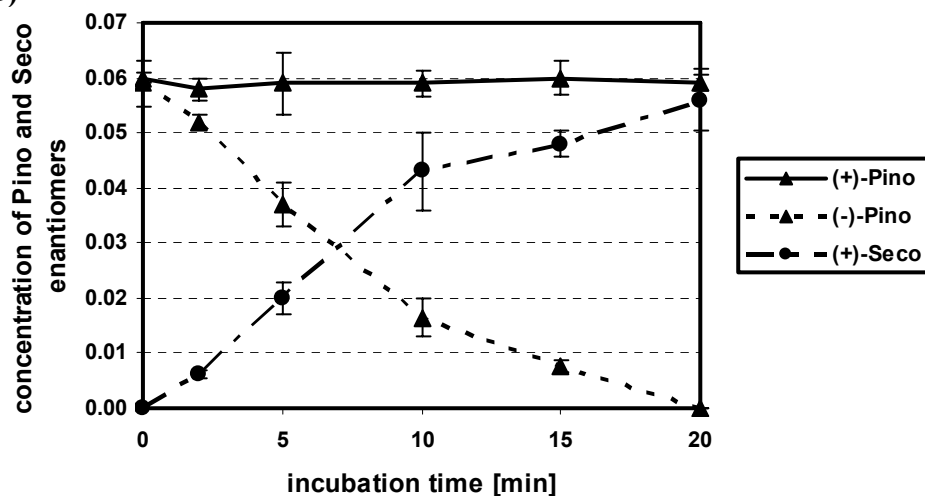
3.2.3. *Organ specific expression of PLR-Lu1 and PLR-Lu2 in L. usitatissimum*

In order to establish the organ specificity of *PLR-Lu1* and *PLR-Lu2* gene expression in *L. usitatissimum*, semiquantitative RT-PCR was conducted. Given the considerable homology (63% identity, 78% similarity), between *PLR-Lu1* and *PLR-Lu2*, specific primers was designed in order to eliminate the potential for unwanted cross reactivity and nonspecific binding (see methods). The specificity of both primers proved further by performing RT-PCR on the DNA-plasmid level of *PLR-Lu1* and *PLR-Lu2* separately. Transcript levels of *PLR-Lu1* and *PLR-Lu2* was evaluated in an organ specific manner after 26 cycles. An *actin* gene was amplified from the same organs as control. As shown in Fig. 3.5 *PLR-Lu1* was strongly expressed in seeds as well as roots whereas in leaves and stems its expression was absent. *PLR-Lu2* was expressed in all tested organs. The strongest signal of *PLR-Lu2* was detected in leaves and to a lesser extent was expressed in other organs.

leaf	stem	root	seed	
				PLR-Lu1
				PLR-Lu2
				actin

Fig. 3.5. RT-PCR analysis of *plr-Lu1* and *plr-Lu2* gene expression after 26 cycles in different organs of *L. usitatissimum*. An *actin* gene from the same lines was amplified to determine equal amounts of cDNA template.

3.3. Detection of PLR activity in cell cultures of *L. perenne*

According to the structures found in *L. perenne* we have proposed a hypothetic biosynthetic pathway (Fig. 1.8) for arylnaphthalene lignans. In order to prove whether the first steps of the biosynthesis of Jus B are similar to the first steps of the lignan biosynthesis in *F. intermedia*, PLR was chosen as an enzyme maybe involved in the biosynthesis of Jus B. In the first step to investigate if any PLR activity can be observed in cell suspension culture of *L. perenne*, proteins were fractionated with $(NH4)_2SO_4$ precipitation. The fractionation was performed in four steps (0-20%, 20-40%, 40-60% and 60-80%). Salting out depends on the hydrophobic nature of the precipitated protein. Proteins with more hydrophobic patches aggregate and precipitate before those with smaller and fewer patches. In the fraction which was precipitated

with 40-60% $(NH4)_2SO_4$, only the conversion of Pino to Lari was observed. Usually the enzymes involve in the biosynthesis of secondary metabolism are expressing in low amounts. Traditional purification of these enzymes is complicated and time consuming. This will be easier by cloning and heterologous overexpression of the related enzymes in different systems like *E. coli*.

3.3.1. Cloning of a sequence encoding a *PLR* from *L. perenne*

A full length cDNA with 1145 bp encoding a putative PLR (*PLR-Lp1*, GenBank accession number EF050530) was cloned by an RT-PCR with degenerated primers followed by 5′- and 3′-RACE PCR. The translational start of the ORF is at nucleotide 75, the TGA stop at nucleotide 1017 encoding a polypeptide of 314 amino acids (Fig. 3.7). The *PLR-Lp1* shows highest similarities to the PLR-Lu1 of *L. usitatissimum* (80% identity and 87% similarity) and the PLR-La1 of *L. album* (66% identity and 79% similarity) on amino acid level. PLR-Lp1 shows lower similarities to PCBERs (48% identity and 65% similarity to a PCBER of *Pinus taeda*; 41% identity and 65% similarity to a PCBER of *Populus balsamifera*). No significant sequence similarity to an IFR was observed. Next, genomic DNA was digested to completion with either *Eco*RI, *Eco*RV, *Xba*I, which do not cut in the cDNA, and *Bgl*II and *Hind*III which cut 13 bp and 67 bp before the 3′-end of the cDNA. The ORF of *PLR-Lp1* was used as probe. For each restriction digest at least two bands were observed indicating that *PLR-Lp1* belongs to a small gene family in the genome of *L. perenne* H (Fig. 3.6).
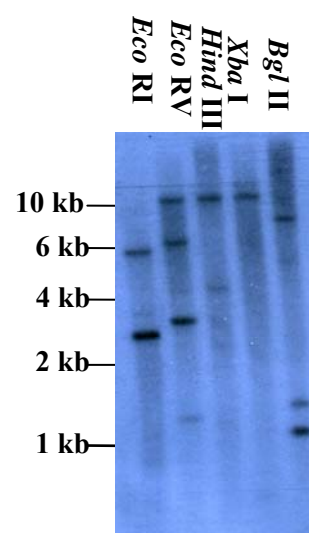
Fig. 3.6. Southern hybridisation of *L. perenne* genomic DNA. DNA was digested with *Eco*RI, *Eco*RV, *Hind*III, *Xba*I, *Bgl*II. The resulting membranes were probed with the open reading frae of m*PLR-Lp1*.

```
   3   AATCTTTTCGAAACGAGAGAAATCTAACTCACTTCTTCCTCGATCACGAATCTCGAGAAA

                       M  K  P  C  S  V  L  V  V  G  G  T  G  Y  I  G
  63   ATTTCTCGAATCATGAAGCCGTGTAGTGTGCTCGTGGTGGGAGGTACAGGGTACATCGGG

        K  R  I  V  S  A  S  L  Y  L  G  H  D  T  Y  V  L  K  R  P
 123   AAGAGGATTGTGAGTGCGAGTCTCTACCTTGGCCACGACACCTATGTCCTCAAGCGACCT

        G  T  G  L  D  I  E  K  L  Q  L  L  L  S  F  K  K  R  G  A
 183   GGGACAGGGCTTGACATCGAGAAGCTCCAGCTCTTGCTGTCGTTTAAAAAACGAGGCGCT

        H  L  V  E  A  S  F  S  D  H  D  S  L  V  R  A  V  R  L  V
 243   CATTTGGTTGAGGCCTCGTTCTCTGATCATGATAGCCTTGTTCGTGCCGTGAGGTTGGTT

        D  V  V  I  C  T  M  S  G  V  H  F  R  S  H  N  I  L  L  Q
 303   GATGTCGTGATATGTACCATGTCTGGGGTTCACTTCCGGTCGCATAACATTCTGCTTCAG

        L  K  L  V  E  A  I  K  E  A  G  N  V  K  R  F  I  P  S  E
 363   TTGAAGCTCGTCGAGGCCATTAAGGAGGCGGGGAATGTTAAGAGGTTCATTCCGTCGGAG

        F  G  M  D  P  A  R  M  G  Q  A  M  E  P  G  R  E  T  F  D
 423   TTTGGGATGGACCCAGCGAGGATGGGACAAGCGATGGAGCCAGGGAGGGAGACGTTCGAT

        Q  K  M  V  V  R  K  A  I  E  E  A  N  I  P  H  T  Y  I  S
 483   CAGAAGATGGTGGTGAGGAAGGCGATCGAGGAGGCGAACATTCCTCACACGTACATCTCG

        A  N  C  F  A  G  Y  F  V  G  N  L  S  Q  L  G  T  L  T  P
 543   GCAAACTGCTTCGCGGGTTACTTCGTCGGCAATCTTTCGCAGCTCGGAACCCTAACCCCG

        P  S  D  K  V  I  I  Y  G  D  G  N  V  K  V  V  Y  V  D  E
 603   CCTTCCGATAAGGTCATCATCTATGGAGATGGCAATGTCAAAGTTGTGTACGTGGACGAG

        D  D  V  A  K  Y  T  I  K  A  I  E  D  D  R  T  V  N  K  T
 663   GACGATGTGGCCAAGTACACGATCAAGGCGATCGAAGATGATCGGACGGTGAACAAGACG

        V  Y  L  R  P  P  E  N  M  M  S  Q  R  E  L  V  A  V  W  E
 723   GTGTACCTAAGGCCGCCGGAGAATATGATGAGTCAAAGAGAGTTGGTGGCCGTTTGGGAG

        K  L  S  G  N  Q  L  E  K  I  E  L  P  P  Q  D  F  L  A  L
 783   AAGCTCTCAGGCAACCAACTTGAGAAGATTGAACTTCCCCCACAAGACTTTCTTGCACTA

        M  E  G  T  T  V  A  E  Q  A  G  I  G  H  F  Y  H  I  F  Y
 843   ATGGAAGGGACAACTGTGGCAGAGCAGGCCGGGATCGGGCACTTCTACCACATCTTCTAC

        E  G  C  L  T  N  F  E  I  N  A  E  N  G  E  E  E  A  S  R
 903   GAGGGATGCCTGACGAACTTCGAGATCAACGCCGAAAACGGGGAAGAAGAAGCTTCGAGA

        L  Y  P  E  V  E  Y  T  R  V  H  D  Y  L  K  I  Y  L  -
 963   TTGTACCCTGAAGTTGAGTACACTCGTGTCCATGATTACTTGAAGATCTACCTTTGAAGA

1023   TAAGTTACTTGGTACTAGTTTCTTTGTACCATTTTGAACAATTTGTACCACTTGTTGTTG

1083   TTGGACACGTGTCACTTTCCCATTAAATGATGTAATTTTTTCAACTAAAAAAAAAAAAAA

1143   AAA
```

Fig. 3.7. Full length cDNA sequence (untranslated regions and open reading frame) of *PLR-Lp1* and the corresponding amino acids (Accession number EF050530). The start and stop codons are shown in red.

### 3.3.2. Functional expression of PLR-Lp1 in *E. coli*

The ORF of *PLR-Lp1* was cloned in an expression vector for the heterologous expression as N-terminal 6-His fusion protein in *E. coli*. An SDS gel was running with fractions obtained during purification process of the recombinant protein (Fig. 3.8).
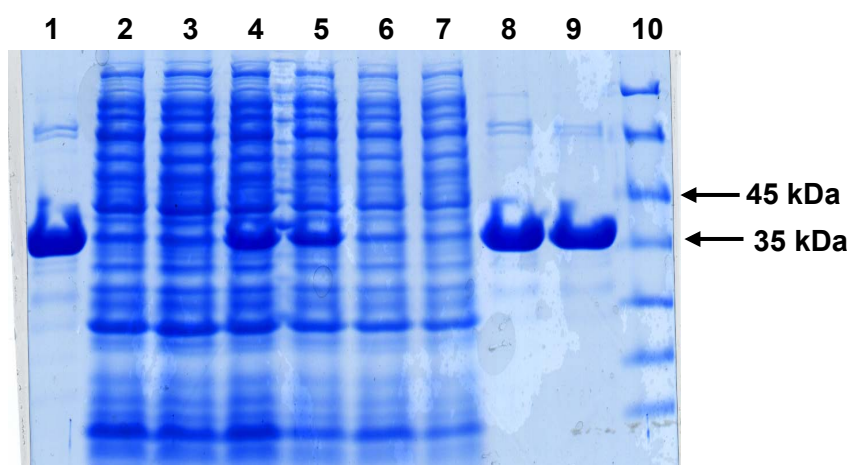

Fig. 3.8. Purification of PLR-Lp1 from a heterologous bacterial system. Lanes 1,8 and 9 show the final purified protein (35 kDa); lanes 2 and 3 are the wash fraction; lanes 4 and 5 are the crude enzyme extract; lanes 6,7 show the affinity purification flowthrough; lane 10 is molecular weight marker

Enzyme assays were performed with purified recombinant PLR-Lp1 protein. The formation of Lari as well as Seco by using racemic Pino as substrate was observed. No activity was measured in extracts from cells containing the expression vector lacking an insert or when either cofactor was omitted or when the enzyme was denatured (boiled for 15 min). DDC, a substrate for PCBERs was not converted by PLR-Lp1. Racemic Pino is completely converted into Lari with protein concentrations as low as 0.1 μg in assays carried out at 30 °C, pH 7.1 for 3 h with different protein concentrations (Fig. 3.10A). With increasing protein concentrations Lari is completely converted into Seco. To determine the enantiospecificity of PLR-Lp1, the Pino, Lari and Seco from the assays was collected and further analysed with chiral column HPLC (Fig. 3.9 and Fig. 3.10B-D). Both enantiomers of Pino have been converted to (+)- and (−)-Lari, respectively, with preference for the (+)- rather than the (−)- enantiomer. Both enantiomers of Lari are used effectively, but, with a preference for (−)-Lari.

Analogous results were obtained for depletion of Pino and formation of Seco with variation of the reaction time from 2 min to 24 h. When pure (+)-Pino or (+)-Lari were used, depletion of these substrates occurred within the same time scale and with the same protein concentrations as for assays with the racemic substrates indicating that one of the enantiomers does not influence the affinity of the other to the protein.
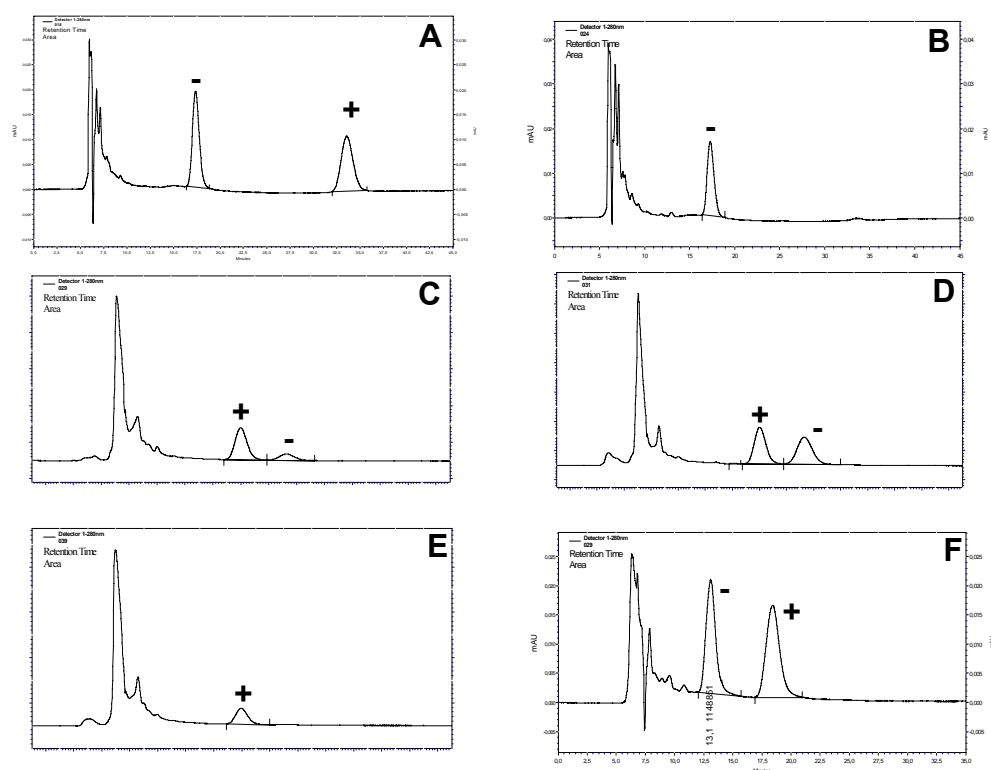
Fig. 3.9. Chiral column HPLC analysis obtained following reduction of racemic Pino by PLR-Lp1. **A)** Pino isolated from the assay with 0.001 μg protein [ratio of (+):(-) = 49:51]; **B)** Pino obtained following the reduction of racemic Pino with 0.05 μg protein [100% (+)]; **C)** Lari obtained following the reduction of racemic Pino with 0.05 μg protein [ratio of (+):(-) = 67:33]; **D)** Lari obtained following the reduction of racemic Pino with 0.1 μg protein [ratio of (+):(-) = 52:48]; **E)** Lari obtained following the reduction of racemic Pino with 7 μg protein [ratio of (+):(-) = 92:8]; **F)** Seco obtained following the reduction of racemic Pino with 15 μg protein [ratio of (+):(-) = 52:48].
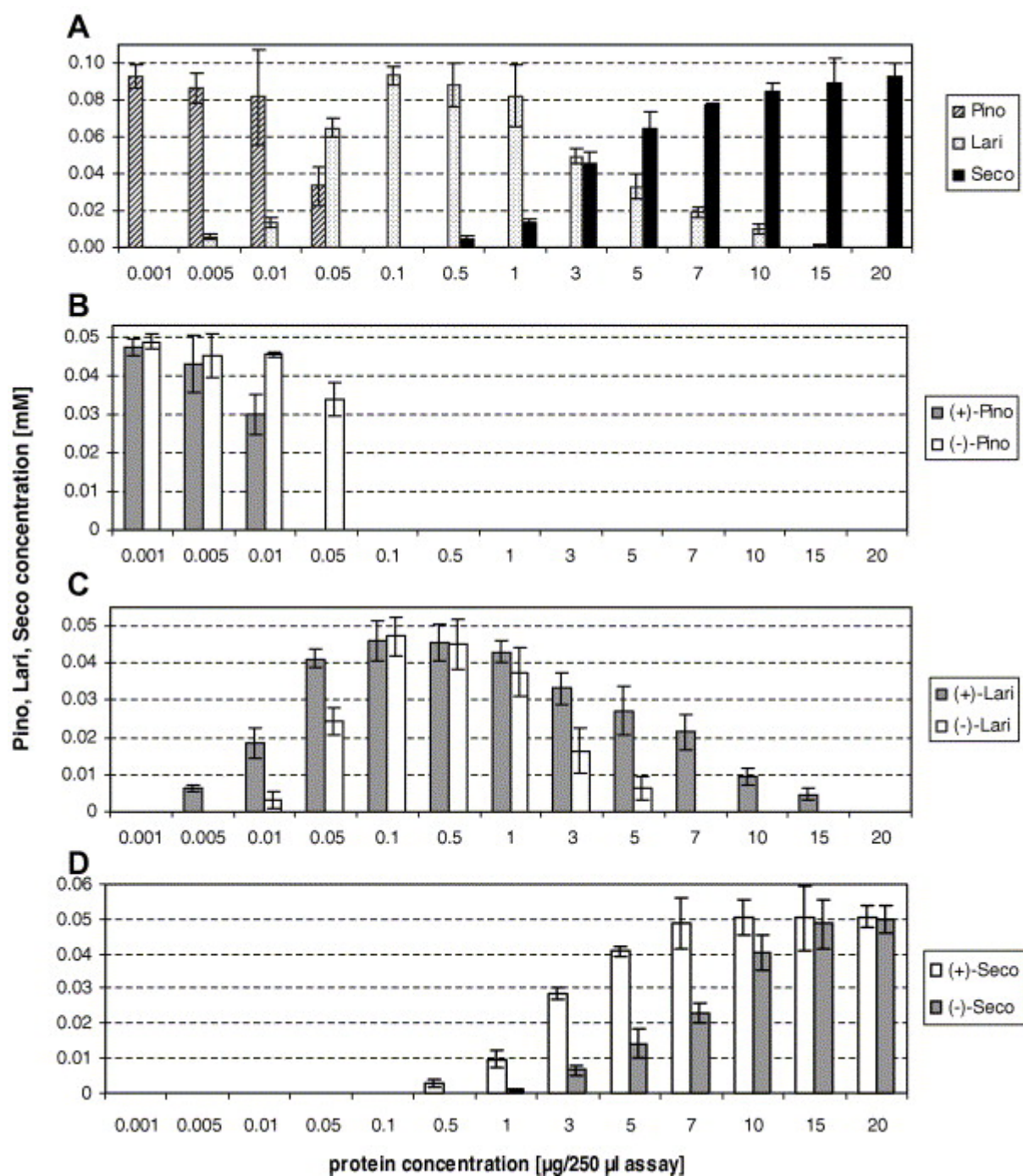
Fig. 3.10. Turnover of pinoresinol (Pino) and formation of lariciresinol (Lari) and secoisolariciresinol (Seco) following incubation of racemic Pino with different amounts of recombinant purified PLR-Lp1 for 3 h **(A)**. Enantiomeric composition of Pino **(B)**, Lari **(C)** and Seco **(D)**. Experiments were carried out six times each in duplicate.

3.4. Sequence homology comparison between PLR-Lu2 and PLR-Lp1

Amino acid sequences are responsible for the structures and properties of proteins. It is evident that despite the enormous variability of proteins, particular structural elements are rather conservative and these elements govern to a large extent the function of the protein molecule. This is more pronounced in the case of proteins possessing the catalytic functions.

In terms of identifying the regions of the polypeptide chain involved in NAD(P)H binding, there is a limited number of invariant amino acids in the sequences of different reductases that are viewed to be diagnostic. These include three conserved glycine residues with the sequence GXGXXG, where X is any conserved hydrophobic residue. The glycin-rich region is viewed to play a central role in positioning NAD(P)H in its correct conformation. This conserved region was observed both for PLR-Lu2 and PLR-Lp1 (Fig. 3.11).

More importantly, a Lys residue that is conserved among all PIP reductases and which is thought to be involved in catalysis as a general base, is also present (Lys^{156} in PLR-Lu2 and Lys^{138} in PLR-Lp1). Four positions of PLRs are important for determining enantiospecificity. In (-)-Seco forming PLRs like PLR-Lu2 these four conserved amino acids are Met^{146}, Gly^{285}, Tyr^{289} and Val^{322} respectively. For PLRs which produce only (+)-Seco like PLR-Lu1 these four conserved positions are Leu^{126}, Val^{265}, Leu^{269} and Met^{304}. In PLR-Tp1 Val^{265} and Leu^{269} are in the binding pocket for the substrate and also suggested by Min et al. (2003) as involved in enantiospecificity. Leu^{128} and Met^{304} are at the borders of the pocket. In PLR-Lp1 three regions are conserved as (-)-Seco forming system corresponding to Met^{128}, Gly^{267} and Val^{306}, but Phe^{271} is found instead of Tyr.

```
PLR-Lu2   MAAGFLFHMG-SLPAIATVGHKSKVLVI GGTGYLG KRLVTASLAAGHETYVLQRPEIGVD 59
PLR-La1   --MGSLGKVNNEIPTKSSGG--SKVLVI GGTGYLG KRLVKASLDSGHDTYVMHRPEIGVD 56
PLR-Fi1   --MG-------------KSKVLII GGTGYLG RRLVKASLAQGHETYILHRPEIGVD 41
PLR-TP2   --MEE------------SSRVLIV GGTGYIG RRIVKASIALGHPTFILFRKEVVSD 42
PLR-Lu1   --MG---------RCRVLVV GGTGYIG KRIVKASIEHGHDTYVLKRPETGLD 41
PLR-TP1   --MDK--------KSRVLIV GGTGYIG KRIVNASISLGHPTYVLFRPEVVSN 42
PLR-Lp1   --MK---------PCSVLVV GGTGYIG KRIVSASLYLGHDTYVLKRPGTGLD 41
                        . **::.*****:*.*:*.**:  ** *:::  *       :

PLR-Lu2   IEKIQLLLSFKKAGASLVSGSFNDYRSLVDAVKLVDVVICAVSGVHIRSHQILLQLKLVD 119
PLR-La1   IEKVQLLLSFKMQGAHLVSASFDDQRSLVDAVKLVDVVICAISGVHIRSHQILLQLKLVE 116
PLR-Fi1   IDKVEMLISFKMQGAHLVSGSFKDFNSLVEAVKLVDVVISAISGVHIRSHQILLQLKLVE 101
PLR-TP2   VEKVEMLLSFKKNGAKLLEASFDDHESLVDAVKQVDVVISAVAGNHMRHH-ILQQLKLVE 101
PLR-Lu1   IEKFQLLLSFKKQGAHLVEASFSDHESLVRAVKLVDVVICTVSGAHSRS--LLLQLKLVE 99
PLR-TP1   IDKVQMLLYFKQLGAKLIEASLDDHQRLVDALKQVDVVISALAGGVLSHH-ILEQLKLVE 101
PLR-Lp1   IEKLQLLLSFKKRGAHLVEASFSDHDSLVRAVRLVDVVICTMSGVHFRSHNILLQLKLVE 101
                  ::*.::*: **   **  *:..*:.*    ** *:: *****.:::*      :* *****:
                                          ▼

PLR-Lu2   AIKEAGNVKRFLPSEFGTDPAT-MENAMEPGRVTFDDKMVVRKAIEEAGIPFTYISANCF 178
PLR-La1   AIKEAGNVKRFVPSEFGTDPAR-MENAMEPGRITFDDKMVVRRAIEEAGIPFTYVSANCF 175
PLR-Fi1   AIKEAGNVKRFLPSEFGMDPAKFMDTAMEPGKVTLDEKMVVRKAIEKAGIPFTYVSANCF 161
PLR-TP2   AIKEAGNIKRFVPSEFGMDPGL-MEHAMAPGNIVFIDKIKVREAIEAASIPHTYISANIF 160
PLR-Lu1   AIKEAGNVKRFIPSEFGMDPAR-MGDALEPGRETFDLKMVVRKAIEDANIPHTYISANCF 158
PLR-TP1   AIKEAGNIKRFLPSEFGMDPDI-MEHALQPGSITFIDKRKVRRAIEAASIPYTYVSSNMF 160
PLR-Lp1   AIKEAGNVKRFIPSEFGMDPAR-MGQAMEPGRETFDQKMVVRKAIEEANIPHTYISANCF 160
                  *******:***:***** **    *   *: **   .:  *   **.*** *.**.**:*:* *

PLR-Lu2   AGYFLGGLCQPG-FILPSREQVTLLGDGNQKAVYVDEDDIARYTIKMIDDPRTLNKTVYI 237
PLR-La1   AGYFLGGLCQPG-YILPSRDHVTLLGDGDKKGVYVDEDDTAAYTLRAIDDPRTLNKTIYV 234
PLR-Fi1   AGYFLGGLCQFG-KILPSRDFVIIHGDGNKKAIYNNEDDIATYAIKTINDPRTLNKTIYI 220
PLR-TP2   AGYLVGGLAQLG-RVMPPSEKVILYGDGNVKAVWVDEDDVGIYTIKAIDDPHTLNKTMYI 219
PLR-Lu1   GGYFVGNLSQLG-PLTPPSDKVTIYGDGNVKVVYMDEDDVATYIMTIEDDRTLNKTMYL 217
PLR-TP1   AGYFAGSLAQLDGHMMPPRDKVLIYGDGNVKGIWVDEDDVGTYTIKSIDDPQTLNKTMYI 220
PLR-Lp1   AGYFVGNLSQLG-TLTPPSDKVIIYGDGNVKVVYVDEDDVAKYTIKAIEDDRTVNKTVYL 219
                  .**: *.*.* .  :  *.  :  *  ***: *  ::  :*** .  *::  *:* :*:***:*:
                                                         ▼      ▼

PLR-Lu2   KPPKNVLSQREVVGIWEKYIGKELKKTTLSVEEFLAMMKEQDYAEQVGLTHYYHVCYEGC 297
PLR-La1   KPPKNVLSQREVVGIWEKYIGKELQKTILSEQDFLATMREQNYAEQVGLTHYYHVCYEGC 294
PLR-Fi1   SPPKNILSQREVVQTWEKLIGKELQKITLSKEDFLASVKELEYAQQVGLSHYHDVNYQGC 280
PLR-TP2   RPPLNILSQKEVVEKWEKLSGKSLNKINISVEDFLAGMEGQSYGEQIGISHFYQMFYRGD 279
PLR-Lu1   RPPENVITHRQLVETWEKLSGNQLQKTELSSQDFLALMEGKDVAEQVVIGHLYHIYYEGC 277
PLR-TP1   RPPMNILSQKEVIQIWERLSEQNLDKIYISSQDFLADMKDKSYEEKIVRCHLYQIFFRGD 280
PLR-Lp1   RPPENMMSQRELVAVWEKLSGNQLEKIELPPQDFLALMEGTTVAEQAGIGHFYHIFYEGC 279
                   ** *::::::::  **:    :.*.*  :. ::*** :.      ::    *  :.: :.*
                                                         ▼

PLR-Lu2   LTNFEIGDEAG--EATKLYPEVGYTTVVEYMKRYV 330
PLR-La1   LSNFEVDDEQ---EASKLYPDVHYTTVEEYLKRYV 326
PLR-Fi1   LTSFEIGDEE---EASKLYPEVKYTSVEEYLKRYV 312
PLR-TP2   LYNFEIGPNG--VEASQLYPEVKYTTVDSYMERYL 312
PLR-Lu1   LTNFDIDAAQDQVEASSLYPEVEYIRMKDYLMIYL 312
PLR-TP1   LYNFEIGPNA--IEATKLYPEVKYVTMDSYLERYV 313
PLR-Lp1   LTNFEINAENGEEEASRLYPEVEYTRVHDYLKIYL 314
                  * .*::.      **: ***:* *  : .*:  *:
```

Fig. 3.11. The conserved sequence "GxxGxxG" of the NADPH binding domain is shown in the square. Black triangles indicate amino acid positions which are discussed to be involved in stereospecificity by Min et al. (2003). (+)-PLR amino acid sequences are indicated in red. (-)-PLR amino acid sequences are shown in blue.

3.5. RNA silencing of *PLR-Lp1* in hairy roots of *L. perenne*

3.5.1. Construction of ihpRNAi vector

To demonstrate if PLR-Lp1 involves in the biosynthesis of Jus B and Diph glycoside derivatives, a part of *PLR-Lp1* gene was used to build an intron containing hairpin RNA construct using the pHANNIBAL vector. The expression of such construct leads to the formation of dsRNA which reduces the mRNA level of the target gene via the RNAi mechanism. Following the construction of hpRNAi cassettes (chapter 2.2.22.1), correctness of each cloning step was proven by restriction hydrolysis and gel electrophoresis. The *PLR* part with *Xba*I, *Xho*I, *Cla*I and *Kpn*I polylinkers was first cloned into the pGEM®-T vector and sequenced (pSH2) (Fig. 3.12A). pSH2 was cloned in the sense orientation of the pHANNIBAL vector (pSH3) (Fig. 3.12B). Digestion of the pSH3 construct with *Kpn*I and *Xho*I resulted in the separation of two bands app. at 652 bp and 6.0 kb corresponding to the *PLR* part in the sense direction and the pHANNIBAL vector cassette, respectively. pSH4 (Fig. 3.12C) was hydrolyzed by *Xba*I and *Cla*I showed two fragment app. at 652 bp (*PLR* in antisense direction) and 6.652 kb (pHANNIBAL + *PLR* in the sense direction). pSH4 DNA-plasmid was separately digested with *Kpn*I and *Xho*I, as the over proof. Hydrolysis with *Kpn*I resulted to the formation of two fragments on the gel, the smaller at 741 bp of pdk intron. By *Xho*I digestion a band at 2.045 kb was detected corresponding to the *PLR* sense + pdk intron + *PLR* antisense. pSH5 construct (Fig. 3.12D) was restrictly hydrolyzed with *Not*I, to prove whether pSH4 is correctly cloned into pART27 vector. As the expression cassette of pHANNIBAL is 3.0 kb, the fragment which was observed at 4.3 kb corresponds to the expression cassette + *PLR* sense + *PLR* antisense; the largest fragment at app. 11 kb is the pART27 vector (10.9 kb). Restriction hydrolysis of the control construct (pDI25) with *Not*I, results to a band at 2.95 kb of pHANNIBAL expression cassette and a 10.9 kb fragment of pART27.

A)

B)

C)

D)
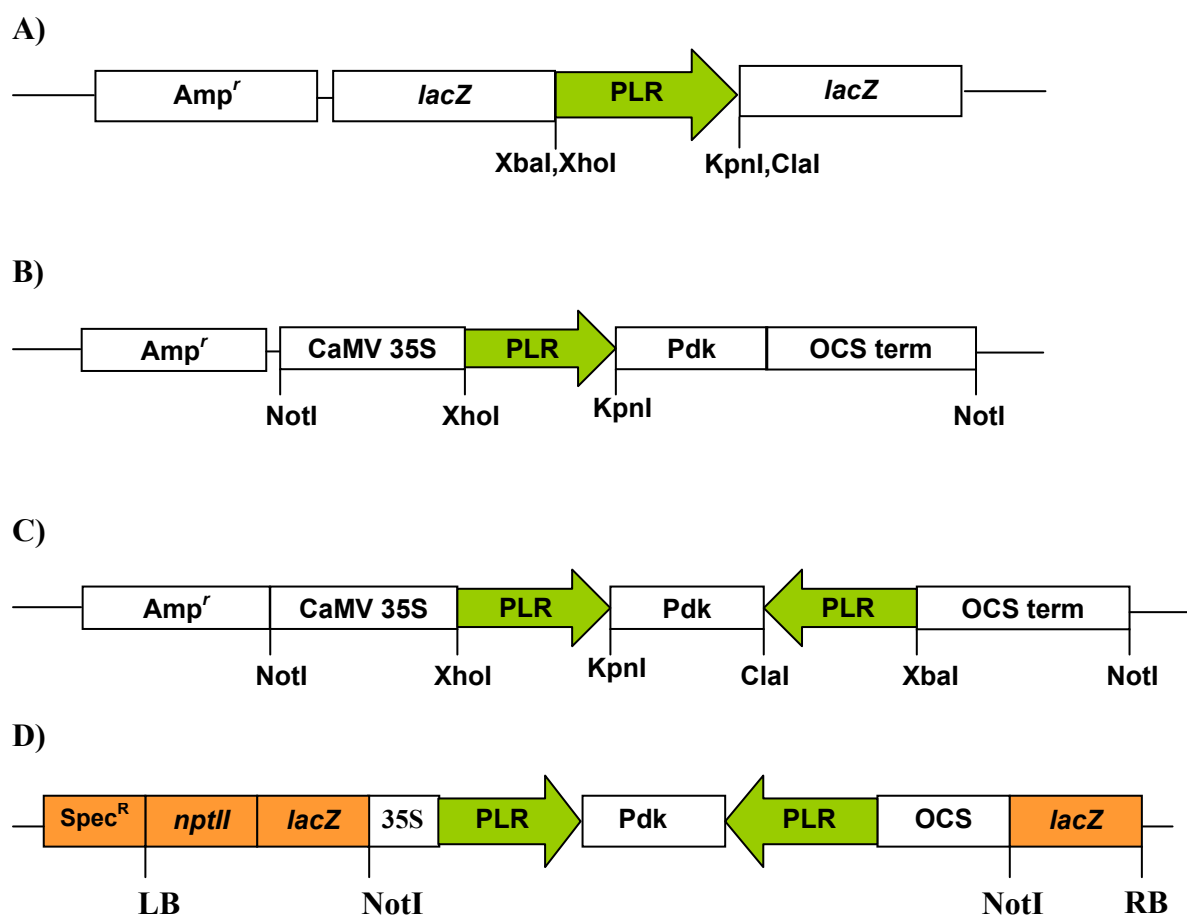
Fig. 3.12. An ihpRNAi construct with the PLR of *L. perenne* in the sense and antisense direction. **A)** pSH2 construct (*PLR-Lp* fragment in pGEM®-T vector). **B)** pSH3 construct (*PLR-Lp* part in the sense direction of the pHANNIBAL vector). **C)** pSH4 construct (*PLR-Lp* part in the sense and antisense direction of the pHANNIBAL vector). **D)** pSH5 construct (*PLR-Lp* part in the sense and antisense direction in the binary vector pART27).

3.5.2. Selection of putative transformants by aminoglycosides

To establish a selection protocol sensitivity of normal *L. perenne* hairy roots without foreign gene constructs, kanamycin was first investigated, as the aminoglycoside which is commonly used for the selection process. The cells appeared to be tolerant to kanamycin with concentrations as much as 250 mgl^{-1} which led only to slightly reduced cell proliferation. Since sensitivity to kanamycin was not sufficient to allow this antibiotic to be used as a selectable marker, the effect of paromomycin, another aminoglycoside inactivated by the *npt*II gene product, was tested as was suggested by others (Belny et al. 1997).

A progressive decline in cell proliferatin with increasing concentration was observed with a total necrosis at 200 mgl^{-1}. Therefore, 200 mgl^{-1} paromomycin was used for selection of transformants (Fig. 3.13).

A   **B**   **C**
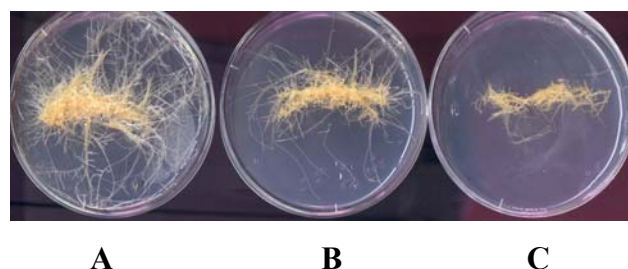
Fig. 3.13. *L. perenne* hairy roots without construct on: **A)** Mc Cown medium, **B)** with 250 mgl^{-1} kanamycin and **C)** with 200 mgl^{-1} paromomycin 8 weeks after inoculation.

3.5.3. Analysis of transgenic hairy roots

Six independent hairy root lines carrying the ihpRNAi transgene (H 1–6), five control lines with the empty construct (E 1–5) and five controls without construct (T 1–5) showed comparable growth and typical hairy root morphology. They were further analyzed after removing the agrobacteria by addition of 100 mgl^{-1} timentin$^{®}$ to the medium, which was shown by PCR for the *virC* gene. The hairy root status was proven via the presence of the *rolC* gene by PCR.

To prove the integration of T-DNA, the *rol*C gene (540 bp) was amplified with specific primers (chapter 2.2.23.1). The rolC gene was detected in transformed lines as well as the positive control (Fig. 3.14A). To confirm whether the detection of the *rol*C gene by PCR in hairy root-derived plants was the result of true transformation and to rule out the possibility of residual growth of *A. rhizogenes* in hairy roots, a second PCR using primers specific for the *vir*C gene was performed. Agarose gel electrophoresis revealed a band of app. 730 bp that corresponded to a fragment of the *vir*C gene only with the DNA from *A. rhizogenes*. After several subcultivation cycles in medium containing timentin$^{®}$ each hairy root line was free from *A. rhizogenes*. If any line had still *vir* amplicone addition of timentin$^{®}$ to the medium was further continued.

To confirm integration of the *PLR* into the transgenes the primer combination as mentioned (chapter 2.2.23.2) corresponding to a sequence specific primer for 35S-promoter as the forward primer and PLRPHAN-R as the reverse primer. The 35S primer results only in the amplification of integrated *PLR* but not the endogenous one. A band at app 700 bp was amplified in the hairy root lines with hpRNAi construct, whereas the lines with empty vector did not show any amplicon (Fig. 3.14B).

A
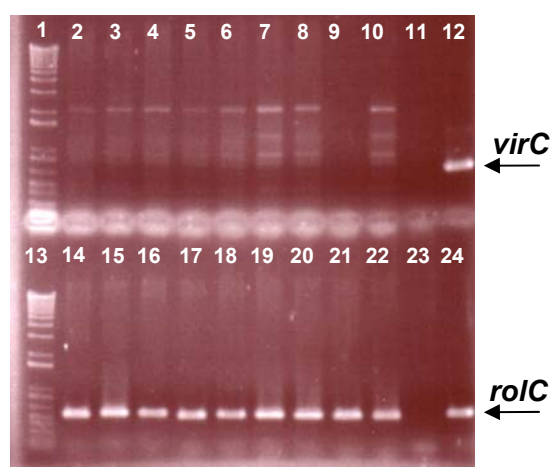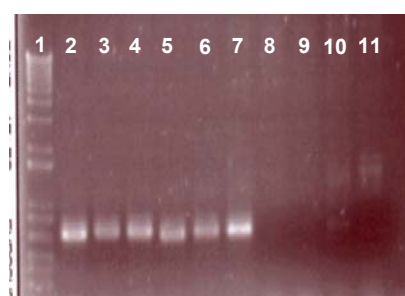
Fig. 3.14. A) Agarose gel electrophoresis of PCR-amplified products from genomic DNA of hairy roots of *L. perenne* with *virC* (lanes 2-12) and *rolC* (lanes 14-24) primers

Lane 1, 13: 1kb$^+$ ladder; lanes 2-5 and 14-17: hairy root lines containing hpRNAi construct; lanes 6-10 and18-22: hairy root lines with empty vector; lane 11 and 23: H_2O as (-)-control, lane 12 and 24: DNA from TR105 as (+)-control.

B) Analysis of the presence of 35S-PLR transgene in hairy roots of *L. perenne*. Lane 1: 1kb$^+$ ladder; Lanes 2-7: hairy root lines containing hpRNAi construct; lanes 8-11: hairy root lines with empty vector.

L. perenne hairy root control lines E and T accumulate 29-38 mg/g DW Jus B as the major lignan beside the two Diph glycosides indicating no influence of the ihpRNAi construct without *PLR-Lp1* sequences on the lignan content (Fig 3.15). The content of Jus B and the Diph glycosides in lines H was significantly reduced to 6–11 mg/g DW Jus B. The identity of the lignans was confirmed by HPLC and LC–MS in comparison to authentic standards. By down regulating the expression of the *PLR* gene not only suppression of the arylnaphthalene compounds as the end product but also the increase in concentration of the substrates for the

PLR gene was expected. This was first observed by overlaying the chromatograms of suppressed and control lines on each other.
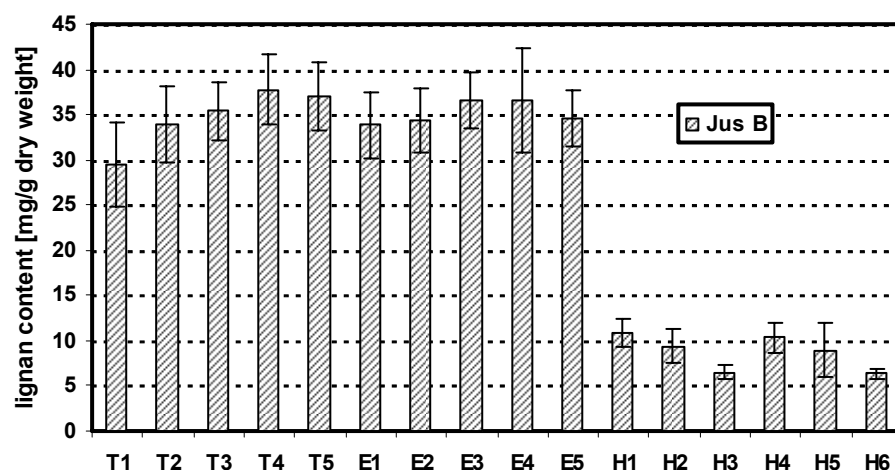
Fig. 3.15. Justicidin B (Jus B) content in hairy roots of *Linum perenne* Himmelszelt: (T1–5) lines without any construct, (E1–5) lines with empty vector, (H1–6) lines with ihpRNAi construct. The lignan content was determined in triplicate.

These two additional peaks with ESI-MS spectra very similar to those of Pino and Lari were observed in ihpRNAi lines beside a slightly increased Pino content. The ESI mass spectra of the more polar compound (eluting at Rt 4.6 min) recorded in the positive and negative ion modes pointed towards the presence of a Lari derivative. The positive ion spectrum showed a quasimolecular peak $[M + NH_4]^+$ at *m/z* 540 along with a base peak at *m/z* 219 characteristic for Lari and Seco. The negative ion spectrum consistently displayed $[M-H]^-$ at *m/z* 521 and a fragment corresponding to the loss of the hexose moiety $[M-H-(C_6H_{10}O_5)]^-$ at *m/z* 359, so that the presence of a Lari monohexoside is likely. The less polar compound (eluting at Rt 6.5 min) mass spectrometrically resembled Pino. However, in the positive ion mode, a quasimolecular ion $[M + NH_4]^+$ was observed at *m/z* 538, followed by fragments at *m/z* 359 and 341, $[M + H-C_6H_{10}O_5]^+$ and $[M + H-C_6H_{12}O_6]^+$, respectively, corresponding to loss of a hexose moiety. In the negative ion spectrum, the quasimolecular peak $[M-H]^-$ appeared at *m/z* 519 and a following fragment was observed at *m/z* 357, resulting from loss of the hexose moiety $[M-C_6H_{11}O_5]^-$. Thus, this latter compound should be a Pino monohexoside.

Transcript levels of *PLR-Lp1* in silenced lines were measured by using semiquantitative RT-PCR with transcript levels of *actin* for comparison (Page et al. 2004). In all ihpRNAi lines the level of *PLR-Lp1* mRNA was significantly reduced (Fig. 3.16).
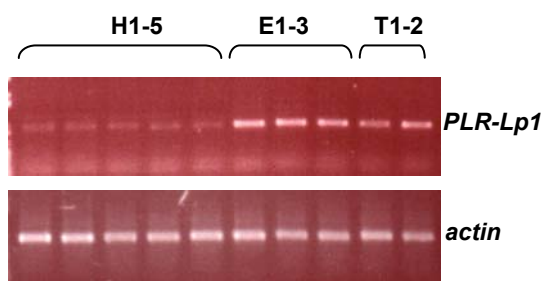
Fig. 3.16. RT-PCR analysis of *plr-Lp1* gene expression in 7 day old *L. perenne* hairy roots containing *plr* ihpRNAi constructs (H) in comparison with lines containing empty vector (E) and lines without any vector (T). An *actin* gene from the same lines was amplified to determine equal amounts of cDNA template.

Specific PLR activity levels decreased from app. 10 nkat/kg protein in control lines in comparison to app. 0.7 nkat/kg protein in ihpRNAi lines at day 7 (Fig. 3.17).
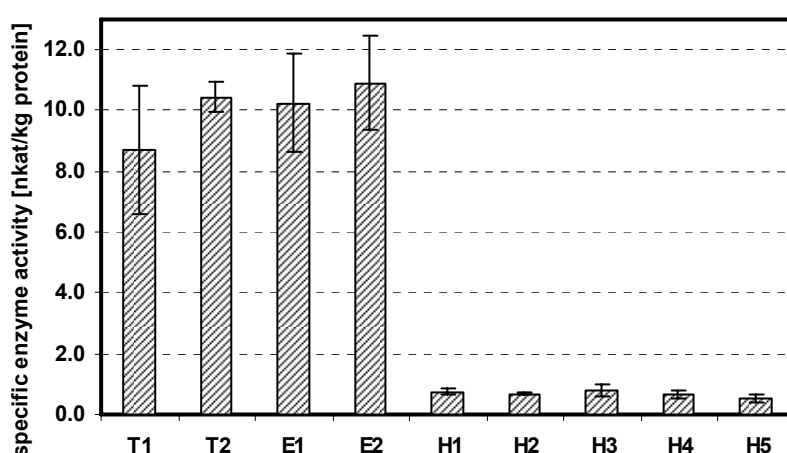
Fig. 3.17. PLR activity with 40 µg protein and 90 min incubation in selected hairy root lines of *L. perenne* containing *plr* ihpRNAi constructs (H) in comparison with lines containing empty vector (E) and lines without any vector (T). (The values are mean ± SD from two times assays conducted in duplicate.)

3.6. Identification of JusB7H from *L. perenne* H as a cytochrome P450-dependent monooxygenase

Jus B and glycosides of 7-hydroxyjusticidin B (Diph) are the main detectable compounds in cell cultures of *L. perenne* H (Hemmati et al. 2007). The introduction of the 7-hydroxyl group into Jus B leading to Diph is an aromatic hydroxylation catalyzed by JusB7H (Fig. 3.18).

justicidin B (MW=364)   **diphyllin** (MW= 380)
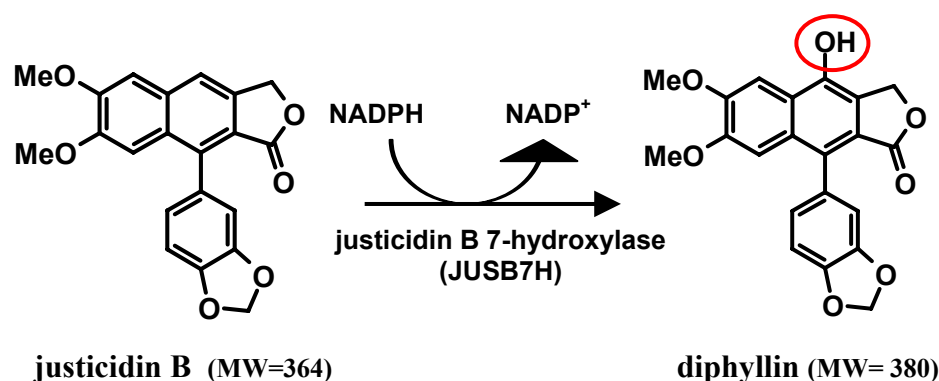
Fig. 3.18. Formation of Diph by introduction of the hydroxyl group to the C7 of Jus B via JusB7H.

Diph has been identified as the enzyme product by HPLC-UV according to Fig. 3.19.
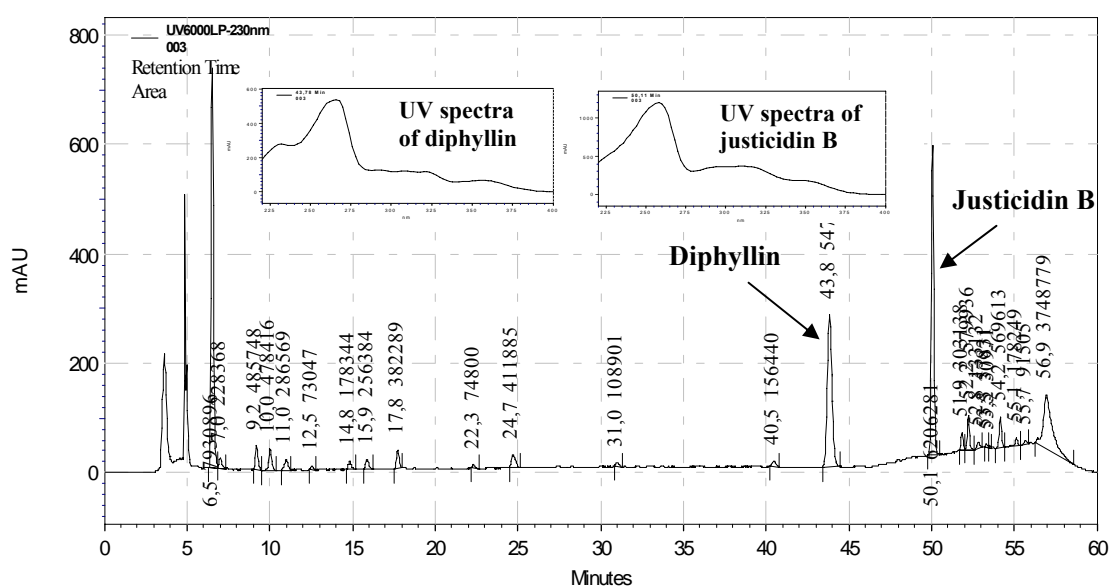
Fig. 3.19. HPLC chromatogram and UV spectrum of Jus B (substrate) and Diph (product) of JusB7H assay. The R_t at 43.8 and 50.1 corresponds to the Diph and Jus B respectively.

The over proof on the identity of the product with Diph was detected by HPLC-SPE-^{1}H NMR spectroscopy based on the following data. (1) The shorter retention time on the reversed phase HPLC column of the product (R_t 28.5 min) compared to the substrate Jus B (R_t 37.3 min) was consistent with the higher polarity of a hydroxylated product. (2) The UV spectrum recorded by the PDA detector during the HPLC-SPE-NMR run was identical with that of an authentic standard. (3) The ^{1}H NMR spectrum of the enzyme product matched that of the authentic standard but differed from that of the substrate in the missing signal of H-7 and a downfield shift of H-6 (δ 7.37 in the spectrum of Jus B versus δ 7.56 in Diph).

NMR data of diphyllin

^{1}H NMR (500 MHz; MeCN-d_3): δ 7.56 (1H, *s*, H-6), 6.96 (1H, *d*, *J* = 8.0 Hz, H-5'), 6.84 (1H, *d*, *J* = 1.9 Hz, H-2'), 6.79 (1H, *dd*, *J* = 8.0, 1.9 Hz, H-6'), 7.04 (1H, *s*, H-3), 6.05 (1H, *d*, *J* = 1.0 Hz, O-C<u>H</u>$_2$-O), 6.04 (1H, *d*, *J* = 1.0 Hz, O-C<u>H</u>$_2$-O), 5.35 (2H, *s*, H-9), 3.99 (3H, *s*, OC<u>H</u>$_3$-5), 3.70 (3H, *s*, OC<u>H</u>$_3$-4).

NMR data of justicidin B

^{1}H NMR (500 MHz; MeCN-d_3): δ 7.84 (1H, *s*, H-7), 7.37 (1H, *s*, H-6), 6.99 (1H, *d*, *J* = 8.0 Hz, H-5'), 6.88 (1H, *d*, *J* = 1.9 Hz, H-2'), 6.83 (1H, *dd*, *J* = 8.0, 1.9 Hz, H-6'), 7.07 (1H, *s*, H-3), 6.07 (1H, *d*, *J* = 1.0 Hz, O-C<u>H</u>$_2$-O), 6.06 (1H, *d*, *J* = 1.0 Hz, O-C<u>H</u>$_2$-O), 5.37 (2H, *s*, H-9), 3.97 (3H, *s*, OC<u>H</u>$_3$-5), 3.71 (3H, *s*, OC<u>H</u>$_3$-4).

The hydroxylation required NADPH as electron donor. The enzyme system was localized in the microsomal fractions. Assays with the supernatant containing soluble enzymes did not result to any hydroxylation reaction. The requirement for NADPH and the localization of the enzyme in the so called microsomal fraction were hints that JusB7H might be a cytochrome P450-dependent monooxygenase. Further data sustaining this indication, are the strong inhibition of JusB7H by Cyt *c*, a competitive electron acceptor of the NADPH:cytochrome P450 reductase complex (Oritz de Montellano and Correia 1995), and imidazol derivatives like clotrimazole as well known cytochrome P450 inhibitors. JusB7H activity was severely inhibited by very low concentration of Cyt *c*; 50% inhibition of JusB7H was achieved by 0.76 $\times$ 10^{-6} M Cyt *c* (Fig. 3. 20). 5.6 $\times$ 10^{-4} M clotrimazole or 10^{-3} M NDA another known inhibitor of cytochrome-P450-dependent monooxygenases led to a 50% inhibition of JusB7H activity.
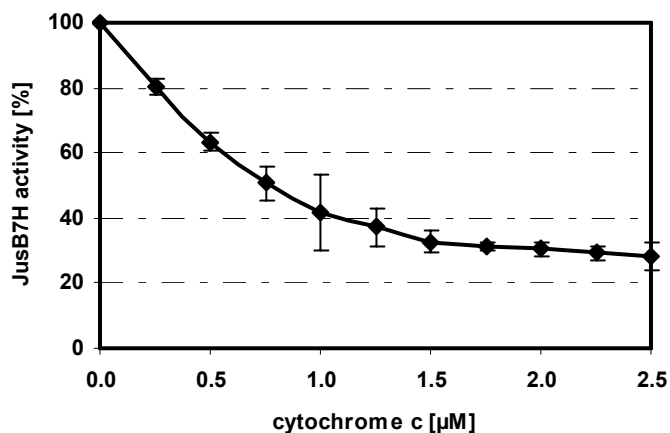
Fig. 3.20. Inhibition of JusB7H from suspension cultures of *Linum perenne* H by cytochrome *c* (100% activity corresponds to 0.2 ± 0.007 µkat kg^{-1}). Values are mean $\pm$ SD of two independent assays each conducted in duplicate.

3.6.1. Basic characteristics of JusB7H

The basic characteristics of JusB7H are typical of cytochrome P450 monooxygenases. No activity was observed when either cofactor (NADPH) was omitted or after heat inactivation of the microsomal preparation. The pH optimum was determined in the range of 6-9 in 0.1 M Tris-HCl buffer with different pH values. The conformation of a protein is influenced by pH and as enzyme activity is crucially dependent on its conformation, its activity is likewise affected. The pH values measured in the assay mixture at 26 °C as follows 6.2, 6.62, 7.03, 7.25, 7.44, 7.73, 7.82, 8.24 and 8.56. The maximum Maximal JusB7H activities were measured at a reaction pH around 7.4, a value corresponding to the cytoplasmic pH (Fig. 3.21). The optimum temperature was determined by incubating assay mixtures in the range of 0-100 °C. As the temperature rises, molecular motion - and hence collisions between enzyme and substrate - speed up. But as enzymes are proteins, there is an upper limit beyond which the enzyme becomes denatured and ineffective. The optimal reaction temperature was 26 °C. However, considerable JusB7H activities were observed at 0 °C and 40 °C with 36% and 52% of the activity at 26 °C, respectively, indicating a rather broad temperature window with high enzyme activity (Fig. 3.22).

Fig. 3.21. pH dependency of JusB7H in 0.1 M Tris HCl buffer with 700 μg protein at 26 °C.
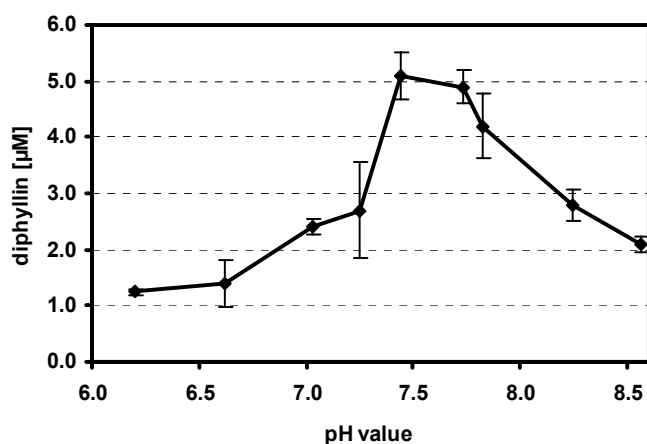

Fig. 3.22. Temperature dependency of JusB7H in 0.1 M Tris HCl buffer (pH 7.5) with 700 μg protein.
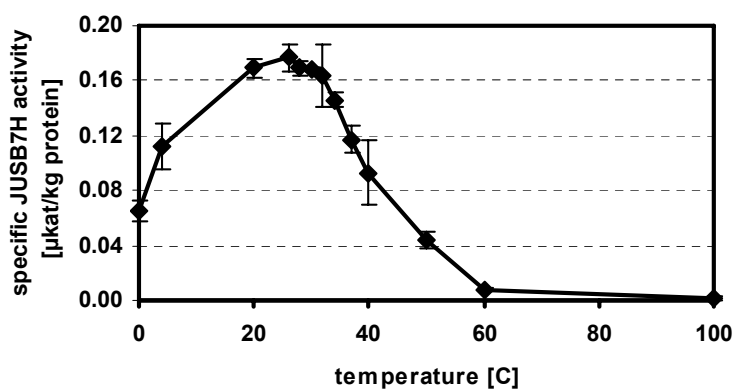
0, 300, 500, 600, 700, 800 and 1000 μg microsome were added to assay mixtures to determine the optimum concentration of protein needs to be added to the assays. In one experiment until 500 μg and in the repeated experiment until 700 μg protein the formed Diph was linear (Fig. 3.23).

Fig. 3.23. Protein dependency of JusB7H in 0.1 M Tris HCl buffer (pH 7.5) with at 26 °C.
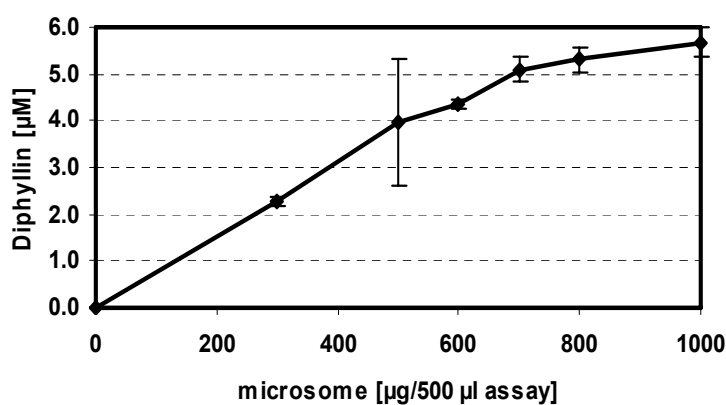
To determine the time dependency the enzyme assays were performed until 120 min. In one series of the experiment until 60 min and in the repeated experiment until 75 min the product formation was linear (Fig. 3.24).

Fig. 3.24. Time dependency of JusB7H in 0.1 M Tris HCl buffer (pH 7.5) with at 26 °C with 700 µg.
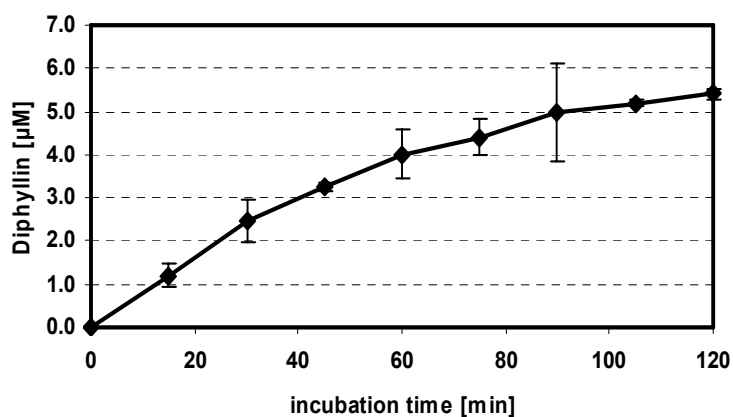

3.6.2. Substrate specificity of JusB7H

JusB7H catalyzes the formation of Diph from Jus B. Deoxypodophyllotoxin, 7(8),7'(8')-dehydrodeoxypodophyllotoxin, podophyllotoxin, 7(8),7'(8')-dehydropodophyllotoxin, 5'-demethyljusticidin B, *β*-peltatin A-methylether, matairesinol and yatein did not serve as a substrate for JusB7H (Fig. 3.25). Microsomal preparations from two cell cultures of *L. album* accumulating either podophyllotoxin (line PT) or 6-methoxypodophyllotoxin (line 6M) (Federolf et al. 2007) did not catalyze the hydroxylation of Jus B. JusB7H shows only affinity toward Jus B.

matairesinol   yatein   deoxypodophyllotoxin   podophyllotoxin

β-peltatin A-methylether   5′-demethyl justicidin B   dehydrodeoxypodophyllotoxin   dehydropodophyllotoxin
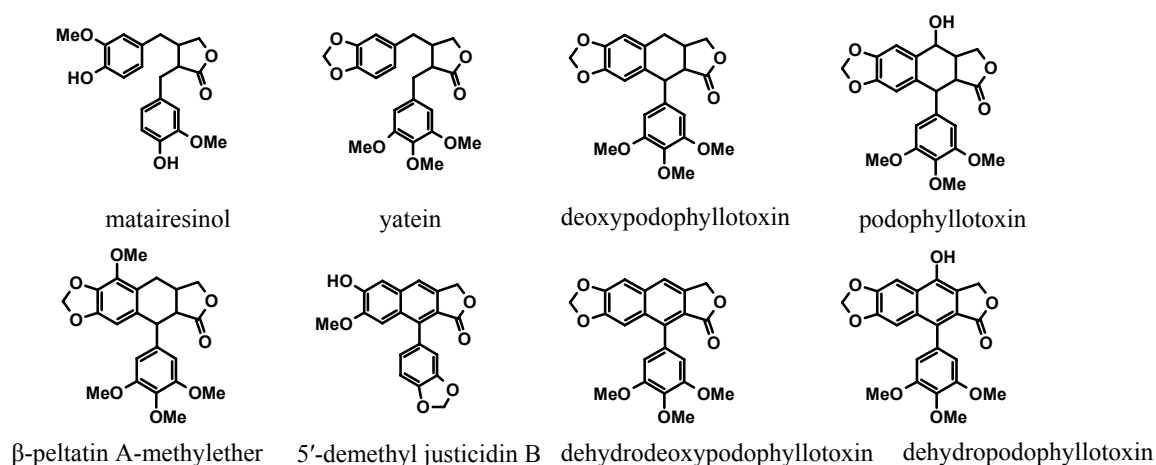
**Fig. 3. 25.** Compounds with similar structures with Jus B which were tested for JusB7H assays.

3.6.3. Determination of Michaelis-Menten constants for Jus B and NADPH

Enzyme kinetics is the study of the rates of chemical reactions that are catalyzed by enzymes. Based on Michaelis-Menten kinetic model, as enzyme-catalyzed reactions are saturable, their rate of catalysis does not show a linear response to increasing substrate. If the initial rate of the reaction is measured over a range of substrate concentrations (denoted as [S]), the reaction rate (v) increases as [S] increases. However, as [S] gets higher, the enzyme becomes saturated with substrate and the rate reaches V_{max}, the enzyme's maximum rate. JusB7H has a high affinity toward Jus B. The apparent K_m value for this substrate determined by Lineweaver-Burk was 3.9 ± 1.3 µM with a saturation concentration of 50 µM (Fig. 3.26). The apparent K_m for NADPH as the co-substrate for JusB7H was 102 ± 9.8 µM, as shown by Lineweaver-Burk diagrams (Fig. 3.27).
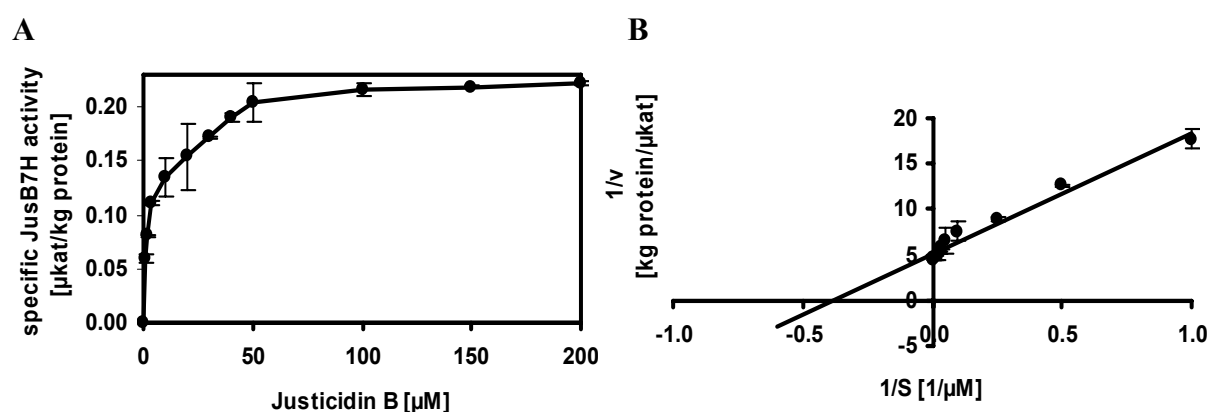

Fig. 3.26. A) Substrate saturation curve of JusB7H from cell cultures of *L. perenne* H for justicidin B. **B)** The corresponding Lineweaver-Burk digram. The apparent K_m was determined to be 3.9 ± 1.3 µM. Kinetic constants are mean $\pm$ SD of three independent assay series each carried out in duplicate.

Addition of NADP$^+$ alone did not lead to a hydroxylation reaction. NADH could only sustain a very low hydroxylation activity. Simultaneous addition of 0.05-0.25 mM NADPH together with 0.5 mM NADH resulted only in additive activities but the so-called synergistic effect was not observed (Fig. 3.28).
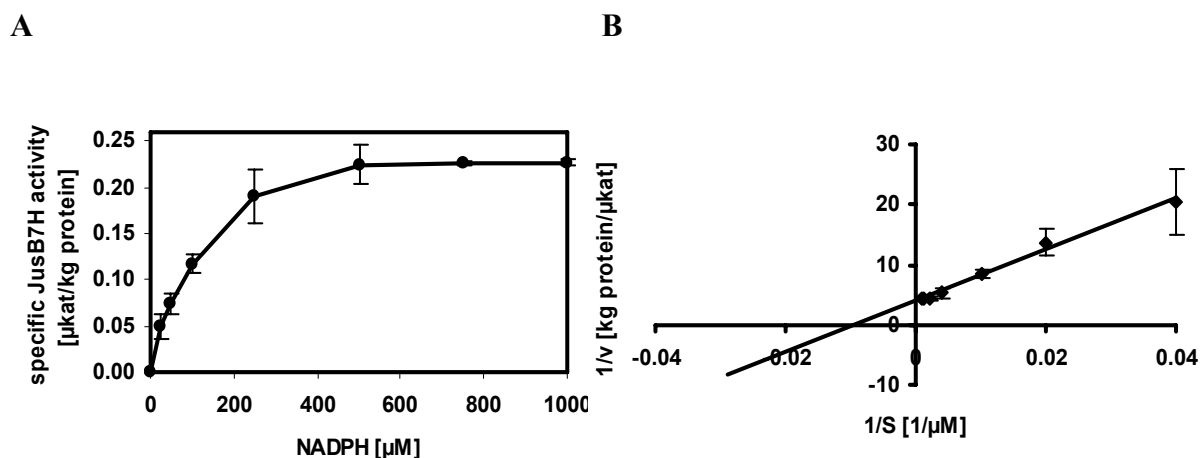
Fig. 3.27. A) Substrate saturation curve of JusB7H from cell cultures of *L. perenne* H for NADPH. **B)** The corresponding Lineweaver-Burk digram. The apparent K_m was determined to be 102 ± 9.8 µM. Kinetic constants are mean $\pm$ SD values of three independent assay series each carried out in duplicate.
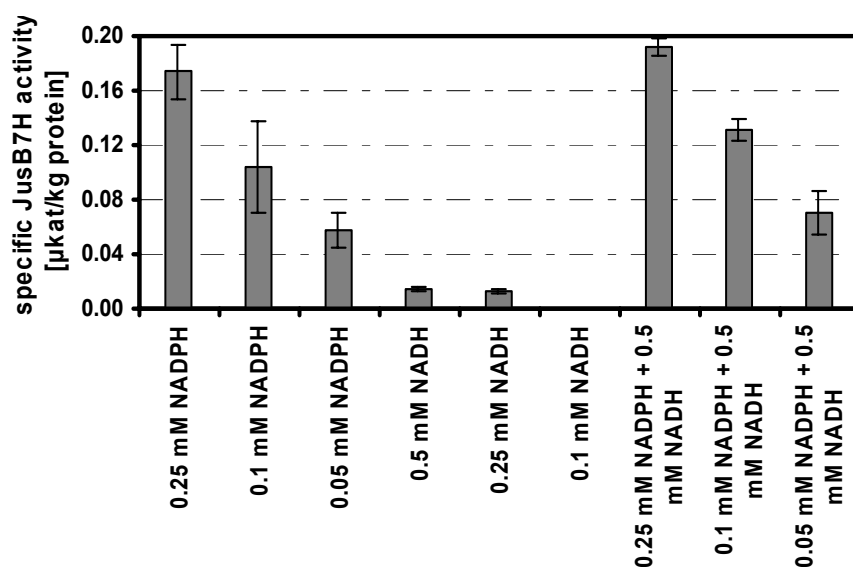
Fig. 3.28. Activity of JusB7H with different electron donors. Values are mean $\pm$ SD of two independent assays each conducted in duplicate.

Addition of 5 µM FAD, the prosthetic cofactor of the NADPH: cytochrome P450 reductase, did not lead to an enhancement of JusB7H activity, on the contrary activities were about 28% lower.

4. Discussion

4.1. Biosynthesis of arylnaphthalene type lignans

Investigating plants from several *Linum* species has shown that plants from the section *Syllinum* accumulate mainly aryltetralin type lignans, whereas simple lignans or arylnaphthalene type lignans are found in the section *Linum* (Schmidt et al. unpublished results). The biosynthetic pathway of aryltetralin lignans in the section *Syllinum* (Fig. 1.1) was partly described previously (von Heimendahl et al. 2005; Federolf et al. 2007). Arylnaphthalene type lignans can be found only in plant species of the section *Linum* like *L. austriacum* and *L. perenne* Himmelszelt. Cell suspension and hairy root cultures of *L. perenne* Himmelszelt accumulate up to 23 mg/g DW justicidin B (Jus B) in 8–10 days and 37 mg/g DW in 14 days, respectively (Hemmati et al. 2007). That is 2–3 times more than observed for in vitro cultures of *L. austriacum* (Mohagheghzadeh et al. 2002). Besides Jus B we identified two glycosylated derivatives of diphyllin (Diph). To our knowledge, this is the first report on the occurrence of 7-oxygenated arylnaphthalene lignans and their derivatives in a *Linum* species. Although plant cell cultures are a valubale source of secondary metabolites (Fuss 2003), but the aryldihydronaphthalene and dihydro derivatives of isojusticidin B, which were found in the aerial parts of *L. perenne* plants by Schmidt et al. (2006); could not be detected in cell suspension cultures of this species. This is related to the essential difference between disorganized cultures and organized systems. Although the responsible genes for the appropriate pathway are present in disorganized cultures, they are frequently not expressed. This may be due to the fact that the appropriate transcription factors are not active. If the formation of an appropriate transcription factor can be switched on, then secondary product formation occurs, as was shown by Grotewold et al. (1998), with the induction of formation of anthocyanins in formerly unproductive cells of maize. If we understand more completely how molecular-genetic regulation of natural product formation occurs in whole organs, it may become possible to trigger unorganized cell suspension cultures to produce natural compounds of interest. On the other hand, secondary products are produced and/or stored in specialized cellular structures, like trichomes, glands etc. The failure of cell suspension cultures to produce secondary compounds has been attributed to the lack of these structures. This is because, in the first place, such structures are likely to be necessary for expression of

the biosynthetic pathway, and secondly, the products are probably phytotoxic and failure to sequester them may inhibit growth or kill the culture.

Biosynthesis of arylnaphthalene lignans was not investigated up to now but we have assumed that the first steps of their biosynthetic pathway are catalyzed by the bifunctional enzyme pinoresinol lariciresinol reductase (PLR). We cloned a *PLR* cDNA from *L. perenne* Himmelszelt cell cultures (*PLR-Lp1*). The recombinant PLR-Lp1 completely used up the racemic Pino before the resulting Lari was completely converted to Seco. Therefore, PLR-Lp1 seems to work more like a pinoresinol reductase than a pinoresinol lariciresinol reductase. It becomes obvious that the number of metabolites found in one species exceeds the number of genes involved in their biosynthesis. The concept of one gene-one mRNA-one protein is collapsing (Schwab 2003). Many present-day proteins are known to have the capability of accepting more than one substrate, catalyzing more than one reaction and forming more than one product. They are called multifunctional enzymes. The presence of multifunctional proteins significantly enhances the metabolic efficiency of a cell and also metabolome diversity. Since many proteins involved in the biosynthesis of secondary plant metabolites are multifunctional, fewer enzymes are required to synthesize the various structures. Schwab (2003) has reviewed examples of alcohol acyl-CoA transferases, O-methyltransferases, terpene synthases and glycosyltransferases which have multifunctional activity. PLR catalyzes the two consequent early steps of lignan biosynthesis and works as a bifunctional enzyme.

To prove whether PLR-Lp1 is involved in the biosynthesis of arylnaphthalene lignans, ihpRNAi experiments were carried out. The effect of gene suppression to find metabolic pathway intermediates has been shown in many studies (Allen et al. 2004; Courdavault et al. 2005; Frick et al. 2004; Kumagai and Kouchi 2003; Nishihara et al. 2005). Chimeric genes in which the coding regions are fused to regulatory sequences from other sources to create artificial genes can be generated for transcription and translation in plants (Miki 2002). The PLR part of *L. perenne* was amplified with polylinkers and cloned in the pGEM®-T vector. To form the ihpPRNA constructs the fragment was subcloned in the sense and antisense orientation of a pHANNIBAL vector. hpRNA constructs require two copies of the target sequence in an inverted-repeat orientation, in order to produce duplex RNA. Smith et al. (2000) have found that it is necessary to introduce a spacer region between the arms of hpRNA constructs for the stability of the inverted repeats in *E. coli*. However, replacing the

spacer region of hpRNA constructs with a functional intron sequence increases the proportion of independent silenced lines recovered from 50% to 100%. Hence Wesely et al. (2001) built up a generic intron-spliced hpRNA (ihpRNA) vector by the name of pHANNIBAL, into which the gene of choice could be directionally cloned to make sense and antisense arms. Enhancement of the silencing efficiency by the presence of intron is that, the process of intron excision from the construct by spliceosome might help to align the complementary arms of the hairpin in an environment favouring RNA hybridization, promoting the formation of a duplex. Alternatively, splicing may transiently increase the amount of hairpin RNA by facilitating, or retarding, the hairpin′s passage from the nucleus, or by creating a smaller, less nuclease-sensitive loop (Smith et al. 2000). pHANNIBAL based constructs are driven by the constitutive 35S promoter. The 35S promoter is a typical example of a plant promoter from cauliflower mosaic virus (CaMV), which is often used for constitutive expression. 35S as a strong promoter causes high levels of gene expression in dicot plants. *Trans*-acting *vir* functions encoded by the Ri plasmids and by the *Agrobacterium* chromosome act to promote the integration into the plant genome of DNA segments which are delimited by *cis*-acting T-DNA border sequences. This has led to the construction of binary vectors for use in *Agrobacterium*-mediated plant transformation (MacBride and Summerfelt 1990). pART27 as a binary vector, carries the RK2 minimal replicon for maintenance in *Agrobacterium*, the ColE1 origin of replication for high-copy maintenance in *E. coli* and the Tn7 spectinomycin/stereptomycin resistance gene as a bacterial selectable marker. The organizational structure of the T-DNA of pART27 has been constructed taking into account the right to left border, 5′ to 3′ model of T-DNA transfer. The T-DNA carries the chimaeric kanamycin resistance gene (nopaline synthase promoter-neomycin phsphotransferase-nopaline synthase terminator) distal to the *lac*Z′ region. Timentin® which is mixture of ticarcillin disodium and clavulanate potassium in the ratio of 15:1 (Duchefa 2003) was added to the media to remove the agrobacteria two days after transformation. Since hairy roots of *L. perenne* accumulate a very high amount of Jus B it was a good starting point to conclude the influence of downregulation of possible genes maybe involved in arylnaphthalene biosynthesis. The hairy roots without construct had shown resistance to kanamycin, paromomycin (200 mgl^{-1}) was next used as the selection marker for transformed lines. Park and Facchini (2000) have used 50 mgl^{-1} paromomycin for the selection of the hairy roots of *Papaver somniferum* and *Eschscholzia californica* but it can result in the observation of

false positive lines. The hairy root lines harboring the RNAi construct containe the *npt*II gene. *npt*II encodes the neomycin phosphotransferase II which results in the phosphorylation of paromomycin. The comparison of *PLR-Lp1* mRNA level, PLR-Lp1 activities and lignan accumulation in hairy root lines which were transformed with only agrobacteria or with agrobacteria with an empty vector control showed no difference between these lines. In contrast, lines transformed with the ihpRNAi construct for *plr* gene suppression show significant reduction of mRNA level and enzyme activities for PLR-Lp1 and significantly lowered accumulation of Jus B and the Diphs. The level of Pino increased in these lines. Two additional peaks never observed in the control lines which could be glycosides of Pino and Lari were detected. The compounds can not be Pino and Lari monoglucosides since β-glucosidases are used in our lignan extraction method. But, it is possible that Pino and Lari can serve as substrates for the same enzymes which add the sugar moieties to the Diphs accumulated in the in vitro cultures of *L. perenne* H. Nevertheless, the exact structures of the compounds still remain to be identified. Since the RNAi construct was cloned in such a manner that it is not highly specific for *PLR-Lp1* but to silence possible *PLR*-like genes too, it can be concluded that at least *PLR-Lp1* is involved in the biosynthesis of Jus B and Diph derivatives.

In order to be converted to Diph, Jus B has to be hydroxylated at position 7 of the aromatic ring B. Several hydroxylases introducing OH-groups into aromatic rings have been shown to be cytochrome P450-dependent monooxygenases, e.g. cinnamic acid 4-hydroxylase (Russell and Conn 1967; Russell 1971), tabersonine 16-hydroxylase (St-Pierre and De Luca 1995), Xanthon 6-hydroxylase (Schmidt et al. 2000), 8-dimethylallylnaringenin 2'-hydroxylase (Yamamoto et al. 2001) and deoxypodophyllotoxin 6-hydroxylase (Molog et al. 2001; Federolf et al. 2007). Subcellular localization in the microsomal fraction is typical of this enzyme class. JusB7H activity was determined in the microsomal fraction after $MgCl_2$-precipitation and centrifugation at 48000 *g*. The supernatant of this centrifugation step contained no hydroxylating activities. The CYP450 from plant sources are usually obtained in microsomes. The microsomal preparations may include vesicles derived from the breakage of various membranes such as those of ER, Golgi, plasma membrane, tonoplast, plastid envelopes, nucleus and peroxisomes. The subcellular origins of microsomal membranes have been determined in only a few cases. They are often ER bound however immunohistochemical localization, would be specifically useful for this purpose (Donaldson

and Luster 1991). This first hint that JusB7H is a cytochrome P450-dependent monooxygenase was verified by the inhibition of the reaction by Cyt c, an electron acceptor competing for electrons transferred from a NADPH:cytochrome P450 reductase to cytochrome P450. As shown in the Fig. 1.15 NADPH:CYP450 reductase can donate electrons in vitro to Cyt c as well as to CYP450, thus addition of exogenous Cyt c to a CYP450 reaction can inhibit the reaction [some reversible inhibitors compete with substrates for occupancy of the active site by coordinating to the heme iron atom (Oritz de Montellano 2005)]. 50% inhibition of JusB7H activity was reached by the addition of 0.76×10^{-6} M Cyt c. This value is comparable to concentrations necessary to inhibit other cytochrome P450 monooxygenases. 1.6×10^{-6} M Cyt c leads to a 50% inhibition of DOP6H of *L. album* (Federolf et al. 2007). 50% inhibition of tabersonine 16-hydroxylase is achieved by 10^{-6} M Cyt c (St-Pierre and De Luca 1995). An inhibition of 90% for DOP6H of *L. flavum* was observed at a concentration of 2.5 μM Cyt c (Molog et al. 2001). The N-substituted imidazols like CLOT (Fig. 4.1) were effective inhibitors for JusB7H. 5.6×10^{-4} M CLOT led to a 50% inhibition of JusB7H activity. The activity of DOP6H from *L. album* and tabersonine 16-hydroxylase from *Catharanthus roseus* is inhibited to 50 % by 1.1×10^{-5} M and 5×10^{-5} M CLOT respectively (Federolf et al. 2007; St-Pierre and De Luca 1995). Tetcyclacis (NDA), a potent inhibitor of cytochrome P450 enzymes showed less pronounced inhibition of JusB7H. 50% inhibition of JusB7H activity is reached by the addition of 10^{-3} M NDA. 1.1×10^{-5} M and 10^{-4} M NDA is sufficient to reach a 50% inhibition of DOP6H from *L. album* and tabersonine 16-hydroxylase from *Catharanthus roseus*, respectively (Federolf et al. 2007; St-Pierre and De Luca 1995). A structural feature common to tetcyclacis and the triazole-type compounds is an sp^2-hybridised nitrogen atom located at the periphery of the molecule in a heterocycle. It appears likely that the electron-pair on this atom interacts with the central iron atom of cytochrome P-450 in the enzymes, resulting in inhibition (Rademacher et al. 1987). Ancymidol as pyrimidine derivative did not inhibit JusB7H, this was the case for a lot of other CYP450s like monoterpene hydroxylation in mints (Karp et al. 1990). Further characteristics of JusB7H are typical of cytochrome P450-dependent hydroxylases, e.g. the pH optimum is around 7.4, the pH range of the cytoplasm. JusB7H is strictly dependent on NADPH as an electron donor, whereas NADH can only sustain very low hydroxylation activities. For some cytochrome P450-dependent reactions, simultaneous addition of NADPH and NADH lead to a synergistic effect of these two reducing equivalents (Clemens et al. 1993; Gerardy and Zenk 1993).

clotrimazole (CLOT)   tetcyclacis (NDA)   cytochrome *c* (Cyt *c*)
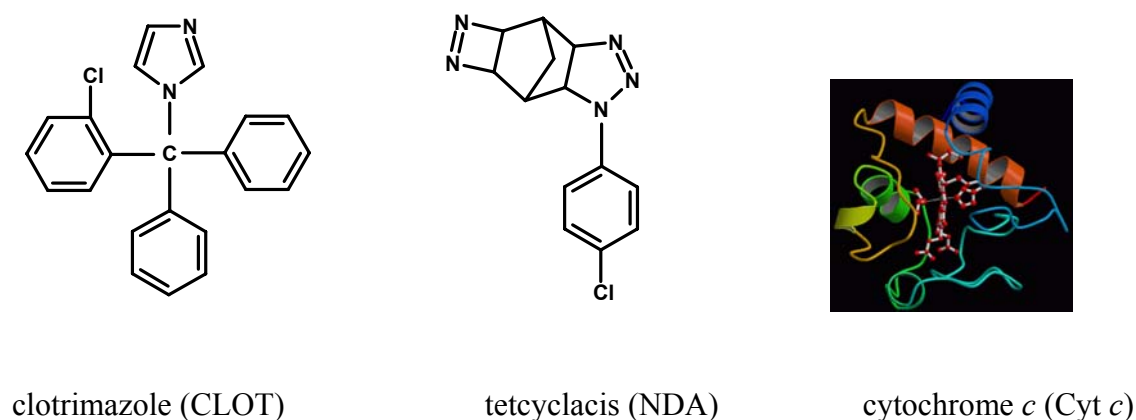
Fig 4.1. Structures of CYP450 inhibitors.

(Cyt c adopted from http://www.fccc.edu/research/labs/roder/rodproj.html)

This phenomenon is explained by the participation of a NADPH:cytochrome P450 reductase as well as cytochrome b_5 in the electron transfer to the cytochrome P450 monooxygenases (De Vetten et al. 1999). JusB7H only showed additive effects of NADPH and NADH, but no synergistic effect. The so called synergistic effect was neither observed for some other cytochrome P450 enzymes like DOP6H in *L. flavum* (Molog et al. 2001). NADPH:cytochrome P450 reductase is known to contain FAD and FMN as prosthetic groups. These flavine nucleotides might be partially lost during enzyme preparation and purification (Petersen 1997). Addition of FAD to the JusB7H assay did not lead to an enhancement of enzyme activity. This might indicate that FAD is tightly bound to the reductase and not lost during the preparation of microsomes. The low apparent K_m value for Jus B (3.9 ± 1.3 µM) which shows a high enzyme substrate specificity is also found with other cytochrome P450 enzymes like the low apparent K_m for Geranylhydroquinone 3"-hydroxylase from *Lithospermum erythrorhizon* with a value of 1.5 µM for geranylhydroquinone (Yamamoto et al. 2000). However the range of K_m values is variable. The high apparent K_m for NADPH in the JusB7H assay is also observed for other cytochrome P450 enzymes. Cinnamic acid 4-hydroxylase from *Anthoceros agrestis* shows an apparent K_m value of around 60 µM for NADPH (Petersen 2003). Cytochrome P450 enzymes exist in various forms, which confer substrate specificity. Most cytochrome P450 enzymes from plants exhibit a narrow substrate

specificity (Donaldson and Luster 1991, Sandermann 1992), which is also true for JusB7H. Structurally related substances were not converted to the related hydroxylated products with microsomal preparations of *L. perenne* H. Neither 7(8),7'(8')-dehydrodeoxypodophyllotoxin nor deoxypodophyllotoxin and *β*-peltatin A-methylether with an aromatic and aliphatic ring C, respectively, served as substrate for JusB7H. Jus B is the only known substrate for JusB7H until now. These observations demonstrate that JusB7H of *L. perenne* H cell cultures is a cytochrome P450-dependent monooxygenase which hydroxylates the C7 position of Jus B to give Diph as the only product. Cloning and characterization of a cDNA encoding JusB7H will be the topic for further studies. Since the cell cultures of *L. perenne* H accumulate Diph only in glycosidic form Diph has to be converted to diglycosides which are more water soluble and can be stored in the vacuole. Our data together with the cloning of a PLR of *L. perenne* H and the findings of dihydroarylnaphthalenes in the aerial part of this plant species support our hypothetical pathway leading to diphyllin glycosides (Fig. 1.8).

4.2. Enantiospecificity in lignan biosynthesis

The majority of naturally occurring lignans are optically active as one enantiomer or mixtures with various enantiomeric compositions (Ayers and Loike, 1990). While the Seco isolated from *Forsythia* plants was the pure (-)- enantiomer (Umezawa et al. 1990), this lignan isolated from *Wikstroemia sikokiana* and *A. lappa* is a mixture of both (+)- and (-)-enantiomers (Suzuki et al. 2002). The hydrolytically released SDG derived from the various lignan oligomers in flax seeds is composed of ~99% (+)- and ~1% (-)-Seco. But in contrast the aerial parts of flowering *L. usitatissimum* plants, only contain (-)-enantiomers of lignans derived from (-)-Seco (Schmidt et al. 2006). Regardless the sign of optical rotation, Matai as a dibenzylbutyrolactone lignan is the first enantiomeric pure compound in lignan biosynthesis in many cases (Umezawa, 2003). Therefore, it seems that enantiomeric purity in lignan biosynthesis is determined during the first steps, but on different levels.

Based on the SDG diastereomers two distinct forms of stereoselective coupling control should be mediated in *L. usitatissimum*: that is each differentially engenders the formation of either (+)-Pino or its corresponding antipode from coniferyl alcohol (Davin and Lewis, 2005). It is argued that a dirigent gene homolog forming (+)-Pino has been heterologously expressed from flaxseed (Davin and Lewis, 2003). The dirigent gene responsible for the formation of

(-)-Pino is not reported yet. A cDNA encoding (-)-PLR (PLR-Lu1) was isolated from cell cultures of *L. usitatissimum* (von Heimandahl et al. 2005). Enzyme assays with purified recombinant PLR-Lu1 results in the formation of (+)-Seco. By action of PLR-Lu1, (+)-Seco was rapidly formed by the reduction of (-)-Pino. Same as the PLR-Tp1 from *T. plicata* (Fujita et al. 1999), the formation of (-)-Lari as an intermediate was not observed for PLR-Lu1. Southern analysis indicated that the genome of *L. usitatissimum* contains a small gene family of PLRs (von Heimendahl et al. 2005). The question is that whether consequent reductive transformations to (+)- and (-)-Seco are performed by a nonspecific PLR enzyme or via at least two PLR isoforms with different enantiospecificity. We have cloned a PLR cDNA (PLR-Lu2) from the leaves of *L. usitatissimum* responsible for the formation of (-)-Seco. Thus it could be rationalized that two pathways utilizing (-)- and (+)-PLR, being involved in the formation of (+)- and (-)-Seco, respectively (Fig. 1.11). By the recombinant PLR-Lu2 approximately 50% of Pino was used up and the resulting Lari was completely converted to Seco. Enantiomeric composition of the substrates and the products of the assays during 40 min was analysed. First (+)-Lari forms from (+)-Pino until no (+)-Pino is left. Then (-)-Seco can be formed from (+)-Lari. In *F. intermedia* formation of Seco was only retarded and occurred already when (+)-Pino was still in the reaction mixture (Katayama et al. 1993). PLRs of *T. plicata* work only strictly enantiospecific in the formation of Seco from Lari (Fujita et al. 1999).

In plant species like *A. lappa* which accumulate lignans with opposite stereochemistry in different organs no PLR cDNAs were cloned and also in *T. plicata* containing two PLR classes with opposite enantiospecificity the relationship between the expression of PLRs and enantiomeric composition of lignans in the plant is not reported. Now, with the *PLR-Lu1* and *PLR-Lu2* sequence in hand it was possible to compare the expression patterns of both PLRs with enantiomeric composition of the lignans in different organs of *L. usitatissimum*. As it is expected in leaves and stems of *L. usitatissimum* accumulating the (-)-enantiomers of lignans, only PLR-Lu2 which is responsible for the formation of (-)-Seco was transcriptionally active (Fig. 3.5). Both *PLR-Lu1* and *PLR-Lu2* transcripts were present in seeds and contribute to the synthesis of (+)- and (-)-Seco, respectively. As an additional complexity, *PLR-Lu1* and *PLR-Lu2* were similarly expressed in seeds which is in contrast to the ratio of the SDG diastereomers reported for the flaxseed. An explanation is that (+)-Seco is used mainly as a

substrate for UDPG:glucosyltransferase to yield (+)-SDG but the (-)-Seco is further channeled to the biosyntheis of (-)-yatein. However, the precise ratio of (+)- to (-)-SDG and other types of lignans in flaxseed should be defined and the expression pattern of dirigent proteins responsible for the formation of (+)- and (-)-Pino should be investigated.

Thus far it can be concluded that the enantiomeric composition of lignans in *L. usitatissimum* is controlled by at least two separate gene subsets. *PLR-Lu1* which is responsible for the upstream steps in (+)-Seco biosynthesis and *PLR-Lu2* in contrast catalyzes the formation of (-)-Seco leads to the downstream products like (-)-yatein. The pattern of transcription levels of both genes suggests that PLRs with different enantiospecificity are essential components of metabolic control in various organs of the *L. usitatissimum* plant.

As mentioned , PLR of *L. perenne* (PLR-Lp1) was not enantiospecific and could utilize both (+)- and (-)-enantiomers of Pino and Lari. However Fujita et al. (1999) have emphasized that in assays with PLR-Tp1, if allowed to continue until depletion of the (±)-Pino occurs the (-)-antipode is fully converted to (+)-Seco, whereas the (+)-antipode is only transformed to (+)-Lari.

We analysed the enantiomeric composition of the substrate and the products of assays with different protein concentrations in order to get hints for the enantiospecificity of PLR-Lp1. The protein shows preference for (+)-Pino (*R,R* configuration at C-atoms 8,8′) in the first reaction step, but preference for (−)-Lari (*S,S* configuration at C-atoms 8,8′) in the second reaction step. All other PLRs cloned so far, like PLRs from *T. plicata*, *F. intermedia*, *L. album* and *L. usitatissimum*, at least prefer for both reaction steps either the *R,R* configurated or *S,S* configurated lignans (Dinkova-Kostova et al. 1996; Fujita et al. 1999; von Heimendahl et al. 2005). Therefore, PLR-Lp1 is the first PLR with opposite enantiospecificity toward Pino and Lari. This fact together with the preference for both Pino enantiomers before Lari indicates that another gene encoding a PLR which is at least more specific for the conversion of Lari to Seco could be present in the genome of *L. perenne* Himmelszelt which is also indicated by Southern analysis. Katayama et al. (1993) have shown that the enzyme PLR is not only highly enantiospecific, as it can also distinguish between the diastereomers (+)-Pino and (+)-epipinoresinol, with the later apparently not serving as a substrate for reduction, i. e. the difference in stereochemistry at C7' between Pino and epiPino deleteriously affects either molecular recognition (binding) by the enzyme, or its subsequent reduction on the enzyme active site.

4. Discussion

Several enzymes like PLR-Lu1 and PLR-Lu2 are encoded by multiple genes that are regulated differently in response to a range of environmental and developemental stimuli, adding genetic complexity. The isoenzymes encoded by a gene family show overlapping catalytic activities towards the different substrates. This implies that mutations in one gene does not necessarily lead to the loss of secondary plant metabolites but results in the moderate shift of the product pattern. A single amino acid alteration in a protein can lead to a modified substrate preference and an increase of a small number of metabolites or even formation of new compounds depending on substrate availability. If the compounds are profitable for the plant the individuals carrying the mutation will rapidly propagate. A mutation in a multifunctional enzyme leads to a gradual shift in the composition of secondary plant metabolite rather than the appearance of a new metabolite at the expense of an existing compound.

Multifunctional isoenzymes are an ideal playground for evolution. Plants appear to have adapted existing enzymes to their evolving needs, rather than inventing entirely novel mechanisms. Multifunctional enzymes have already been proposed as the ancestor of present-day enzyme (Jensen 1976). These broad specificity enzyme may be recruited for new metabolic pathways, followed by further evolution toward more specific and efficient catalysts. Its follows that gene duplication is an important factor in this concept as it provides the raw material for the acquisition of new biosynthetic pathways.

As mentioned in the chapters 3.2.1 and 3.3.1 both PLR-Lu2 and PLR-Lp1 have high levels of similarity to the other members of the PIP family. PCBERs, PLRs and IFRs are quite closely related from a sequence homology perspective, i.e. PCBER is ~66% similar/~45% identical to PLRs and ~65% similar/50% identical to IFRs (Davin and Lewis 2003). Significant homology was noted for (+)-PLR with various IFRs from the legumes. This is of considerable interest since isoflavonoids are formed via a related branch of the phenylpropanoid-acetate metabolism. For example, in *Medicago sativa*, its IFR catalyzes the stereospecific conversion of 2'-hydroxyformononetin to (3*R*)-vestitone in the biosynthesis of the phytoalexin, (-)-medicarpin. This sequence similarity is more than a coincidence, given that both lignans and isoflavonoids are offshoots of the general phenylpropanoid metabolism, with comparable plant defense functions and pharmacological roles, e.g. as phytoestrogens. Both reductases catalyze very similar reactions. It is tempting to speculate that the IFRs may have evolved from PLRs. This is considered likely since the lignans are present in the pteridophytes,

hornworts, gymnosperms, and angiosperms; hence, their pathways apparently evolved prior to the isoflavonoids. Together, these similarities suggest that although plant defense mechanism have been maintained, evolutionary divergence of the plant biochemical pathway has occurred (Dinkova-Kostova et al. 1996). IFRs are enantiospecific toward their substrates. For all of the IFRs identified to date, only the (-)-enantiomers of their products are formed. On the other hand, the PLRs at least can exist in two distinct forms like *T. plicata* or *L. usitatissimum* wich have both (+)- and (-)-PLRs. Gang et al. (1999b) have suggested that since PCBERs are apparently highly ubiquitous in the plant kingdom and they are only regiospecific. In this regard, PCBERs (being regiospecific) is the evolutionary forerunners of both PLRs and IFRs (with the latter present thus far mainly in the Fabaceae), as the result enantiospecificity evolving later. PCBER regiospecificity is best explained by a larger space in the substrate binding pocket (in comparison to PLR-Tp1) were both (+)- and (-)-DDC can fit among the hydrophobic side chains (Min et al. 2003). All three classes posses NADPH binding sites and appear to be cytosolic enzymes, since they lack signal sequence for targeting to the secretory pathway, mitochondria, chloroplast, or peroxisomes. Additionally, they may be regulated in a comparable manner, not only at the transcriptional level (Dixon et al. 1995) but also at the enzymatic level by protein phosphorylation, as evidenced by several potential phosphorylation sites that are conserved among all of the members. Recently Fuss (2007) has established a phylogenetic tree for the PIP family. One of the main clusters contains the PLRs and the second main cluster involves IFRs and PCBERs. Interestingly, the group of PLRs is divided into two subclusters. One contains PLRs of Coniferopsida, the other of Magnoliopsida. The Magnoliopsida PLRs build two clusters. One cluster contains PLRs with enantioselectivity for (+)-Pino (e.g. PLR-Lu2, PLR-La1, PLR-Fi1). A broad variety in enantiospecificity can be found for the PLRs of the second cluster (e.g. PLR-Lp1 which is relative enantiospecific or PLR-Lu1 with highly enantiospecificity toward (-)-Pino). Hence two gene copies for encoding PLRs had to be in the genome of the *Linum* ancestor because the PLRs of *L. usitatissimum* are closer related to other *Linum* species than to each other. Von Heimendahl et al. (unpublished data) have found in parallel with PLRs with variable enantiospecificity, a PCBER in *A. thaliana* with PLR activity which is also enantiospecific toward (+)-Pino. Therefore, the progenitor of both PLRs and PCBERs has to be present in primitive plants. This progenitor could show enantiospecificity because at least a PCBER of *A. thaliana* prefers (+)-Pino in the assay for PLR activity. This is in contrast with Gang et al.

(1999b) who predicted PCBERs as the ancestors for the enantiospecific PLRs and IFRs. Therefore, enantiospecificity is an old invention in evolution of PIP family, which can be changed or lost during evolution. Thus, new genes almost always arise by gene duplication followed by divergence (Ober 2005). This leaves the organism with one gene that maintains the original function and a second copy that is not restricted by natural selection. This second copy can then accumulate mutations until, rarely, it has acquired a new function and might be then become fixed in the population (Pichersky and Gang 2000).

5. Summary

Lignans are a class of secondary metabolites derived from two phenylpropanoid units that are linked by a C-C bond between 8 and 8′ of the side chain carbon atoms. *Linum usitatissimum* and *Linum perenne* H, two species of the section *Linum* of the Linaceae mainly accumulate dibenzylbutan [secoisolariciresinol (Seco)] and arylnaphthalene [justicidin B (Jus B) or diphyllin (Diph)] type lignans, respectively. Seco reduces the incidence of hormone dependent cancers. Jus B shows cytotoxicity against chronic leukemias.

The first steps in the biosynthesis of lignans are discussed to be ubiquitous leading to all kind of structures. The coupling of two molecules of coniferyl alcohol yields pinoresinol (Pino) which is reduced by the pinoresinol-lariciresinol reductase (PLR) via lariciresinol (Lari) to Secoisolariciresinol (Seco). Seco is converted to matairesinol the predicted central intermediate in lignan biosynthesis.

Since nothing was known about the biosynthesis of arylnaphthalene lignans, a pathway for the biosynthesis of arylnaphthalene lignans like Jus B and Diph, based on the lignan structures found in *L. perenne* was proposed. Firstly, a cDNA encoding a PLR (PLR-Lp1) from a cell culture of *L. perenne* was cloned. Hairy root lines which were transformed with an ihpRNAi construct to suppress *PLR-Lp1* gene expression show less mRNA accumulation for the *PLR-Lp1* gene and PLR enzyme activity. Jus B accumulation was reduced to 24% in comparison to control lines. These results prove the involvement of PLR in the biosynthesis of arylnaphthalene lignans. As a second enzyme of the proposed pathway, Justicidin B 7-hydroxylase (JusB7H) was characterized from a microsomal fraction prepared from a *L. perenne* H suspension culture. The enzyme catalyzes the last step in the biosynthesis of Diph by introducing a hydroxyl group in position 7 of Jus B. The hydroxylase activity was strongly inhibited by cytochrome *c* as well as other cytochrome P450 inhibitors like clotrimazole indicating the involvement of a cytochrome P450-dependent monooxygenase. JusB7H has a pH optimum of 7.4 and a temperature optimum of 26 °C. Jus B was the only substrate accepted by JusB7H with an apparent K_m of 3.9 ± 1.3 μM. NADPH is predominantly accepted as the electron donor, but NADH was a weak cosubstrate. A synergistic effect of NADPH and NADH was not observed. The apparent K_m for NADPH was 102 ± 10 μM.

Most isolated naturally occurring lignans are optically active as a single enantiomer or mixtures with various enantiomeric compositions. Enantiomeric purity in lignan biosynthesis is determined during the first steps, but on different levels. Seeds of *Linum usitatissimum* contain almost 99% (+)- and 1% (-)-Seco-diglucoside. Aerial parts of *L. usitatissimum* accumulate only the (-)-enantiomers of lignans which should be derivatives of (-)-Seco. A recombinant PLR (PLR-Lu1) from *L. usitatissimum* seeds converts only (-)-pinoresinol (Pino) to (+)-Seco. A second cDNA *PLR-Lu2* from the leaves of *L. usitatissimum* was isolated during this work. The recombinant protein converts only (+)-Pino to (-)-Seco. Expression profiling of both *PLR*s revealed that *PLR-Lu1* was strongly expressed in seeds as well as roots whereas in leaves and stems its expression was absent. *PLR-Lu2* was expressed in all tested organs with the strongest signal in leaves. Therefore, the enantiomeric composition of lignans in the organs of *L. usitatissimum* is determined by the relative action of two PLRs with opposite enantiospecificity rather than a single enzyme with low enantiospecificity. In contrast, experiments with the recombinant PLR of *L. perenne*, PLR-Lp1, revealed that it prefers (+)-Pino in the first reaction step, but (-)-Lari in the second step. It is the first PLR described with opposite enantiospecificity within the two reaction steps catalyzed by PLRs.

Zusammenfassung

Lignane sind Dimere aus zwei Phenylpropanmolekülen, die jeweils über ihre 8-8′ Kohlenstoffatome der Seitenketten miteinander verknüpft sind. *Linum usitatissimum* und *Linum perenne* H, zwei Arten der Sektion *Linum* (Linaceae) akkumulieren hauptsächlich Lignane vom Typ der Dibenzylbutane [Secoisolariciresinol (Seco)] beziehungsweise Aryl-naphthalene [Justicidin B (Jus B) oder Diphyllin (Diph)]. Seco schützt vor Hormon-abhän-gigen Krebsarten. Jus B zeigt Cytotoxicität gegen chronische Leukämie.

Die ersten Schritte der Biosynthese verschiedenster Lignane sollen gleich sein. Die Kopplung von zwei Molekülen Coniferylalkohol liefert Pinoresinol, welches von der Pinoresinol-Larici-resinol-Reduktase (PLR) über Lariciresinol (Lari) zu Secoisolariciresinol (Seco) reduziert wird. Seco wird zu Matairesinol, dem vermutlich zentralen Intermediat der Lignanbiosyn-these, umgesetzt.

Da zu Beginn der vorliegenden Arbeit nichts zu Biosynthese der Arylnaphthalen-Lignane bekannt war, wurde hier ein Biosyntheseweg für JusB und Diph vorgeschlagen. Als erstes wurde eine cDNA für eine PLR (PLR-Lp1) aus Zellkulturen von *L. perenne* kloniert. „Hairy Root"-Linien, die zur Suppression der *PLR-Lp1* Genexpression mit ihpRNAi Konstrukten transformiert waren, zeigten geringere Akkumulation des *PLR-Lp1*-Gens, so wie reduzierte PLR-Enzymaktivität. Die Akkumulation von JusB war auf 24 % im Vergleich zu Kontroll-linien abgesenkt. Diese Ergebnisse beweisen, dass die PLR an der Biosynthese des JusB beteiligt ist. Als zweites Enzym aus dem vorgeschlagenen Biosyntheseweg wurde die JusB-7-Hydroxylase (JusB7H) in Mikrosomen von Zellkulturen von *L. perenne* charakterisiert. Versuche mit Inhibitoren für Cytochrom P450 Monooxygenasen (Cytochrom *c* und Clotri-mazol) zeigen, dass die Hydroxylierung des Jus B zu Diph an Position 7 von einer Cytochrom P450 Monooxygenase katalysiert wird. Die JusB7H hat ein pH-Optimum von ca. 7.4 und ein Temperaturoptimum um 26 °C. Jus B wurde als einziges der getesteten Substrate akzeptiert mit einem apparenten Km von 3.9 ± 1.3 µM. NADPH ist der vorherrschende Elektronendonor. NADH ist ein nur schwaches Cosubstrat. Der apparente Km für NADPH ist 102 ± 10 µM.

Die meisten in der Natur gefundenen Lignane sind optisch aktiv, wobei sie entweder als einzelnes Enantiomer oder Mischungen von Enantiomeren in variabler Zusammensetzung vorkommen. Enantiomerenreinheit scheint während der ersten Schritte der Biosynthese auf verschiedenen Ebenen festgelegt zu werden. In Samen von *L. usitatissimum* liegt zu 99 % (+)-Secoisolariciresinoldiglucosid, aber zu 1% auch das andere Enantiomer vor. In blühenden Pflanzen von *L. usitatissimum* kommen nur die (-)-Enantiomere von Lignanen vor. Eine rekombinante PLR (PLR-Lu1) aus *L. usitatissimum* Samen ist spezifisch für die Umwandlung von (-)-Pino zu (+)-Seco. Im Zuge dieser Arbeit wurde eine zweite cDNA für eine PLR (PLR-Lu2) aus Blättern von *L. usitatissimum* isoliert. Das heterolog exprimierte und gereinigte Protein ist enantiospezifisch für die Umwandlung von (+)-Pino zu (-)-Seco. Der Vergleich der Expressionsmuster der beiden PLRs ergab, dass die *PLR-Lu1* in sich entwickelnden Samen und Wurzeln, nicht aber Blättern und Stängeln exprimiert wird. Die Transkripte der *PLR-Lu2* wurden in allen untersuchten Organen besonders zahlreich aber in Blättern nachgewiesen. Daraus ist zu schließen, dass die enantiomere Zusammensetzung der Lignane in den Organen von *L. usitatissimum* durch das Wechselspiel von PLR-Lu1 und PLR-Lu2 bestimmt wird und nicht durch das Vorhandensein einer mehr oder weniger enantiounspezifischen PLR. Im Gegensatz dazu stehen die Befunde zur Enantiospezifität der PLR aus *L. perenne*, PLR-Lp1. Das heterolog exprimierte Protein bevorzugt im ersten Reaktionsschritt (+)-Pino, im zweiten aber (-)-Lari. Damit ist zum ersten Mal eine PLR kloniert worden, die in den beiden Reaktionschritten entgegengesetzte Enantioselektivität zeigt.

6. References

Adlercreutz, H., Bannwart, C., Wähälä, K., Mäkelä, T., Brunow, G., Hase, T., Arosemena, P.J., Kellis Jr, J.T. Vickery, L.E. (1993) Inhibition of human aromatase by mammalian lignans and isoflavonoid phytoestrogens. J. Steroid Biochem. Mol. Biol. 44: 147-153

Akashi, T., Koshimizu, S., Aoki, T., Ayabe, S. (2006) Identification of cDNAs encoding pterocarpen reductase involved in isoflavon phytoalexin biosynthesis in *Lotus japonicus* by EST mining. FEBS Lett. 580: 5666-5670

Al-Abed, Y., Sabri, S., Abu Zarga, M. (1990) Chemical constituents of the flora of Jordan. Part V-B. Three new arylnaphthalene lignan glucosides from *Haplophyllum buxbaumii*, J. Nat. Prod. 53: 1152–1161

Alfermann, A.W., Petersen, M., Fuss, E. (2003) Production of natural products by plant cell biotechnology: results, problems and perspectives. In: Laimer, M., Rücker, W. (eds) Plant Tissue Culture, 100 years since Gottlieb Haberlandt. Springer, pp. 153-166

Allen, R.S., Millgate, A. G., Chitty, J. A., Thisleton, J., Miller, J. A. C., Fist, A. J., Gerlach, W, L., Larkin, P. J. (2004) RNAi-mediated replacement of morphine with the nonnarcotic alkaloid reticulin in Opium poppy. Nat. Biotechnol. 22: 1559-1566

Anterola, A.M., Jeon, J.H., Davin, L.B., Lewis, N.G. (2002) Transcriptional control of monolignol biosynthesis in *Pinus taeda*. J. Biol. Chem. 277: 18272-18280

Axelson, M., Setchell, K.D.R. (1981) The excretion of lignans in rats-evidence for an intestinal bacterial source for this new group of compounds. FEBS Lett. 123: 337–342

Ayers, D.C. and Loike, J.D. (1990) Lignans: Chemical, biological and clinical properties. Cambridge Univ. Press. pp. 12-84

Baba, A., Kawamura, N., Makino, H., Ohta, Y., Taketomi, S., Sohda, T. (1996) Studies on disease-modifying antirheumatic drugs: Synthesis of novel quinoline and quinazoline derivatives and their anti-inflamatory effect. J. Med. Chem. 39: 5176-5182

Belny M, Hérouart D, Thomasset B, David H, Jacquin-Dubreuil A, David A. (1997) Transformation of *Papaver somniferum* cell suspension cultures with sam1 from *A. thaliana* results in cell lines of different S-adenosyl-L-methionine synthetase activity. Phisiol. Plant. 99: 233-240

Bernstein, E., Caudy, A.A., Hammond, S.M., Hannon, G. (2001) Role of a bidentate ribonuclease in the initiation step of RNA interference. Nature 49: 363-366

Bradford, M.M. (1976) A rapid and sensitive method for the quantitation of microgram quantities of protein utilizing the principle of protein-dye binding. Anal. Biochem. 72: 248-254

Croteau, R., Kutchan, T.M., Lewis, N.G. (2000) Natural Products (Secondary Metabolites). In: Buchanan, B.B., Gruissem, W., Jones, R.L. (eds) Biochemistry & Molecular Biology of Plants. Courier Companies, Inc., pp. 1250-1318

Chapple, C. (1998) Molecular genetics analysis of plant cytochrome P450-dependent monooxygenases. Ann. Rev. Plant Physiol. Mol. Biol. 49: 311-343

Chen, C.C., Hsin, W.C., Ko, F.N., Huang, Y.L., Ou, J.C., Teng, C.M. (1996) Antiplatelet arylnaphthalide lignans from *Justicia procumbens*. J. Nat. Prod. 59: 1149-1150

Chen, H., Nelson, R.S., Sherwood, J.L. (1994) Enhanced recovery of transformants of *Agrobacterium tumefacience* after freez-thaw transformation and drug selection. Biotechniques 16: 664-670

Clemens, S., Hinderer, W., Wittkampf, U., Barz, W. (1993) Characterization of cytochrome P450 dependent isoflavone hydroxylase from chickpea. Phytochemistry 32:653-657

Chu, A., Dinkova, A., Davin, L.B., Bedgar, D.L., Lewis, N.G. (1993) Stereospecificity of (+)-pinoresinol and (+)-lariciresinol reductases from *Forsythia intermedia*. J. Biol. Chem. 268: 27026-27033

Chung, S.M., Vaidya, M., Tzfira, T. (2006) *Agrobacterium* is not alone: gene transfer to plants by viruses and other bacteria. Trends Plant Sci. 11: 1-4

Courdavault, V., Thiersault, M., Courtois, M., Gantet, P., Oudin, A., Doireau, P., St-Pierre, B., Giglioli-Guivarc'h, N. (2005) CaaX-prenyltransferase are essential for expression of genes involved in the early stages of monoterpenoid biosynthetic pathway in *Catharanthus roseus* cells. Plant Mol. Biol. 57: 855-870

Cullmann, F., Adam, K-P., Becker, H. (1993) Bisbenzyls and lignans from *Pellia epiphylla*. Phytochemistry 34: 831-834

Davin, L.B., Bedgar, D. L., Katayama, T., Lewis, N. G. (1990) On the stereoselective synthesis of (+)-pinoresinol in *Forsythia suspensa* from its achiral precursor, coniferyl alcohol. Phytochemistry 31: 3869-3874

Davin, L.B., Lewis, N.G. (2000) Dirigent Proteins and Dirigent sites Explain the Mystery of Specificity of Radical Precursor Coupling in Lignan and Lignin Biosynthesis. Plant. Physiol. 123: 453-461

Davin, L.B., Lewis, N.G. (2003) An historical perspective on lignan biosynthesis: monolignol, allyphenol and hydroxycinnamic acid coupling and downstream metabolism. Phytochem. Rev. 2: 257-288

Davin, L.B., Lewis, N.G. (2005) Dirigent phenoxy radical coupling: advances and challenges. Curr. Opin. Biotech. 16: 398-406

Davin, L.B., Wang, H.-B., Crowell, A.L., Bedgar, D.L., Martin, D.M., Sarkanen, S., Lewis, N.G. (1997) Stereoselective bimolecular phenoxy radical coupling by an auxiliary (dirigent) protein without an active center. Science 275: 362-366

De Vetten, N., Ter Horst, J., Van Schaik, H.P., De Boer, A., Mol, J., Koes, R. (1999) A cytochrome b_5 is required for full activity of flavonoid 3', 5'-hydroxylase, a cytochrome P450 involved in the formation of blue flower colors. Proc. Natl. Acad .Sci. USA 96: 778-783

Dewick, P.M. (2002) Medicinal Natural Products A Biosynthetic Approach. Second Edition; Wiley.

Diederichsen, A., Richards, K. (2003) Cultivated flax and the genus *Linum* L. Taxonomy and germplasm conservation. In: Muir, A.D., Westcott, N.D. (eds) Taylor and Francis Inc., London, UK and NY, USA, pp 22-54

Dinkova-Kostova, A.T., Gang, D.R., Davin, L.B., Bedgar, D.L., Chu, A., Lewis, N.G. (1996) (+)-Pinoresinol/(+)-lariciresinol reductase from *Forsythia intermedia*. J. Biol. Chem. 271: 29473-29482

Dixon, R.A., Harrison MJ, Paiva NL. (1995) The isoflavonoid phytoalexin pathway: From enzymes to genes to transcription factors. Physiol. Plant. 93: 385-392

Dixon, R.A., Reddy, M.S.S. (2003) Biosynthesis of monolignols. Genomic and reverse genetic approaches. Phytochem. Rev. 2: 289-306

Donaldson, R.P., Luster, D.G. (1991) Multiple forms of plant cytochrome P-450. Plant Physiol. 96: 669-674

Doyle, J.J., Doyle, J.L. (1990) Isolation of plant DNA from fresh tissue. Focus 12: 13-15

Duchefa catalogue 2003-2005, Haarlem, The Netherlands

Elbashir, S.M., Lendeckel, W., Tuschl, T. (2001) RNA interference is mediated by 21- and 22-nucleotide RNAs. Genes & Development 15: 188-200

Empt, U., Alfermann, A. W., Pras, N., Petersen, M. (2000) The use of plant cell culture for the production of podophyllotoxin and related lignans. J. Appl. Bot-Angew. Bot. 74: 145-150

Fagard, M., Vaucheret, H. (2000) (Trans) Gene silencing in plants: How many mechanism? Annu. Rev. Plant Physiol. Plant Mol. Biol. 51: 167-194

Federolf, K., Alfermann, A.W., Fuss, E. (2007) Aryltetralin-lignan formation in two different cell lines of *Linum album*: deoxypodophyllotoxin 6-hydroxylase, a key-enzyme for the formation of 6-methoxypodophyllotoxin. Phytochemistry 68:1397-1406

Fire, A., Xu, S.Q., Montgomery, M.K., Kostas, S.A., Driver, S.E., Mello, C.C. (1998) Potent and specific genetic interference by double-stranded RNA in *Caenorhabditis elegans*. Nature 391: 806-811

Floss, G.H. (1979) The shikimate pathway. In: Swain, T., Harborne, J.B., van Sumere, C.F. (eds) Recent advances in phytochemistry, vol 12: Biochemistry of plant phenolics. Plenum Press, New York, pp 59-89

Ford, J.D., Huang, K.–S., Wang, H.B., Davin, L.B., Lewis, N.G. (2001) Biosynthetic pathway to the cancer chemopreventive secoisolariciresinol diglucoside-hydroxymethylglutaryl ester-linked lignan oligomers in flax (*Linum usitatissimum*) seed. J. Nat. Prod. 64: 1388-1397

Frick, S., Chitty, J. A., Kramell, R., Schmidt, J., Allen, R. S., Larkin, P. J., Kutchan, T. M. (2004). Transformation of Opium poppy (*Papaver somniferum* L.) with antisense berberine bridge enzyme gene (anti-bbe) via somatic embryogenesis results in altered ratio of alkaloids in latex but not in roots. Transgenic Res. 13: 607-613

Fujita, M., Gang, D.R., Davin, L.B., Lewis NG. (1999) Recombinant pinoresinol-lariciresinol reductase from Western Red Cedar (*Thuja plicata*) catalyze opposite enantiospecific conversions. J. Biol. Chem. 274: 618-627

Fuss, E. (2003) Lignans in plant cell and organ culture: An overview. Phytochem. Rev. 2:307-320

Fuss, E. (2007) Biosynthesis of lignans. Habilitationsschrift. Heinrich-Heine University, Düsseldorf

Gang, D.R., Costa, M.A., Fujita, M., Dinkova-Kostova, A.T., Wang, H.-B., Burlat, V., Martin, W., Sarkanen, S., Davin, L.B., Lewis, N.G., (1999a) Regiochemical control of monolignol radical coupling: a new paradigm for lignin and lignan biosynthesis. Chem. Biol. 6: 143-151

Gang, D.R., Kasahara, H., Xia, Z.-Q., Vander Mijnsbrugge, K., Bauw, G., Boerjan, W., Van Montagu, M., Davin, L.B., Lewis, N.G. (1999b) Evolution of plant defense mechanism. J. Biol. Chem. 274: 7516-7527

Gerardy, R., Zenk, M.H. (1993) Formation of salutaridine from (R)-reticuline by a membrane bound cytochrome P-450 enzyme from *Papaver somniferum*. Phytochemistry 32: 79-86

Gertsch, T., Tobler, R.T., Brun, R., Sticher O., Heilmann, S. (2003) Antifungal, antiprotozoal, cytotoxic and piscicidal properties of justicidin B and a new arylnaphthalide lignan from *Phyllanthus piscatorum*. Planta Med. 69: 420-424

Gleave, A.P. (1992) A versatile binary vector system with a T-DNA organisational structure conductive to efficient integration of cloned DNA into the plant genome. Plant Mol. Biol. 20: 1203-1207

Graham, S.E., Peterson, J.A. (1999) How similar are P450s and what can their differences teach us. Arch. Biochem. Biophys. 369: 24-29

Grotewold, E., Chamberlin, M., Snook, M., Siame, B., Butler, L., Swenson, L., Maddock, S., St. Clair, G., Bowen, B. (1998) Engineering secondary metabolism in maize cells by ectotopic expression of transcription factors. Plant Cell 10: 721-740

Guillon, S., Trémouillaux-Guiller, J., Pati, P.K., Rideau, M., Gantet, P. (2006) Hairy root research: recent scenario and exciting prospects. Curr. Opin. in Plant Biol. 9: 341-346

Hadacek, F. (2002) Secondary Metabolites as Plant Traits: Current Assessment and Future Perspectives. Critic. Rev. Plant Sci. 21: 273-322

Hamilton, A.J., Baulcombe, D.C. (1999) A species of small antisense RNA in posttranscriptional gene silencing in plants. Science 286: 950-952

Hanahan, D. (1983) Studies on transformation of Escherichia coli with plasmids. J. Mol. Biol. 166: 557-580

Hano, C., Martin, I., Fliniaux, O., Legrand, B., Gutierrez, L., Arroo, Mesnard, F., Lamblin, F. and Lainé, E. (2006) Pinoresinol-lariciresinol reductase gene expression and secoisolariciresinol diglucoside accumulation in developing flax (*Linum usitatissimum*) seeds. Planta 224: 1291-1301

Hartmann, T. (1996) Diversity and variability of plant secondary metabolism: a mechanistic view. Entomol. Gen. Appl. 80: 177-188

von Heimendahl, C.B., Schäfer, K.M., Eklund, P., Sjöholm, R., Schmidt, T.J., Fuss, E. (2005) Pinoresinol-lariciresinol reductase with different stereospecificity from *Linum album* and *Linum usitatissimum*. Phytochemistry 66: 1254-1263

Hellens, R., Mullineaux, P., Klee, H. (2000) A guide to *Agrobacterium* binary Ti vectors. Trends plant Sci. 5: 446-451

Hemmati, S., Schmidt, T.J., and Fuss, E. (2007) (+)-Pinoresinol/(-)-lariciresinol reductase from *Linum perenne* Himmelszelt involved in the biosynthesis of justicidin B. FEBS Lett. 581: 603-610

Humphreys, J.M., Chapple, C. (2002) Rewriting the lignin roadmap. Curr. Opin. in Plant Biol. 5: 224-229

Imbert, T.F. (1998) Discovery of podophyllotoxin. Biochimie 80: 207-222

Jefcoate, C.R. (1978) Measurement of substrate and inhibitor binding to microsomal cytochrome P450 by optical difference spectroscopy. Methods Enzymol. 52: 258-279

Jensen, R.A. (1976) Enzyme recruitment in the evolution of the new function. Ann. Rev. Microbiol. 30: 409-425

Van der Krol, A.R., Mur, L.A., Beld, M., Mol, J.N.M., Stuitje, A.R. (1990) Flavonoid genes in Petunia: addition of a limited number of gene copies may lead to a suppression of gene expression. Plant Cell 2: 291-299

Karp, F., Mihailiak, C.A., Harris, J.L., Croteau, R. (1990) Monoterpen biosynthesis: specificity of the hydroxylations of (-)-limonene by enzyme preparations from peppermint (*Mentha piperita*) spearmint (*Mentha spicata*) and Perilla (*Perilla frutescens*) leaves. Arch Biochem. Biophys. 276: 219-226

Katayama, T., Davin, L.B., Chu, A., Lewis N.G. (1993) Novel benzylic ether reductions in lignan biogenesis in *Forsythia intermedia*. Phytochemisty 33: 581-591

Klee, H., Horsch, R., Rogers, S. (1987) *Agrobacterium*-mediated plant transformation and its applications to plant biology. Ann. Rev. Plant Physiol. 38: 467-486

Koeduka, T., Fridman, E., Gang, D.R., Vassao, D.G., Jackson, B.L., Kish, C.M., Orlova, I., Spassova, S.M., Lewis, N.G., Noel, J.P., Baiga, T.J., Dudareva, N., Pichersky, E. (2006)

Eugenol and isoeugenol, characteristic aromatic constituents of spices, are biosynthesized via reduction of a coniferyl alcohol ester. Proc. Natl. Acad. Sci. 27: 10128-10130

Kranz, K., Petersen, M. (2003) β-Peltatin 6-O-methyltransferase from suspension cultures of *Linum nodiflorum*. Phytochemistry 64: 453-458

Kraus, C., Spiteller, G. (1997) Comparison of phenolic compounds from galls and shoots of *Picea glauca*. Phytochemistry 44: 59-67

Kumagai, H., Kouchi, H. (2003) Gene silencing by expression of hairpin RNA in *Lotus japonicus* roots and root nodules. MPMI 16: 663-668

Kutchan, T.M. (1995) Alkaloid biosynthesis: the basis for metabolic engineering of medicinal plants. Plant Cell 7: 1059-1070

Kutchan, T., Diettrich, H., Bracher, D., Zenk, M.H. (1991) Enzymology and molecular biology of alkaloid biosynthesis. Tetrahedron 47: 5945-5954

Kwon, M., Davin, L.B., Lewis, N.G. (2001) In situ hybridization and immunolocalization of lignan reductases in woody tissues: implications for heartwood formation and other forms of vascular tissue preservation. Phytochemistry 57: 899-914

Laemmli, U.K. (1970) Cleavage of structural proteins during the assembly of the head of bacteriophage T4. Nature 227: 680-685

Lee, K-H., Xiao, Z. (2003) Lignans intreatment of cancer and other diseases. Phytochem. Rev. 2: 341-362

Lin, R.C., Skaltsounis, A.L., Seguin, E., Tilleguin, F., Koch, M. (1994) Phenolic constituents of *Selaginella doederleinii*. Planta Med. 60: 168-170

MacBride, K.E., Summerfelt, K.R. (1990) Improved binary vectors for *Agrobacterium*-mediated plant transformation. Plant Mol. Biol. 14: 269-276

MacRae, W.D., Hudson, J.B., Towers, G.H. (1989) The antiviral action of lignans. Planta Med. 55: 531-535

Martin, P.M., Horwitz, KB., Ryan, D.S. and McGuire, W.L. (1978) Phytoestrogen interaction with estrogen receptors in human breast cancer cells. Endocrinology 103: 1860-1867

Mansoor, S., Amin, I., Hussain, M., Zafar, Y., Briddon, R.W. (2006) Engineering novel traits in plants through RNA interference. Trends Plant Sci.11: 559-565

Miki, B. (2002) Transgene expression and control. In vitro Cell Dev. Biol. Plant 38: 139-145

Min, T., Kasahara, H., Bedgar, D.L., Youn, B., Lawrence, P.K., Gang, D.R., Halls, S.C., Park, H., Hilsenbeck, J.L., Davin, L.B., Lewis, N.G. Kang, C.H. (2003) Crystal Structures of Pinoresinol-Lariciresinol and Phenylcoumaran Benzylic Ether Reductases and Their Relationship to Isoflavone Reductases. J. Biol. Chem. 278: 50714-50723

Mohagheghzadeh, A., Schmidt, T.J., Alfermann, A.W. (2002) Arylnaphthalene lignans from in vitro cultures of *Linum austriacum*. J. Nat. Prod. 65: 69-71

Molog, G.A., Empt, U., Kuhlmann, S., van Uden, W., Pras, N., Alfermann, A.W., Petersen, M. (2001) Deoxypodophyllotoxin 6-hydroxylase, a cytochrome P450 monooxygenase from cell cultures of *Linum flavum* involved in the biosynthesis of cytotoxic lignans. Planta 214: 288-294

Moss, G.P. (2000) Nomenclature of lignans and neolignans (IUPAC recommendations 2000). Pure Appl. Chem. 72: 1493-1523

Murashige, T. Skoog, F. (1962) A revised medium for rapid growth and bioassays with tobacco tissue cultures. Physiol. Plant 15: 473

Napoli, C., Lemieux, C., Jorgensen, R. (1990) Introduction o a chimeric chalcone synthase gene into Petunia results in reversible co-suppression of homologous gene in trans. Plant Cell 2: 279-289

Nishihara, M., Nakatsuka, T., Yamamura, S. (2005) Flavonoid components and flower color change in transgenic tobacco plants by suppression of chalcone isomerase gene. FEBS Lett. 579: 6074-6078

Nukul, G.S., Abu Zarga, M.H., Sabri, S.S., Al-Eisawi, D.M. (1987) Chemical constituents of the Flora of Jordan, part III. Mono-O-acetyl diphyllin Apioside, a new arylnaphthalene lignan from *Haplophyllum buxbaumii*. J. Nat. Prod. 50: 748-750

Ober, D. (2005) Seeing double: gene duplication and diversification in plant secondary metabolism. Trends Plant Sci. 10: 444-449

Ockendon, D.J., Walters, S.M. (1968) *Linum*. In: Tutin, T.G., Heywood, V.H., Burges, N.A., Moore, D.M., Valentine, D.H., Walters, S.M., Webb, D.A. (eds) Flora Europaea, Cambridge University Press, Cambridge, vol 2 pp 206-211

Okigawa, M., Maeda, T., Kawano, N. (1970) The isolation and structure of three new lignans from *Justica procumbens* Linn. VAR. Leucantha honda. Tetrahedron 26: 4301-4305

Oksman-Caldentey, K.M., Inzé, D. (2004) Plant cell factories in the post-genomic era: new ways to produce designer secondary metabolites. Trends Plant Sci. 9: 433-440

Omura, T., Sato, R. (1964) The carbon monoxide-binding pigment of liver microsomes. I. Evidence for its hemoprotein nature. J. Biol. Chem. 239: 2370-2378

Oritz de Montellano, P.R., Correia, M.A. (1995) Inhibition of cytochrome P450 enzymes. In: Oritz de Montellano, P.R. (eds) Cytochrome P450: structure, mechanism, and biochemistry, 2nd edn. Plenum, New York, pp 305-364

Oritz de Montellano, P.R. (2005) Cytochrome P450: Structure, Mechanism and Biochemistry. Springer.

Osawa., T., Nagata, M., Namiki, M., Fukuda, Y. (1985) Sesamolinol, a novel antioxidant isolated from sesame seeds. Agric. Biol. Chem. 49: 3351-3352

Page, J. E., Hause, G., Raschke, M., Gao, W., Schmidt, J., Zenk, M. H., Kutchan, T. M. (2004) final steps of the 1-deoxy-D-xylose 5-phosphate (DXP) pathway to isoprenoids in plants using virus induced gene silencing. Plant physiol. 134: 1401-1413

Paré, P.W., Wang, H.B., Lewis, N.G. (1994) (+)-Pinoresinol synthase: a stereoselective oxidase catalyzing 8, 8'-lignan formation in Forsythia intermedia. Tetrahedron Lett. 35: 4731-4734

Park, S., Facchini, P. (2000) *Agrobacterium rhizogenes*-mediated transformation of opium poppy, *Papaver somniferum* L., and California poppy, *Eschscholzia californica* Cham., root cultures. J. Exp. Bot. 51: 1005-1016

Petersen, M. (1997) Cytochrome P450-dependent hydroxylation in the biosynthesis of rosmarinic acid in *Coleus*. Phytochemistry 45: 1165-1172

Petersen, M. (2003) Cinnamic acid 4-hydroxylase from cell cultures of hornwort *Anthoceros agrestis*. Planta 217: 96-101

Petersen, M., Szabo, E., Mainhard, J., Krawatzki, B., Gertlowski, C., Kempin, B., Fuss, E. (1995) Biosynthesis and accumulation of rosmarinic acid in suspension cultures of *Coleus blumei*. Plant Cell Tiss. Org. Cul. 43: 89-93

Pfeiffer, J., Kühnel, C., Brandt, J., Duy, D., Punyasiri, P.A.N., Forkmann, G. Fischer, T.C. (2006) Biosynthesis of flavan 3-ols by leucoanthocyanidin 4-reductases and anthocyanidin reductases in leaves of grape (*Vitis vinifera* L.), apple (*Malus x domestica* Borkh.) and other crops. Plant Physiol. Biochem. 44: 323-334

Pichersky, E., Gang, D.R. (2000) Genetics and biochemistry of secondary metabolites in plants: an evolutionary perspective. Trends Plant Sci. 5: 439-445

Prieto, J.M., Giner. R.M., Recio, M.C., Schinella, G., Máñez, S., Rios, J.L. (2002) Diphyllin acetylapioside, a 5-lipoxygenase inhibitor from *Haplophyllum hispanicum*. Planta Med. 68: 359-360

Puricelli ,L., Innocenti, G., Piacente, S., Caniato, R., Filippini, R., Cappelletti, E.M. (2002) Production of lignans by *Haplophyllum patavinum in vivo* and *in vitro*. Heterocycles 56: 607-612

Rademacher, W., Fritsch, H., Graebe, J.E., Sauter, H., Jung, J. (1987) Tetcyclacis and triazole-type plant growth retardants: their influence on the biosynthesis of gibberellins and other metabolic processes. Pestic. Sci. 21: 241-252

Rao, Y.K., Fang, S.H., Teng, Y.M. (2006) Anti-inflammatory activities of constituents isolated from *Phyllantus polyphyllus*. J. Ethnopharmacol.103: 181-186

Rogers, C.M. (1972) The taxonomic significance of fatty acid content of seeds of *Linum*. Brittonia 24: 415-419

Russell, D.W. (1971) The metabolism of aromatic compounds in higher plants. X. Properties of the cinnamic acid 4-hydroxylase of pea seedlings and some aspects of its metabolic and developmental control. J. Biol. Chem. 246: 3870-3878

Russell, D.W., Conn, E.E. (1967) The cinnamic acid 4-hydroxylase of pea seedlings. Arch. Biochem. Biophys. 122: 256-258

Sakakibara, N., Suzuki, S., Umezawa, T., Shimada, M. (2003) Biosynthesis of yatein in Anthriscus sylvestris. Org. Biomol. Chem. 1: 2474-2485

Sandermann, H. Jr. (1992) Plant metabolism of xenobiotics. Trends Biochem. Sci.17: 82-84

Schlichting, I., Berendzen, J., Chu, K., Stock, A.M., Maves, S.A., Benson, D.E., Sweet, R.M., Ringe, D., Petsko, G.A., Sligar, S.G. (2000) The catalytic pathway of cytochrome P450cam at atomic resolution. Science 287: 1615-1622

Schmidt, T. J., Hemmati, S., Fuss, E., Alfermann, A. W. (2006) A combined HPLC-UV and HPLC-MS method for the identification of lignans and its application to the lignans of *Linum usitatissimum* L and *L. bienne* Mill. Phytochem. Anal. 17: 299-311

Schmidt, W., Peters, S., Beerhues, L. (2000) Xanthone 6-hydroxylase from cell cultures of *Centaurium erythraea* RAFN and *Hypericum androsaemum* L. Phytochemistry 53: 427-431

Schmidt, T.J., Vößing, S. (2006) A novel aryldihydronaphthalene lignan from *Linum perenne* L. Planta Med. 72: 1006-1006

Schwab, W. (2003) Metabolome diversity: too few genes, too many metabolites? Phytochemistry 62: 837-849

Setchell, K.D.R., Lawson, A.M., Conway, E., Taylor, N.F., Kirk, D.N., Cooley, G., Farrant, R.D., Wynn, S., Axelson, M. (1981) The definite identification of the lignans *trans*-2,3-bis(3-hydroxybenzyl-γ-butyrolactone and 2,3-bis(3-hydroxybenzyl)butane-1,4-diol in human and animal urine. Biochem. J. 197: 447–458

Sevón, N., Oksman Caldentey, K.M. (2002) *Agrobacterium* rhizogenes-Mediated Transformation: Root Cultures as a Source of Alkaloids. Planta Med. 68: 859-868

Sicilia, T., Niemeyer, H.B., Honig, D.M., Metzler, M. (2003) Identification and stereochemical characterization of lignans in flaxseed and pumpkin seeds. J. Agric. Food Chem. 51: 1181-1188

Seidel, V., Windhövel, J., Eaton, G., Alferman, A. W., Aroo, R.R., Medarde, M., Petersen, M., Woolley, J.G. (2002) Biosynthesis of podophyllotoxin in *Linum album* cell cultures. Planta 215: 1031-1039

Small, I. (2007) RNAi for revealing and engineering plant gene functions. Curr. Opin. Biotech. 18: 148-153

Smith, C.J.S., Watson, C.F., Bird, C.R., Ray, J., Schuch, W., Grierson, D. (1990) Expression of a truncated tomato polygalactronase gene inhibits expression of the endogenous gene in transgenic plants. Mol. Gen. Genet. 224: 477-481

Smith, N.A., Singh, S.P., Wang, M.B., Stoutjesdijk, P.A., Green, A.G., Waterhous, P.M. (2000) Total silencing by intron-spliced hairpin RNAs. Nature 407: 319-320

Stévigny, C., Jiwan, J-L.H., Rozenberg, R., de Hoffmann, E., Quetin-Leclercq J. (2004) Key fragmentation patterns of aporphine alkaloids by electrospray ionization with multistage mass spectrometry. Rapid Commun. Mass Spectrom. 18: 523-528

Strack, D. (1997) Phenolic metabolism. In: Dey, P.M., Harborne, J.B. (eds) Plant Biochemistry. Academic Press, London, pp 387-416

St-Pierre, B., De Luca, V. (1995) A cytochrome P-450 monooxygenase catalyzes the first step in the conversion of tabersonine to vindoline in *Catharanthus roseus*. Plant Physiol. 109: 131-139

Suzuki, S., Umezawa, T. and Shimada, M. (2002) Stereochemical diversity in lignan biosynthesis of *Arctium lappa* L. Biosci. Biotech. Biochem. 66: 1262-1269

Taiz, L., Zeiger, E. (2006) Plant Physiology. Fourth Edition. Sinauer Associates, Inc. Sunderland

Umezawa, T. (2003) Diversity in lignan biosynthesis. Phytochem. Rev. 2: 371-390

Umezawa, T., Davin, L.B., Lewis, N.G. (1990) Formation of the lignan, (-)-secoisolariciresinol, by cell free extracts of *Forsythia intermedia*. Biochem. Biophys. Res. Commun. 171: 1008-1014

Umezawa, T., Kuroda, H., Isohata, T., Higuchi, T., Shimada, M. (1994) Enantioselective lignan synthesis by cell-free extracts of *Forsythia koreana*. Biosci. Biotech. Biochem. 58: 230-234

Umezawa, T., Okunishi, T. and Shimada, M. (1997) Stereochemical diversity in lignan biosynthesis. Wood Res. 84: 62-75

Vasilev, N., Elfahmi, Bos, R., Kayser, O., Momekov, G., Konstantinov, S., Inokova, I. (2006) Production of jucticidin B, a cytotoxic arylnaphthalene lignan from genetically transformed root cultures of *Linum leonii*. J. Nat. Prod. 69: 1014-1017

Velasco, L., Goffman, F.D. (2000) Tocopherol, plastochromanol and fatty acid patterns in the genus *Linum*. Plant Syst. Evol. 221: 77-88

Wang, M-B., Metzlaff, M. (2005) RNA silencing and antiviral defense in plants. Curr. Opin. Plant Biol. 8: 216-222

Werck-Reichhart, D. Feyereisen, R. (2000) Cytochrome P450: a success story. Genome Biol. 1: 3003. 1-3003.9

Watson, J., M. Fusaro, A. F., Wang,M., Waterhous, P. M. (2005) RNA silencing platforms in plants. FEBS Lett. 579: 5982-5987

Westcott, N.D., Muir, A.D. (2003) Flax seed lignan in disease prevention and health promotion. Phytochem. Rev. 2: 401-417

Wesley, S.V., Helliwell, C.A., Smith, N.A., MingBo, W., Rouse, D.T., Liu, Q., Gooding, P.S., Singh, S.P., Abbott, D., Stoutjesdijk P.A., Robinson, S.P., Gleave, A.P., Green, A.G., Waterhouse, P.M. (2001) Construct design for efficient, effective and highthoughput gene silencing in plants. Plant J. 27: 581-590

Wong, S-K., Tsui, S-K., kwan, S-Y., Su, X-L., Lin, R-C. (2000) Identification and characterization of *Podophyllum emodi* by API-LC/MS/MS. J. Mass Spectrom. 35: 1246-1251

Xia, Z.-Q., Costa, M. A., Péllisier, H., Davin, L.B., Lewis, N.G. (2001) Secoisolariciresinol dehydrogenase purification, cloning and functional expression. J. Biol. Chem. 276: 12614-12623

Yamamoto, H., Inoue, K., Li, S.M., Heide, L. (2000) Geranylhydroquinone 3"-hydroxylase, a cytochrome P-450 monooxygenase from *Lithospermum erythrorhizon* cell suspension cultures. Planta 210:312-317

Yamamoto, H., Yatou, A., Inoue, K. (2001) 8-Dimethylallylnaringenin 2'-hydroxylase, the crucial cytochrome P450 monooxygenase for lavandulylated flavanone formation in Sophora flavescens cultured cells. Phytochemistry 58: 671-676

Yang, D.-C., Choi, Y.-E. (2000) Production of transgenic plants via *Agrobacterium rhizogenes* mediated transformation of *Panax ginseng*. Plant Cell Rep. 19: 491-496

Zamore, P.D., Tuschl, T., Sharp, P.A., Bartel, D.P. (2000) RNAi: double-stranded RNA directs the ATP-dependent cleavage of mRNA at 21 to 23 nucleotide intervals. Cell 101: 25-33

Zenk, M.H. (1991) Chasing the enzymes of secondary metabolism: Plant cell cultures as a pot of gold. Phytochemistry 30: 3861-3863

Zhou, C., Yang, Y., Jong, A.Y. (1990) Mini-prep in ten minutes. Biotechniques 8: 172-173

Zupan, J.R., Zambryski, P. (1995) Tansfer of T-DNA from *Agrobacterium* to the plant cell. Plant Physiol. 107: 1041-1047

7. Appendix

7.1. Markers
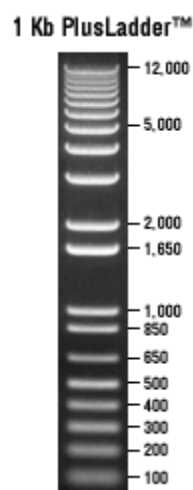
Fig. 7.1. 1 kb Plus DNA Ladder (Invitrogen)
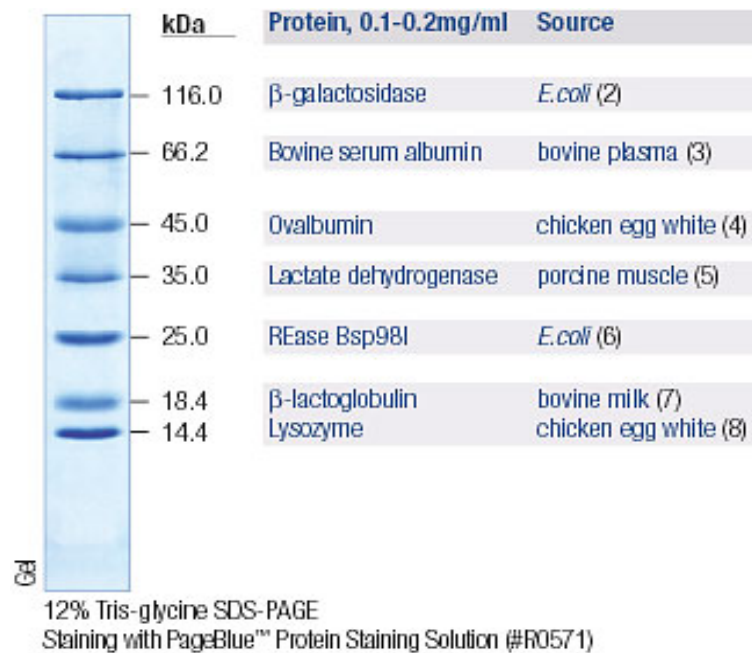
Fig. 7.2. Protein Molecular Weight Marker (MBI-Fermentas).

7.2. Vectors
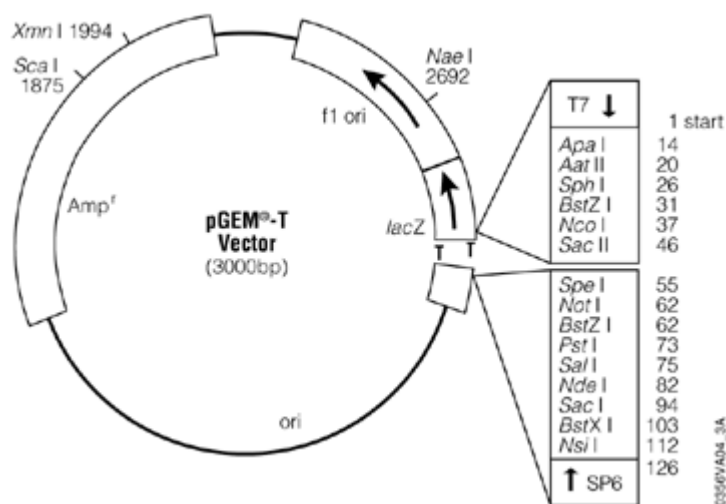
T7 RNA Polymerase transcription initiation site 1

SP6 RNA Polymerase transcription initiation site 126

T7 RNA Polymerase promoter 2987-6

SP6 RNA Polymerase promoter 121-143

multiple cloning site 10-113

lacZ start codon 165

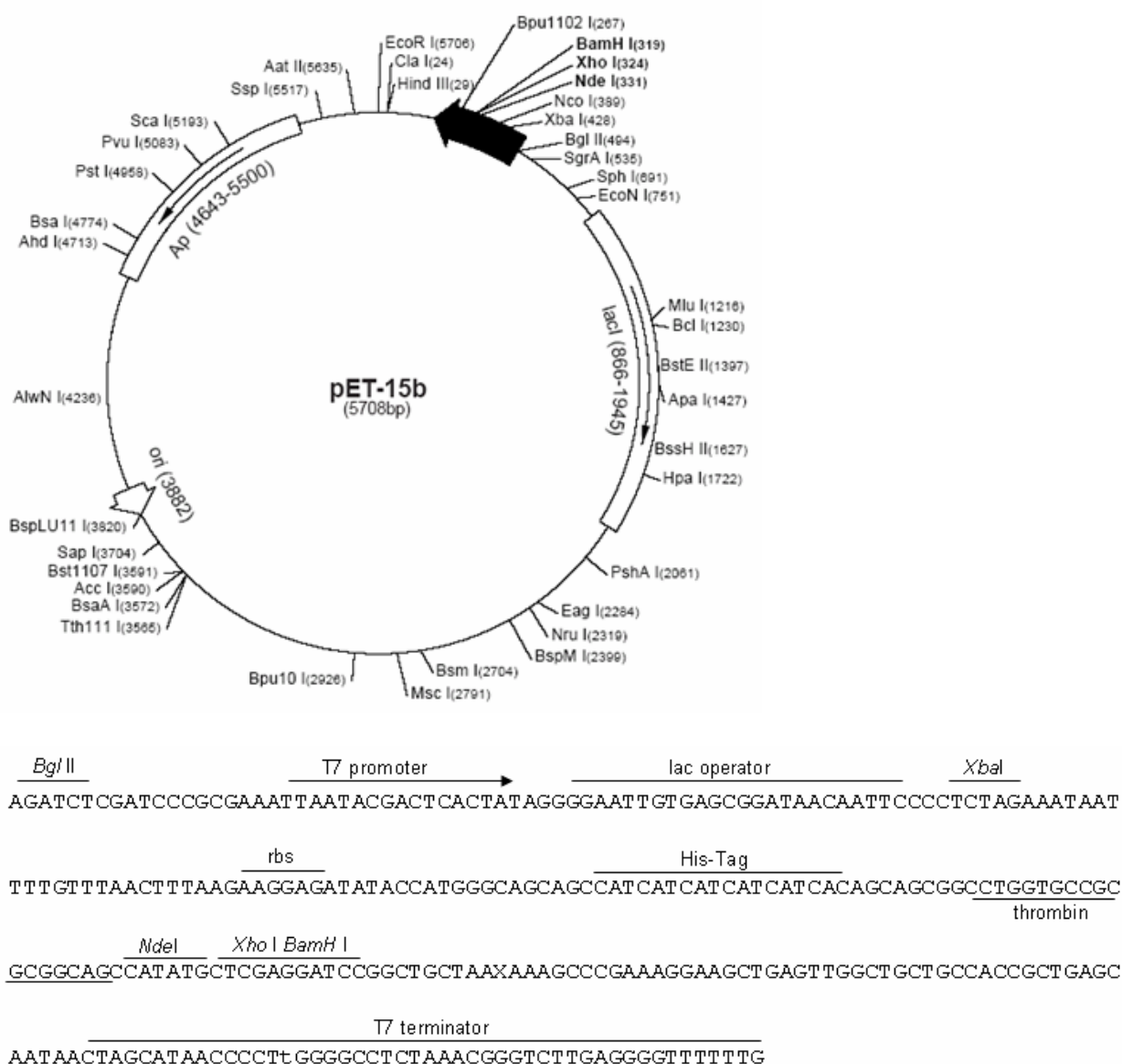lac operon sequences 2824-2984, 151-380

lac operator 185-201

β-lactamase coding region 1322-2182

phage f1 region 2368-2823

binding site of pUC/M13 Forward Sequencing Primer 2944-2960

binding site of pUC/M13 Reverse Sequencing Primer 161-177

Fig. 7.3. Circle Map of pGEM®-T vector (cloning vector) and sequence reference points (Promega).

Fig. 7.4. pET15b cloning/expression vector (Novagen).
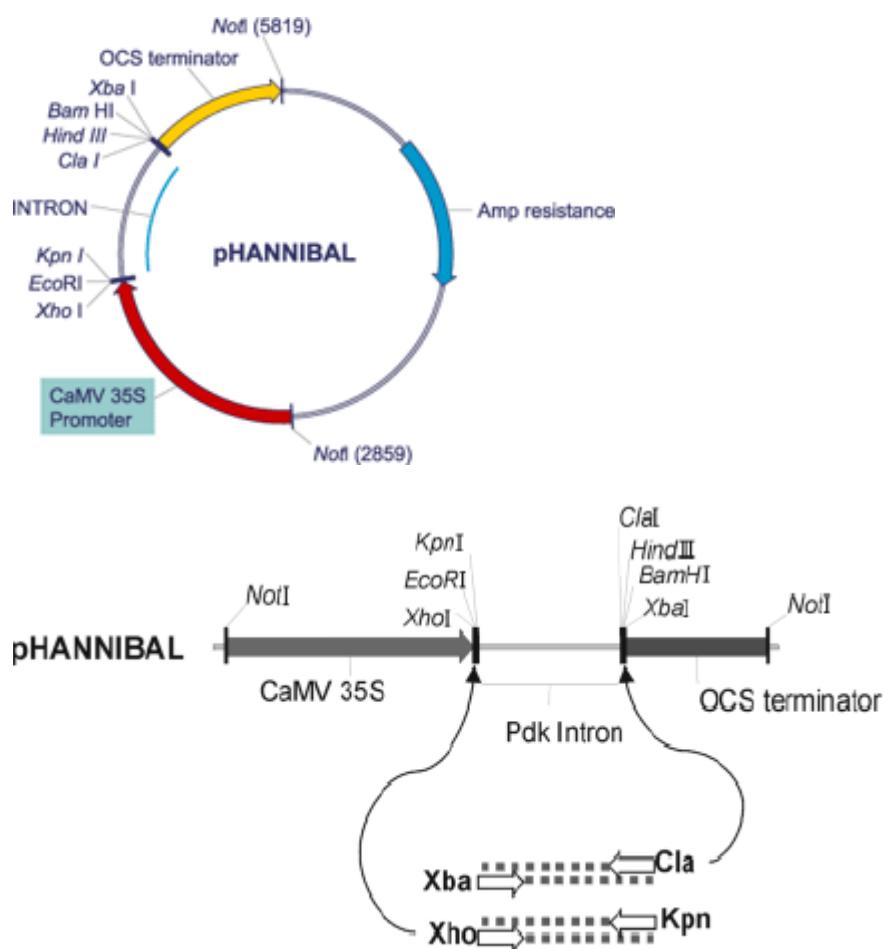
Fig. 7.5. Circle map and expression cassette of pHANNIBAL vector (Wesely et al. 2001).
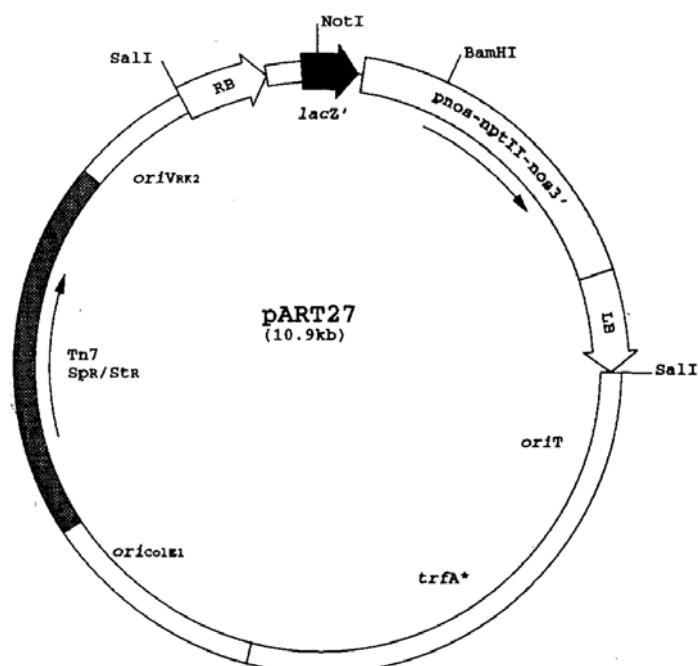
Fig. 7.6. Map of the pART27 binary vector (Gleave 1992).

8. Acknowledgements

I certify that this thesis is entirely my own work. All used sources and resources are cited.

Düsseldorf, 19.11.2007

……………………………..

Shiva Hemmati

PUBLICATIONS

Hemmati S, von Heimendahl CBI, Fuss E. Pinoresinol-lariciresinol reductases with opposite enantiospecificity determine the enantiomeric composition of lignans in *Linum usitatissimum*. (in preparation)

Hemmati S, Schneider B, Schmidt TJ, Federolf K, Alfermann AW, Fuss E. Justicidin B 7-hydroxylase, a cytochrome P450 monooxygenase from cell cultures of *Linum perenne* involve in the biosynthesis of diphyllin. Phytochemistry (in press)

Hemmati S, Schmidt TJ, Fuss E. (+)-Pinoresinol/(-)-lariciresinol reductase from *Linum perenne* Himmelszelt involved in the biosynthesis of justicidin B. FEBS Letters (2007) 581: 603-610

Mohagheghzadeh A, Gholami A, Hemmati S, Ardakani MR, Schmidt TJ, Alfermann AW. Root cultures of linum species section Syllinum as rich sources of 6-methoxypodophyllotoxin. Zeitschrift fur Naturforschung-Section C, Journal of Biosciences (2007), 62 (1-2): 43-49

Schmidt, TJ, Hemmati, S, Fuss, E, Alfermann, AW. A combined HPLC-UV and HPLC-MS method for the identification of lignans and its application to the lignans of *Linum usitatissimum* L. and *L. bienne* Mill. Phytochemical Analysis (2006) 17: 299-311

Ardakani MS, Hemmati S, Mohagheghzadeh A. Effect of elicitors on the enhancement of podophyllotoxin biosynthesis in suspension cultures of *Linum album*. DARU (2005) 13: 56-60

Mohagheghzadeh A, Gholami A, Soltani M, Hemmati S, Alfermann AW. *Linum mucronatum*: organ to organ lignan variation. Zeitschrift fur Naturforschung-Section C, Journal of Biosciences (2005), 60 (5-6): 508-510

Mohagheghzadeh A, Hemmati S, Mehregan I, Alfermann AW. *Linum persicum*: Lignans and placement in Linaceae. Phytochemistry Reviews (2003) 2: 363-369

SEMINARS AND CONGRESSES

(+)-Pinoresinol/(-)-lariciresinol reductase from *Linum perenne* Himmelszelt involved in the biosynthesis of justicidin B. In: 50 years of the phytochemical society of Europe, Cabridge, UK, April 11-14, 2007 (poster)

Evolution and diversity of lignan biosynthesis in the genus *Linum.* In: 5th Kurt-Mothes-Doctoral Student-Workshop, Halle, Germany, October 5-7, 2005 (lecture)

Pinoresinol-lariciresinol reductase in justicidin B producing cell cultures of *Linum perenne*. In: XVII International Botanical Congress, Vienna, Austria, July 17-23, 2005 (poster)

Lignans in *Linum perenne*. In: Section Plant Natural Product, German Society of Botany, Kaub on Rhein, Germany, March 16-18, 2005 (lecture)

Chemodiversity of lignan accumulation in the genus *Linum*. In: Botany Symposium, Braunschweig, Germany, September 5-10, 2004 (poster)

Diversity of lignans in *Linum* species. In: Future Trends in Phytochemistry, Gargnano, Italy, May 5-8, 2004 (poster)

Quantification of aryltetralin lignans in plant parts and ontogenic stages of *Linum album*. In: Phytochemistry and Biology of Lignans, Bornheim-Walberberg, Germany, April 6-9, 2003 (poster)

In vitro cultures of *Linum album* and screening for high lignan producing lines. In: Future Trends in Phytochemistry, Gargnano, Italy, May 22-25, 2002 (poster)